Mussel Attachment in a Dynamic Ocean: An Ecomechanical Perspective

Matthew Nicholas George

A dissertation

submitted in partial fulfillment of the

requirements for the degree of

Doctor of Philosophy

University of Washington

2018

Reading Committee:

Emily Carrington, Chair

Thomas L. Daniel

Jeffery A. Riffell

Program Authorized to Offer Degree:

Biology

University of Washington

Abstract

Mussel Attachment in a Dynamic Ocean: An Ecomechanical Perspective

Matthew Nicholas George

Chair of Supervisory Committee:

Dr. Emily Carrington

Biology

Marine mussels are masters of underwater adhesion, attaching to a wide variety of substrates using an array of collagen-like fibers (byssal threads) that are each tipped with a powerful protein-based adhesive (plaque). The molecular mechanisms that underlay plaque adhesion are an integral part of a worldwide mussel aquaculture industry, while also inspiring the development of anti-fouling coatings for use in the maritime industry, and the design of medical adhesives for use as sutures in the human body. In this dissertation, I seek to understand the mechanisms underlying plaque adhesion using an 'ecomechanical' perspective, by exploring the direct interaction between the local environment and the adhesive plaque after it is deposited on a surface. To accomplish this, in Chapter 1 I perform a series of laboratory experiments wherein mussels make attachments to surfaces under standard 'open-ocean' conditions, and attachments are separated from the animal and matured in different seawater treatments. When sampled overtime, plaque attachment strength increased over time, nearly doubling in adhesion strength

(+94%) after 12 days in seawater at pH 8.0. However, holding plaques in low pH conditions (<7.0) prevented this strengthening, causing the material to tear more frequently under tension. These results point to the role of seawater pH as a 'molecular trigger' during the adhesive curing process, necessitating that plaques have access to a basic pH after initial substrate adhesion is achieved. Chapter 2 expands on this finding by investigating the influence of other seawater parameters, such as seawater temperature, salinity, and dissolved oxygen concentration on the plaque curing process. In contrast to pH, high temperature (30^{o}C) and low salinity (1 PSU) had no effect on adhesion strength, while incubation in hypoxia (0.9 mg L^{-1}) for 12 days left plaques with a mottled coloration. Oxygen deprived plaques were more likely to peel from substrates before the thread could be loaded, leading to a 51% decrease in adhesion strength. Atomic force microscopy (AFM) imaging of the plaque cuticle found that plaques cured in hypoxia had regions of lower stiffness throughout, indicative of reductions in crosslinking between DOPA residues of mussel foot proteins (Mfps). Given the demonstrated sensitivity of the plaque during the adhesive's cure window, Chapter 3 explores the implications observed interactions with the seawater environment, given the dynamic conditions that mussels experience as inhabitants of the nearshore. Five-day excursions in pH and dissolved oxygen measured at a local shellfish farm were replicated in fluctuating laboratory experiments, wherein pH excursions (<5.0) delayed plaque strengthening when applied early in the curing process, while hypoxia decreased adhesion strength after the adhesive had fully matured (<2 mg L^{-1}). In both cases, adhesion strength was rescued after re-immersion in open-ocean seawater conditions. Altogether, these results emphasize that mussel attachment strength is vulnerable to environmental modification, but only if deleterious pH or oxygen conditions are maintained during critical periods of the biomaterial's lifespan.

Acknowledgments

I wish to express my deepest gratitude to those who have supported me during my time at the University of Washington.

To my advisor Emily Carrington, for not only recognizing my potential, but also being among the first to commit to supporting my growth into an independent, thoughtful, and skeptical scientist. Your patience, guidance, humor, knowledge, and grace in the face of both personal and professional hardships gave me something to strive for thought-out my Ph.D. and will continue to do so as I continue in my career.

To my committee members, Tom Daniel, Jeff Riffell, and Carolyn Friedman, for always providing helpful feedback, advice, and challenging me to ask targeted questions.

To my lab members over the years, Hilary Hayford, Mike Nishizaki, Laura Newcomb, Lyda Harris, Emily (Molly) Roberts, Rebecca (Becca) Guenther, Michael (Moose) O'Donnell, and Jaquan Horton, it was a pleasure to work with you and be influenced by your passion for marine science. Our discussions and your input on my work not only made this dissertation better, but opened up my thinking to new avenues and perspectives. I'm grateful to have had your help, support, and friendship along the way.

To the members of Friday Harbor Laboratories, Michelle Herko, Jeannie Meredith, Aimee Urata, Scott Schwinge, Craig Staude, Alan Cairns, and countless others, your logistical support, scientific expertise, and friendship made this work possible.

To Ian Jefferds, Jim Nagel, Dominic Pangelinan, Brad Woolf, and all of the members of Penn Cove shellfish for opening up their shellfish operation and making me feel at home. Your unwavering dedication to scientific discovery and knowledge inspired me throughout my time on the mussel rafts in Quilcene.

To all of the members of the biology department at the University of Washington's Seattle campus, especially Marissa Heringer, whose advice was invaluable when it came to navigating the expansive policies and deadlines associated with my graduate program.

And last, but certainly not least, I owe now and always, my success to the unwavering support and love I have received from my wife Anahita, my parents, Nick and Robin, and all of my extending family who inspire daily. Thank you.

Tables of Contents

Chapter 1

Environmental post-processing increases the adhesion strength of mussel byssus adhesive

Matthew N. George[1,2] and Emily Carrington[1,2]

1 – University of Washington, Department of Biology, BOX 358100, Seattle, WA 98195

2 – Friday Harbor Laboratories, 620 University Rd., Friday Harbor, WA 98250

Keywords**:** protein cross-linking; underwater adhesion; mussel foot protein (Mfp); *Mytilus trossulus*; 3,4-dihydroxyphenly-L-alanine (DOPA)

1.1. Abstract

Marine mussels (*Mytilus trossulus*) attach to a wide variety of surfaces underwater using a protein adhesive that is cured by the surrounding seawater environment. In this study, the influence of environmental post-processing on adhesion strength was investigated by aging adhesive plaques in a range of seawater pH conditions. Plaques took 12 days to achieve full strength at pH 8, nearly doubling in adhesion strength (+94%) and increasing the work required to dislodge (+59%). Holding plaques in low pH conditions prevented strengthening, causing the material to tear more frequently under tension. The timescale of strengthening is consistent with the conversion of DOPA to DOPA-quinone, a pH dependent process that promotes cross-linking between adhesive proteins. The precise arrangement of DOPA containing proteins away from the adhesive-substrate interface emphasizes the role that structural organization can have on function, an insight that could lead to the design of synthetic adhesives and metal-coordinating hydrogels.

1.2. Introduction

The design of strong adhesives that persist on wet surfaces remains one of the most difficult challenges for the adhesives industry today. Water molecules provide a multitude of problems for adhesion, including competition for molecular interactions at the adhesive-substrate interface, erosion through hydrolysis, and deformation by means of water absorption (Comyn 1981; Stewart et al. 2011). These complications are then multiplied in seawater environments, where polar macromolecules, salts, and biological films compete for ionic interactions (Yu, Kan, et al. 2013). In light of these challenges, one increasingly popular approach is to borrow engineering concepts from biological systems that have evolved novel underwater attachment strategies (Kamino 2008; Hagenau et al. 2014). One such system is the marine mussel (*Mytilus spp.*), which routinely forms robust attachments in harsh ocean environments using proteinaceous fibers (byssal threads) tipped with an adhesive plaque (Waite 1983). Adhesive plaques are capable of binding to a wide variety of traditionally challenging materials (ie, glass, plastics, wood, and Teflon®), while the mussel remains fully submerged (Waite 1987).

Mussels adhere to surfaces underwater through the secretion, deposition, and complexation of polyphenolic proteins, known as mussel foot proteins (Mfps). Mfp-3 and -5 are found at the adhesive-substrate interface (Waite & Qin 2001; Zhao et al. 2006) and contain a high abundance of 3,4-dihydroxyphenly-L-alanine (DOPA) side chains, a post-translationally modified amino acid that forms hydrogen bonds with surfaces (Papov et al. 1995; Anderson et al. 2010; Danner et al. 2012). Interestingly, DOPA is also indispensable in forming crosslinks between like proteins within the plaque itself (Haemers et al. 2003; Wilker 2010a; Holten-Andersen et al. 2011), a task that requires the incorporation of oxygen. For DOPA to play these two contradictory roles, the sequencing, positioning, and chemical environment under which

mussel proteins are secreted, and form complexes, must be tightly controlled (Yu & Deming 1998).

Formation of an adhesive plaque begins when a mussel presses the distal depression, a small indentation at the tip of the animal's foot, against a surface. Glands along the depression then sequentially secrete different Mfps into the cavity, where they interact with each other and the surface (Tamarin & Keller 1972). In situ measurements from within the distal depression during plaque secretion suggest that Mfps are deposited under highly acidic (pH 2-4), ionically sparse (0.15 mol L^{-1}), and highly reduced redox conditions (Yu, Wei, Danner, Ashley, et al. 2011; Martinez Rodriguez et al. 2015; Miller et al. 2015; Nicklisch et al. 2016). In this environment, many DOPA-rich Mfp secretions exist as coacervates (Wei et al. 2014); fluid-fluid phase separations (similar to droplets of oil in water) that are metastable, forming micro-droplets that preferentially form hydrogen bonds with surfaces (Zhao et al. 2016). After Mfp secretion is complete, a mussel's foot is removed and seawater rushes in, causing a drastic shift in the pH (~8.1), ionic concentration (~0.7 M), and dissolved oxygen concentration (~8 mg L^{-1}) surrounding the plaque (Waite 2017). The result is a transition from a fluid to a porous solid over the course of minutes.

The molecular mechanics of DOPA-mediated adhesion has garnered the majority of the attention in this system, with several notable successes when it comes to incorporating DOPA into mussel-inspired hydrogels (Lee et al. 2002; Lee et al. 2006) with pH dependent properties (Barrett et al. 2013; Krogsgaard et al. 2013). Through the use of surface force analysis (SFA), Mfp-3 and -5, the two Mfps with the highest molecular DOPA concentrations, display high adhesion energies at a pH of 3.0 (Yu, Wei, Danner, Israelachvili, et al. 2011; Danner et al. 2012). This effect is lost at a pH around 7.5, as DOPA side chains are converted to DOPA-quinone, a

process that instead facilitates protein-protein crosslinking (Holten-Andersen et al. 2011; Yu, Wei, et al. 2013).

While an investigation of how DOPA adheres to surfaces has been fruitful, a focus solely on the molecular mechanics of Mfps ignores how they interact to form a composite material under tension. Adhesive plaques are made up of several Mfps with variable molecular concentrations of DOPA (2-30%), arranged into a structural core and iron fortified coating (Wilker 2010a; Wilker 2010b). Given the structural complexity of the plaque, it is perhaps not surprising that adhesion strength calculations based solely on the adhesion energy of Mfp-5, the Mfp with the most DOPA sidechains, underestimate plaque attachment strength by a factor of 10,000 (Desmond et al. 2015). One explanation for this discrepancy is that, while DOPA is important for adhesion at the adhesive-substrate interface, elements of the local seawater environment 'cure' the plaque, causing structural changes within the protein network that increase adhesion strength (Waite & Broomell 2012). To test this hypothesis, the adhesion strength and material stiffness of adhesive plaques were measured when aged under typical seawater conditions. The effect of seawater pH on the curing process was then examined to determine whether pH is an important factor governing adhesion strength after Mfps have already bound to a surface. Our results show that environmental post-processing is an important driver of the curing process of adhesive plaques, an exciting insight that could inform the design of new DOPA-modified medical adhesives for use in body cavities with specific pH regimes, or inspire the development of novel anti-fouling strategies for use in the maritime industry.

1.3. Materials and Methods

Mytilus trossulus (Gould 1850) were collected during the winter months of December-February, 2015-2016, from Penn Cove Shellfish, located off the coast of Whidbey Island, Washington, USA (48°13'N 122°42'W). Mussels were kept in 50 liter aquaria with recirculating, 0.2 µm filtered seawater (pH = 8.1, T = 10^{o}C, Sal = 31 PSU) for up to two weeks, and were fed Shellfish Diet 1800 (Reed Mariculture, Campbell, CA) up to 5% of wet tissue mass day^{-1} at an algal concentration of 2000 cells ml^{-1}. At the time of collection, shell length was measured using Vernier calipers to the nearest 0.1 cm. After use in experimental trials, mussels were sacrificed and their gonads were separated from their somatic tissue by pulling back the gills and cutting away the underlying tissue with a scalpel. The gonads and remaining somatic tissue were dried separately at 60^{o}C in aluminum weigh dishes until a constant dry weight was achieved (~3 days). Reproductive and physiological condition for all individuals was determined after experimental trials to control for tank and cohort level effects. Reproductive condition was determined using gonad index (GI), calculated as the dry gonad mass divided by the dry body (gonad plus somatic tissue) mass (Carrington 2002). Physiological condition was measured as condition index (CI), defined as dry body mass divided by shell length^{3} (Moeser et al. 2006). Body size and condition metrics for mussels, grouped by experiment and treatment, are reported in supplementary tables S1-S4.

1.3.1. Thread Production

In order to direct the site of plaque deposition, mussels were arranged on sheets of mica and fastened with a rubber band, orienting the mussel's foot towards the substrate. Mica was

chosen to limit the impact of surface roughness and for its characteristic atomic structure. Mussels were allowed to attach over four hours, then byssal threads were cut away from the animal at the proximal region's interface with the shell. Threads from individuals that made less than three attachments were not included in a treatment group. Mica sheets with plaque attachments were stored dry at room temperature (~21^{o}C, ~30-40% RH) for up to two weeks and then moved into treatment conditions.

1.3.2. Experimental Manipulations

Mica sheets with more than three threads attached were incubated in one of six seawater pH treatments (pH_{NBS} target = 1.0, 3.0, 5.0, 7.0, 8.0, 12.0) and allowed to age for either 0.17, 1, 3, 5, 8, 12, or 20 days. Constant pH treatment levels of pH 3.0-8.0 were achieved by bubbling 3 liter containers of filtered seawater with a dynamically controlled mixture of air and CO_2 gas (O'Donnell et al. 2013). Seawater pH was monitored in each container with a Durafet III pH electrode (Martz et al. 2010; Honeywell, Fort Washington, PA; accuracy ± 0.01), attached to a UDA2182 analyzer that controlled a solenoid valve in line with a CO_2 gas canister. Treatments were constantly bubbled with air to maintain a dissolved oxygen concentration above 8 mg L^{-1}, which was monitored with a Honeywell DirectLine DL5000 equilibrium probe (accuracy ± 0.1). Salinity was measured daily with a Honeywell DL4000 conductivity cell (accuracy ± 1 PSU). pH (NBS scale), dissolved oxygen (mg L^{-1}), and temperature (^{o}C) were logged every ten minutes. Endpoint pH treatments of pH 1.0 and 12.0 were accomplished through the addition of either 1N phosphoric acid or a mixture of 0.5M potassium hydroxide and 0.5M potassium carbonate. Additions were accomplished using the pH stat system described above with the addition of drip irrigators. These treatments were not intended to accurately mimic the carbonate chemistry

regime found in nearshore environments, but rather served to bookend the response curve generated through the manipulation of pCO_2.

pH electrodes were calibrated using NBS standards before use in each treatment. Bottle samples were collected at three time points throughout each 20-day treatment (1, 12, and 20 days) and poisoned with 0.02% saturated mercuric chloride ($HgCl_2$) to halt all biological activity. All samples that contained mercuric chloride were handled and disposed of in accordance with NIOSH guidelines. For each bottle, total alkalinity (T_A) was measured in µmol kg^{-1} using end-point titration (DL15 titrator, Mettler Toledo, Schwerzenbach, Switzerland; accuracy ± 50 µmol kg^{-1}) following SOP 3b from Dickson et al. (2007). Treatment averages for pCO_2 (µatm) and total dissolved inorganic carbon (T_C) were calculated using CO2Calc (Van Heuven et al. 2011) with the following constants: CO_2: Mehrbach et al. (1973); $KHSO_4$: Dickson (1990); and Boron: Uppström (1974). Means (± s.d.) for each treatment are listed in Table 1.1.

1.3.3. Mechanical Testing and Atomic Force Microscopy

Each individual adhesive plaque was pulled until failure according to the protocol outlined in Bell & Gosline (1996). Plaques were pulled at a 90^o angle relative to the substrate to ensure uniformity across samples. It should be noted that this testing angle may not be biologically relevant, given the variable positioning of a mussel's foot during deposition (Desmond et al. 2015). For each test, a hemostat was used to grip the distal region, 1 mm above the attachment plaque, and attached to a 10 N digital force gauge (OMEGA, Stamford, CT; accuracy ± 0.01 N) mounted on a motor-driven testing frame. Extension rate was 10 mm min^{-1} and force (N) was recorded at 20 Hz. All threads were rehydrated (>5 mins) in their respective seawater treatment prior to testing. Each plaque was imaged before tensile testing using an

AmScope MU1000 camera (Irvine, CA) attached to a dissection microscope. Plaque attachment area (planform area) in mm^2 was measured using AmScopeX imaging software by tracing the outline of each plaque. Adhesion strength (kPa) was recorded as the maximum force required to remove a plaque from the substrate, normalized by the attachment area (Burkett et al. 2009). Work of adhesion ($N\ m^{-1}$) was calculated as the area under the force-extension curve (Hamada et al. 2017). The mean of 3-5 plaque pulls was reported for each mussel. The failure mode of each plaque was scored visually as either an adhesive failure (plunger failure), a peeling failure (failure propagated from one side of the plaque to the other), or tearing failure (part of the plaque remained after failure) following the guidelines of Young & Crisp (1982).

Nanoscale surface characteristics of the cuticle of adhesive plaques were determined using a Bruker (Billerica, MA) Dimension ICON atomic force microscope (AFM). A ScanAsyst-Air probe with silicon-nitride tip was used to approach the surface of dry plaque samples, scanning 1 μm^2 regions of the cuticle's topography. Scans of the plaque surface were haphazardly taken 1 mm away from the distal root, avoiding large topographical features on the plaque's surface and parts of the distal region that innervated the plaque architecture. A region free of large topographical features was chosen from each 1 μm^2 scan for analysis, moving the tip to that section and recording a 10 nm^2 adhesion image (see Figure S1.1 for explanation). DMT modulus (GPa) was calculated within each scan as the slope of the force curve during tip-sample separation (Young et al. 2011), with a resolution of 512 samples per line and calibrated against a fused silica standard (Veeco, Plainview, NY). The over 260,000 measurements obtained from each 10 nm^2 scan were averaged to get a representative stiffness of the cuticle at that position. Three samples were taken per plaque, averaging the mean of three plaques from each mussel.

1.3.4. Air Exposure and Plaque Maturation

Previous work from our laboratory has shown that storing mature byssal threads in air does not significantly alter a thread's mechanical properties (Brazee & Carrington 2006). To confirm that storage in air did not affect the maturation process in this study, the adhesion strength (kPa) and appearance of freshly made plaques (F, 4 hours after deposition) were compared to plaques subjected to three storage treatments. In the first treatment, plaques were removed from seawater 4 hours after deposition, stored in air for two weeks, and rehydrated in seawater before testing (FD). Freshly made plaques in the second treatment were cut away from the animal, but remained submerged for 20 days in seawater without air exposure (S). The last treatment stored freshly made plaques in air for two weeks, after which they were returned to seawater and allowed to mature for 20 days (DS). Results are reported in Figure S1.2.

1.3.5. Statistical Analysis

All statistical analyses were performed in R (Version 3.4.1; http://www.r-project.org/) with the RStudio IDE (Version 1.0.153; http://www.rstudio.com/). When appropriate, data transformations to achieve linearity were performed using the Johnson Transformations package (Edgar Santos Fernandez 2014). Linear mixed-effects models were constructed and subsequent ANOVA analyses were performed using the nlme package (Pinheiro et al. 2017). Shell length (cm), plaque area (mm^2), GI, CI, and either adhesive age (days) or pH (NBS) were treated as fixed effects, while each mussel was incorporated as a random effect. When appropriate, interaction terms were added to test whether or not the combination of significant effects explained trends.

1.4. Results

1.4.1. Plaque Maturation Over Time

After deposition, adhesive plaques aged under standard seawater conditions (see Table 1.1) increased in adhesion strength and work of adhesion over time ($p < 0.001$, Figure 1.1., Table 1.2). Strengthening was accompanied by a change in plaque color, from milky white after deposition (4 hours) to dark tan after 20 days in seawater (Figure 1.1. c-f). Tukey HSD comparisons of time points indicate peak strength was achieved at 8-12 days after deposition, when plaques displayed adhesion strengths 94% greater than at the time of deposition and required 59% more work to dislodge from the substrate. Freshly made plaques that were stored dry for two weeks remained white in color (Figure S1.2c) and were not significantly stronger than those tested 4 hours after deposition ($p = 0.99$, Figure S1.2a). When rehydrated in seawater and allowed to mature to 20 days, plaques turned yellow (Figure S1.2d) and were significantly different than plaques collected directly after deposition ($p < 0.001$; Figure S1.2a). Plaques that were collected 4 hours after deposition, dried for two weeks, and returned to seawater for 20 days, displayed adhesion strengths similar to 20 day old plaques that were never exposed to air ($p = 0.84$; Figure S1.2a), turning yellow upon their return to seawater (Figure S1.2e).

Increases in adhesion strength were accompanied with characteristic shifts in how the adhesive plaque failed during tensile testing. The most common mode of failure after deposition was peeling (68%), shifting to loss of adhesion (plunger failure, 75%) as plaques reached 12 days old (Figure 1.3). Trends in adhesive strengthening and failure mode mirrored those seen in the DMT modulus obtained through AFM scans of the plaque cuticle ($p < 0.001$, Figure 1.4, Table 1.2). DMT modulus also peaked 12 days after deposition, increasing by 125% when

compared to plaques that were 4 hours old. Surface roughness did not change significantly (data not shown), and no differences in surface topography were evident over time (Figure 1.4c,d).

Shell length, gonad index, condition index, and plaque area were consistent for mussels across treatments and did not affect adhesion strength, work of adhesion, or material stiffness (Experiment 1, Table 1.2; Table S1.1-S1.2).

1.4.2. Plaque Maturation as a Function of Seawater pH

The seawater pH that adhesive plaques were held in for 12 days after deposition had a significant effect on their adhesion strength ($p<0.001$, Figure 1.2a, Table 1.2), work of adhesion ($p<0.001$, Figure 1.2b, Table 1.2), and DMT modulus ($p=0.004$, Figure 1.4b, Table 1.2). At a pH similar to conditions found within the distal depression (pH 1.0-3.0), attachment strength remained below 100 kPa, work of adhesion below 200 N m^{-1}, and DMT modulus below 0.5 GPa, mimicking results found during the natural aging process at 4 hours (Figure 1.1). Under these conditions, plaques became darker than those previously observed, becoming black at pH 1.0-3.0 (Figure 1.2c-d). Tearing failure was also more frequent at low pH (45% at pH 1.0; 4% at pH 8.0; Figure 1.3b).

A rise in pH above 5.0 was matched with a steep increase in adhesion strength (+138% at pH 8.0; Figure 1.2a), work of adhesion (+94% at pH 8.0; Figure 1.2a), and DMT modulus (+87% at pH 8.0; Figure 1.4b). Plaques also achieved their characteristic tan color (Figure 1.2e-h), and tearing failure drastically decreased in frequency (4% at pH 8), to be replaced by loss of adhesion as the dominant failure mode (75%, Figure 1.3b). As was seen with age, no significant differences were observed in surface roughness (data not shown) or topography as a function of

maturation pH (Figure 1.4e,f). Plaque strengthening plateaued at pH 8.0, after which increasing pH did not increase attachment strength, work of adhesion, or DMT modulus.

Gonad index, condition index, and plaque area were consistent for mussels across treatments and did not affect adhesion strength, work of adhesion, or material stiffness (Experiment 2, Table 1.2; Table S1.3-S1.4). Shell length did affect work of adhesion ($p = 0.04$), but an interaction between pH treatment and shell length was not significant ($p = 0.97$).

1.5. Discussion

This study showed that adhesive plaques undergo a curing process after deposition that increases adhesion strength over time, with peak performance observed after 8-12 days. Plaque curing is also sensitive to the local seawater environment, requiring the maintenance of a pH above 7.0 after deposition, and was arrested when removed from seawater. The time course of strengthening observed here is substantially longer than would be predicted from DOPA-mediated interactions with the surface alone, occurring over the course of days rather than minutes (Mian & Khan 2017). This result underscores that environmental post-processing was not only important for initial DOPA-substrate interactions, but may lead to important structural changes in the plaque away from the adhesive-substrate interface that drastically increase adhesion strength. Given that there is growing evidence that nearshore environments are subject to extreme fluctuations in seawater chemistry due to tidal and seasonal variability, the timescale of strengthening observed could be an important overlooked factor that determines the attachment strength of mussels in the intertidal zone, as well as those suspended on ropes in mariculture operations.

Observed increases in plaque adhesion strength and work of adhesion are consistent with increases in the cohesive strength of the plaque protein network over time. At a seawater pH of 8.0, covalent cross-linking occurs between Mfps containing DOPA rich side chains. Cross-linking involves the incorporation of oxygen from the surrounding environment, and is further mediated by the enzyme catechol oxidase, which also displays peak activity at a pH of 8.0 (Waite 1985; Haemers et al. 2002). Oxidation of DOPA leads to the formation of DOPA-quinone, which forms covalent cross-links with DOPA, Histidine, Cysteine, and Lysine (McDowell et al. 1999; Zhao & Waite 2006a; Miserez et al. 2010). The development of large quantities of DOPA-quinone in mussel adhesive was evidenced in this study by plaques that changed color as they aged, from a milky white to a dark-tan color over the course of 20 days, a process that has been referred to as quinone tanning (Brown 1950).

While not explicitly investigated in this study, the rate at which cross-linking occurs may be environmentally dependent. For example, Dolmer and Svane (1994) showed that when kept in a high flow regime (19.4 cm s^{-1}) over a 24-hour period, *Mytilus edulis* produced stronger attachments (whole animal) than when kept in still water (0 cm s^{1}). One possible interpretation of their findings is that water flow increases the flux of oxygen to the plaque, suggesting our still-water assays may have underestimated the timescale required for plaque maturation. Similarly, increases in plaque di-DOPA cross-link densities from flow-exposed mussels (*Mytilus edulis)* reinforce that the effect of flow is not merely due to mussels producing more threads in response to increases in hydrodynamic loading, but rather changes the composition of the plaque (McDowell et al. 1999). However, neither of these studies controlled for potential phenotypic responses of mussels to flow, such as altered gene expression or morphological changes in plaque size. The same can be said for pH; studies using whole animals from our laboratory

(O'Donnell et al. 2013) and others (Zhao et al. 2017) have shown that ocean acidification can decrease attachment strength in mussels and cause characteristic shifts in Mfp expression.

In this study, plaque area was consistent across treatment groups and all plaques were separated from animals before being exposed to seawater treatments. This experimental design allowed for the isolation of the effect of environmental post-processing on the material itself, eliminating any physiological effects that could alter the composition or quality of the byssal threads that were produced. This separation is an important distinction; the timescale over which the curing process takes places could potentially expose newly made plaques to a wide variety of seawater conditions in nearshore environments where pH and oxygen fluctuate due to tidal cycling, respiration and photosynthesis, and upwelling (Booth et al. 2012; Frieder et al. 2012). Nevertheless, interactions between mussel phenotype, the local seawater environment, and attachment strength remains one of the areas in greatest need of study in this system, with the exciting potential to inspire the synthesis of a wide array of materials with different mechanical properties (Carrington et al. 2015).

While DOPA has widely been studied for its adhesive properties, DOPA-quinone contributes significantly to overall adhesion strength by stabilizing the plaque's architecture as a porous solid. Molecular concentrations of DOPA are highest in Mfps located at the adhesive-substrate interface (Mfp-3F, 20%; Mfp-3S, 10%, Mfp-5, 30%), but are also evident in Mfps that never come in contact with the surface (Waite 2017). Mfp-2, the most abundant protein by weight, contains 5% DOPA and may act as the structural backbone of the plaque (Inoue et al. 1995). Similarly, Mfp-4 contains 2% DOPA, is histidine rich, and is located at the load bearing junction where the plaque connects to the distal region of the byssal thread (Zhao & Waite 2006b). The presence of DOPA in these proteins could point to the structural importance of

cross-linking throughout the plaque, consistent with the failure mode results seen here. Peeling failure was common in newly formed plaques, which were also white in color. DOPA-quinone mediated cross-liking, while in a relatively low concentration within the plaque core, could strengthen the protein network while retaining enough flexibility to dissipate energy across the structure, allowing the plaque to act as a single unit during failure. This shift would explain the high prevalence of adhesive failure that occurred after 8 days, as DOPA-quinone formation in the core develops due to the relative oxygen limitation within the plaque.

High molecular DOPA concentrations occur in plaque proteins that are not located at the adhesive-substrate interface, notably Mfp-1 (15% DOPA), which serves at the outer coating of the plaque. In this case, environmental post-processing may also play an important role in determining the overall mechanical properties of the plaque through DOPA-iron complexation. Iron coordination is pH sensitive, with the formation of increasingly stable mono-, bis-, or tris-(DOPA)Fe^{3+} complexes as pH goes from acidic to basic (Taylor et al. 1996; Xu 2013). In fact, the dark appearance of plaques at pHs below 3.0 may be due to the reduction of Fe^{3+} to Fe^{2+} by DOPA, leading to the precipitation of iron pyrites that are typically black in color (Fullenkamp et al. 2014), although not investigated in this study. Observed increases in DMT modulus at the plaque cuticle as a function of adhesive age and maturation pH could reflect this process, given that no physical changes in plaque surface architecture were observed. While the relative importance of the cuticle in the plaque's overall structural integrity is not known, the reduction in stiffness observed in low pH treatments could explain the increased frequency of tearing and peeling failure observed during tensile testing. With reduced stiffness, localized regions of high stress at the cuticle could cause cracks to form, leading to premature failure of the plaque before energy can be dissipated over the protein network.

Currently, mussel-inspired materials are synthesized through the addition of DOPA functional groups to polymer backbones. This approach has led to success in the design of polymer films that stick to inorganic and organic molecules (Waite 2008; Lee et al. 2011), hydrogels with pH-sensitive storage moduli (Krogsgaard et al. 2013), and coatings with variable surface chemistries (Lee et al. 2007). The results presented here show that, while DOPA-mediated interactions with surfaces have received a lot of attention in this system, the cohesive architecture of the protein network may be just as important. Mussel byssus plaques display complex arrangement of DOPA containing proteins which balance the roles of adhesion and cohesion to form a material that has adhesive properties, while drawing upon the surrounding seawater chemistry to enhance structural integrity. Understanding how DOPA is arranged in mussel adhesive, and what effect its arrangement has on the mechanical properties of the plaque as a whole, could prove invaluable when designing adhesives with specific curing times for use in wet environments and body cavities with specific pH regimes.

1.6. Acknowledgements

We thank Jessie Andino, Benjamin Pedigo, MacKenzie Edelsward, and Chloe Peterschmidt for assistance with tensometer testing, Micah Glaz for support with AFM analysis, and Ian Jefferds, Dominic Pangelinan, and all the mussel growers at Penn Cove Shellfish. We would also like to thank the three anonymous reviewers whose suggestions led to significant improvements of the manuscript.

1.7. Funding

This work was supported by an NSF GRFP fellowship (#DGE-1256082) and the Brooks and Suzanne Ragen FHL Endowed Scholarship to MNG, as well an NSF grant (#EF104113) to EC. Part of this work was conducted at the Molecular Analysis Facility, a National Nanotechnology Coordinated Infrastructure site at the University of Washington which is supported in part by the National Science Foundation (#ECC-1542101), the University of Washington, the Molecular Engineering & Sciences Institute, the Clean Energy Institute, and the National Institutes of Health. The efforts of EC were supported while serving at the National Science Foundation. Any opinion, findings, and conclusions or recommendations expressed in this material are those of the author(s) and do not necessarily reflect the views of the National Science Foundation.

1.8. Disclosure Statement

No potential conflict of interest was reported by the authors.

1.9. Dataset Availability

Datasets described in this publication are archived under project #2250 at www.bco-dmo.org.

1.10. References

Anderson TH, Yu J, Estrada A, Hammer MU, Waite JH, Israelachvili JN. 2010. The contribution of DOPA to substrate–peptide adhesion and internal cohesion of mussel-inspired synthetic peptide films. Adv Funct Mater. 20:4196–4205.

Barrett DG, Fullenkamp DE, He L, Holten-Andersen N, Lee KYC, Messersmith PB. 2013. pH-based regulation of hydrogel mechanical properties through mussel-inspired chemistry and processing. Adv Funct Mater. 23:1111–1119.

Bell E, Gosline J. 1996. Mechanical design of mussel byssus: material yield enhances attachment strength. J Exp Biol. 199:1005–1017.

Booth JAT, McPhee-Shaw EE, Chua P, Kingsley E, Denny M, Phillips R, Bograd SJ, Zeidberg LD, Gilly WF. 2012. Natural intrusions of hypoxic, low pH water into nearshore marine environments on the California coast. Cont Shelf Res. 45:108–115.

Brazee SL, Carrington E. 2006. Interspecific comparison of the mechanical properties of mussel byssus. Biol Bull. 211:263–274.

Brown CH. 1950. Quinone tanning in the animal kingdom. Nature. 165:275–275.

Burkett JR, Wojtas JL, Cloud JL, Wilker JJ. 2009. A method for measuring the adhesion strength of marine mussels. J Adhes. 85:601–615.

Carrington E. 2002. Seasonal variation in the attachment strength of blue mussels: causes and consequences. Limnol Oceanogr. 47:1723–1733.

Carrington E, Waite JH, Sarà G, Sebens KP. 2015. Mussels as a Model System for Integrative Ecomechanics. Annu Rev Mar Sci. 7:443–469.

Comyn J. 1981. The relationship between joint durability and water diffusion. In: Dev Adhes - Part 2. London: Applied Science Publishers; p. 279–313.

Danner EW, Kan Y, Hammer MU, Israelachvili JN, Waite JH. 2012. Adhesion of mussel foot protein Mefp-5 to mica: an underwater superglue. Biochemistry (Mosc). 51:6511–6518.

Desmond KW, Zacchia NA, Waite JH, Valentine MT. 2015. Dynamics of mussel plaque detachment. Soft Matter. 11:6832–6839.

Dickson AG. 1990. Thermodynamics of the dissociation of boric acid in synthetic seawater from 273.15 to 318.15 K. Deep Sea Res Part Oceanogr Res Pap. 37:755–766.

Dickson AG, Sabine CL, Christian JR. 2007. Guide to best practices for ocean CO2 measurements. In: PICES Spec Publ. Vol. 3. Sidney, British Columbia: North Pacific Marine Science Organization.

Dolmer P, Svane I. 1994. Attachment and orientation of Mytilus edulis L. in flowing water. Ophelia. 40:63–74.

Fernandez ES. 2014. Johnson: Johnson Transformation. R package version 1.4. [Internet]. Available from: https://CRAN.R-project.org/package=Johnson

Frieder CA, Nam SH, Martz TR, Levin LA. 2012. High temporal and spatial variability of dissolved oxygen and pH in a nearshore California kelp forest. Biogeosciences. 9:3917–3930.

Fullenkamp DE, Barrett DG, Miller DR, Kurutz JW, Messersmith PB. 2014. pH-dependent cross-linking of catechols through oxidation via Fe3+ and potential implications for mussel adhesion. RSC Adv. 4:25127–25134.

Haemers S, Koper GJ, Frens G. 2003. Effect of oxidation rate on cross-linking of mussel adhesive proteins. Biomacromolecules. 4:632–640.

Haemers S, van der Leeden MC, Koper GJ, Frens G. 2002. Cross-linking and multilayer adsorption of mussel adhesive proteins. Langmuir. 18:4903–4907.

Hagenau A, Suhre MH, Scheibel TR. 2014. Nature as a blueprint for polymer material concepts: Protein fiber-reinforced composites as holdfasts of mussels. Prog Polym Sci. 39:1564–1583.

Hamada NA, Roman VA, Howell SM, Wilker JJ. 2017. Examining potential active tempering of adhesive curing by marine mussels. Biomimetics. 2:16.

Holten-Andersen N, Harrington MJ, Birkedal H, Lee BP, Messersmith PB, Lee KYC, Waite JH. 2011. pH-induced metal-ligand cross-links inspired by mussel yield self-healing polymer networks with near-covalent elastic moduli. Proc Natl Acad Sci. 108:2651–2655.

Inoue K, Waite JH, Matsuoka M, Odo S, Harayama S. 1995. Interspecific variations in adhesive protein sequences of Mytilus edulis, M. galloprovincialis, and M. trossulus. Biol Bull. 189:370–375.

Kamino K. 2008. Underwater adhesive of marine organisms as the vital link between biological science and material science. Mar Biotechnol. 10:111–121.

Krogsgaard M, Behrens MA, Pedersen JS, Birkedal H. 2013. Self-healing mussel-inspired multi-pH-responsive hydrogels. Biomacromolecules. 14:297–301.

Lee BP, Dalsin JL, Messersmith PB. 2002. Synthesis and gelation of DOPA-modified poly (ethylene glycol) hydrogels. Biomacromolecules. 3:1038–1047.

Lee BP, Dalsin JL, Messersmith PB. 2006. Biomimetic adhesive polymers based on mussel adhesive proteins. In: Smith AM Callow JA Eds Biol Adhes. Berlin, Germany: Springer Berlin Heidelberg; p. 257–278.

Lee BP, Messersmith PB, Israelachvili JN, Waite JH. 2011. Mussel-inspired adhesives and coatings. Annu Rev Mater Res. 41:99.

Lee H, Lee BP, Messersmith PB. 2007. A reversible wet/dry adhesive inspired by mussels and geckos. Nature. 448:338–341.

Martinez Rodriguez NR, Das S, Kaufman Y, Israelachvili JN, Waite JH. 2015. Interfacial pH during mussel adhesive plaque formation. Biofouling. 31:221–227.

Martz TR, Connery JG, Johnson KS. 2010. Testing the Honeywell Durafet® for seawater pH applications. Limnol Oceanogr Methods. 8:172–184.

McDowell LM, Burzio LA, Waite JH, Schaefer J. 1999. Rotational echo double resonance detection of cross-links formed in mussel byssus under high-flow stress. J Biol Chem. 274:20293–20295.

Mehrbach C, Culberson C, Hawley J, Pytkowicz R. 1973. Measurement of the apparent dissociation constants of carbonic acid in seawater at atmospheric pressure. Limnol Oceanogr. 18:897–907.

Mian SA, Khan Y. 2017. The adhesion mechanism of marine mussel foot protein: adsorption of L-Dopa on (alpha)- and (beta)-cristobalite silica using density functional theory. J Chem. 2017.

Miller DR, Spahn JE, Waite JH. 2015. The staying power of adhesion-associated antioxidant activity in Mytilus californianus. J R Soc Interface. 12:20150614.

Miserez A, Rubin D, Waite JH. 2010. Cross-linking chemistry of squid beak. J Biol Chem. 285:38115–38124.

Moeser GM, Leba H, Carrington E. 2006. Seasonal influence of wave action on thread production in Mytilus edulis. J Exp Biol. 209:881–890.

Nicklisch SC, Spahn JE, Zhou H, Gruian CM, Waite JH. 2016. Redox capacity of an extracellular matrix protein associated with adhesion in Mytilus californianus. Biochemistry (Mosc). 55:2022.

O'Donnell MJ, George MN, Carrington E. 2013. Mussel byssus attachment weakened by ocean acidification. Nat Clim Change. 3:587–590.

Papov VV, Diamond TV, Biemann K, Waite JH. 1995. Hydroxyarginine-containing polyphenolic proteins in the adhesive plaques of the marine mussel Mytilus edulis. J Biol Chem. 270:20183–20192.

Pinheiro J, Bates D, DebRoy S, Sarkar D, R Core Team. 2017. nlme: Linear and Nonlinear Mixed Effects Models. R package version 3.1-131. [Internet]. Available from: https://CRAN.R-project.org/package=nlme

Stewart RJ, Ransom TC, Hlady V. 2011. Natural underwater adhesives. J Polym Sci Part B Polym Phys. 49:757–771.

Tamarin A, Keller P. 1972. An ultrastructutal study of the byssal thread forming system in Mytilus. J Ultrastruct Res. 40:401–416.

Taylor SW, Chase DB, Emptage MH, Nelson MJ, Waite JH. 1996. Ferric ion complexes of a DOPA-containing adhesive protein from Mytilus edulis. Inorg Chem. 35:7572–7577.

Uppström LR. 1974. The boron/chlorinity ratio of deep-sea water from the Pacific Ocean. In: Deep Sea Res Oceanogr Abstr. Vol. 21. [place unknown]: Elsevier; p. 161–162.

Van Heuven S, Pierrot D, Lewis E, Wallace D. 2011. MATLAB program developed for CO2 system calculations. . ORNL/CDIAC-105b. Carbon Dioxide Inf Anal Cent Oak Ridge Natl Lab US Dep Energy Oak Ridge Tenn.

Waite H. 1983. Adhesion in byssally attached bivalves. Biol Rev. 58:209–231.

Waite JH. 1985. Catechol oxidase in the byssus of the common mussel, Mytilus edulis L. J Mar Biol Assoc U K. 65:359–371.

Waite JH. 1987. Nature's underwater adhesive specialist. Int J Adhes Adhes. 7:9–14.

Waite JH. 2008. Surface chemistry: mussel power. Nat Mater. 7:8–9.

Waite JH. 2017. Mussel adhesion–essential footwork. J Exp Biol. 220:517–530.

Waite JH, Broomell CC. 2012. Changing environments and structure–property relationships in marine biomaterials. J Exp Biol. 215:873–883.

Waite JH, Qin X. 2001. Polyphosphoprotein from the adhesive pads of Mytilus edulis. Biochemistry (Mosc). 40:2887–2893.

Wei W, Tan Y, Rodriguez NRM, Yu J, Israelachvili JN, Waite JH. 2014. A mussel-derived one component adhesive coacervate. Acta Biomater. 10:1663–1670.

Wilker JJ. 2010a. The iron-fortified adhesive system of marine mussels. Angew Chem Int Ed. 49:8076–8078.

Wilker JJ. 2010b. Marine bioinorganic materials: mussels pumping iron. Curr Opin Chem Biol. 14:276–283.

Xu Z. 2013. Mechanics of metal-catecholate complexes: The roles of coordination state and metal types. Sci Rep. 3:2914.

Young GA, Crisp D. 1982. Marine animals and adhesion. In: KW Allend Ed Adhes. Vol. 6. England: Barking, Applied Science Publishers, Ltd.; p. 19–39.

Young TJ, Monclus MA, Burnett TL, Broughton WR, Ogin SL, Smith PA. 2011. The use of the PeakForceTM quantitative nanomechanical mapping AFM-based method for high-resolution Young's modulus measurement of polymers. Meas Sci Technol. 22:125703.

Yu J, Kan Y, Rapp M, Danner E, Wei W, Das S, Miller DR, Chen Y, Waite JH, Israelachvili JN. 2013. Adaptive hydrophobic and hydrophilic interactions of mussel foot proteins with organic thin films. Proc Natl Acad Sci. 110:15680–15685.

Yu J, Wei W, Danner E, Ashley RK, Israelachvili JN, Waite JH. 2011. Mussel protein adhesion depends on interprotein thiol-mediated redox modulation. Nat Chem Biol. 7:588–590.

Yu J, Wei W, Danner E, Israelachvili JN, Waite JH. 2011. Effects of interfacial redox in mussel adhesive protein films on mica. Adv Mater. 23:2362–2366.

Yu J, Wei W, Menyo MS, Masic A, Waite JH, Israelachvili JN. 2013. Adhesion of mussel foot protein-3 to TiO2 surfaces: the effect of pH. Biomacromolecules. 14:1072–1077.

Yu M, Deming T. 1998. Synthetic polypeptide mimics of marine adhesives. Macromolecules. 31:4739–4745.

Zhao H, Robertson NB, Jewhurst SA, Waite JH. 2006. Probing the adhesive footprints of Mytilus californianus byssus. J Biol Chem. 281:11090–11096.

Zhao H, Waite JH. 2006a. Linking adhesive and structural proteins in the attachment plaque of Mytilus californianus. J Biol Chem. 281:26150–26158.

Zhao H, Waite JH. 2006b. Proteins in load-bearing junctions: the histidine-rich metal-binding protein of mussel byssus. Biochemistry (Mosc). 45:14223–14231.

Zhao Q, Lee DW, Ahn BK, Seo S, Kaufman Y, Israelachvili JN, Waite JH. 2016. Underwater contact adhesion and microarchitecture in polyelectrolyte complexes actuated by solvent exchange. Nat Mater. 15:407–412.

Zhao X, Guo C, Han Y, Che Z, Wang Y, Wang X, Chai X, Wu H, Liu G. 2017. Ocean acidification decreases mussel byssal attachment strength and induces molecular byssal responses. Mar Ecol Prog Ser. 565:67–77.

1.11. Tables

Table 1.1. Seawater conditions (± s.d.) in each pH treatment during 20-day exposures. Seawater was 0.2µm filtered, UV sterilized, and kept in the dark to prevent bacterial and algal growth. pH (NBS), temperature (°C), salinity (PSU), and dissolved oxygen (DO; mg L^{-1}) where measured at 10 minute intervals. Total alkalinity (T_A) was measured through acid titration of poisoned bottle samples taken at 1, 12, and 20 days. pCO_2 and total dissolved inorganic carbon (T_C) were calculated from pH, salinity, temperature, and total alkalinity. The bold treatment was considered 'standard seawater conditions' because it most closely represented open ocean conditions.

		Measured				Calculated	
pH Target	Durafet pH (NBS)	T (°C)	Sal (PSU)	DO (mg L^{-1})	T_A (µmol kg^{-1})	pCO_2 (µatm)	T_c (µmol kg^{-1})
1	1.21 ± 0.24	10.1 ± 1.2	29 ± 1	9.2 ± 0.5	2065 ± 55		
3	3.09 ± 0.15	9.8 ± 1.4	28 ± 2	9.3 ± 0.3	2078 ± 40	8.6E7 ± 7.3E6	3.9E6 ± 3.1E5
5	5.04 ± 0.04	10.0 ± 0.8	29 ± 1	8.6 ± 0.5	2092 ± 18	5.9E5 ± 2.6E4	2.9E4 ± 1.3E3
7	7.01 ± 0.02	9.5 ± 0.7	29 ± 2	8.8 ± 0.4	2079 ± 31	6119 ± 283	2346 ± 49
8	**8.02 ± 0.03**	**9.6 ± 1.1**	**28 ± 1**	**9.4 ± 0.7**	**2089 ± 22**	**569 ± 11**	**2004 ± 20**
12	11.98 ± 0.15	10.3 ± 0.5	28 ± 1	9.5 ± 0.5	2087 ± 34		

Table 1.2. ANOVA summary of linear mixed-effects models exploring the effect of multiple factors (shell length, gonad index (GI), condition index (CI), and plaque planform area) on adhesive plaque performance (adhesion strength, work of adhesion, and material stiffness) for two experiments. In the first experiment, adhesive plaques were aged under standard seawater conditions (see Table 1.1) and sampled through time. In the second experiment, plaques were aged to maturity (12 days) in various pH treatments (pH = 1-12). Factors were treated as fixed with the mussel included as a random factor and the degrees of freedom for the denominator are reported. P-values less than 0.05 are marked with an asterisk.

	Adhesion Strength (kPa)			Work of Adhesion ($N\ m^{-1}$)			Material Stiffness (MPa)		
Source	d.f.	F	P-value	d.f.	F	P-value	d.f.	F	P-value
Experiment 1:									
Adhesive Age	188	80.86	<0.001*	187	42.86	<0.001*	57	30.10	<0.001*
Shell length	188	0.01	0.94	187	0.12	0.73	57	0.14	0.71
GI	188	0.10	0.75	187	0.21	0.65	57	0.36	0.55
CI	188	1.64	0.20	187	2.34	0.13	57	0.01	0.91
Plaque area				187	0.04	0.85	57	0.51	0.48
Experiment 2:									
pH	149	20.63	<0.001*	147	14.17	<0.001*	42	9.15	0.004*
Shell length	149	0.37	0.54	147	4.40	0.04*	42	0.62	0.44
GI	149	0.63	0.43	147	0.13	0.72	42	3.50	0.07
CI	149	0.12	0.73	147	2.18	0.14	42	0.03	0.87
Plaque area				147	1.11	0.29	42	2.85	0.10
pH x Shell				147	0.001	0.97			

1.12. Figures

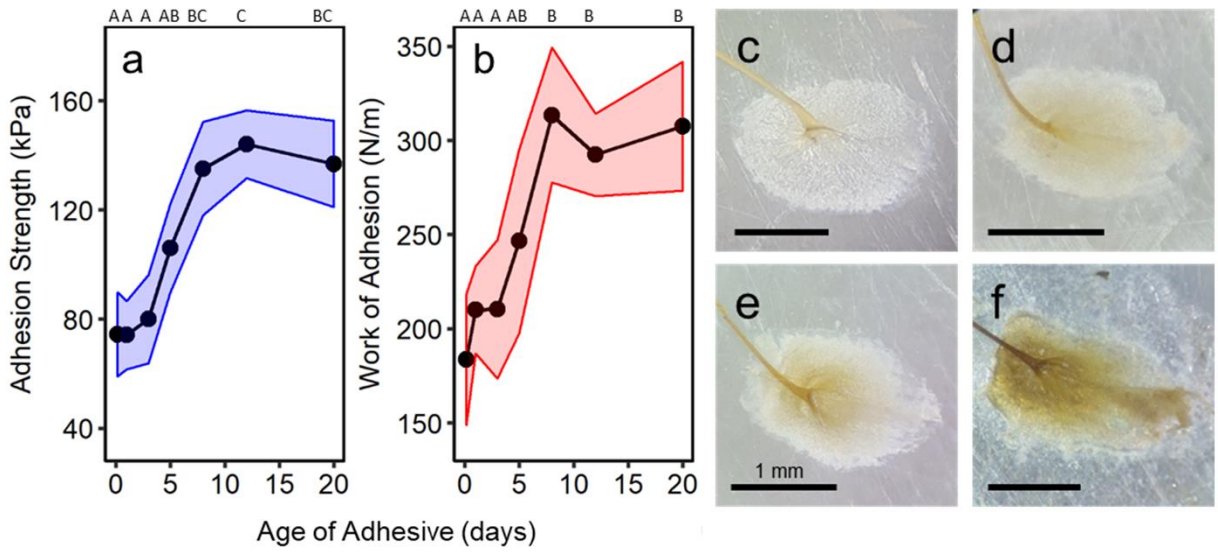

Figure 1.1. Strengthening characteristics of adhesive plaques after deposition on a surface (pH = 8.02 ± 0.03, T = 9.6 ± 1.1°C, Sal = 28 ± 1 PSU). The force required to remove plaques from a substrate normalized to the attachment area (a; adhesion strength, kPa) and the area under the force-extension curve (b; work of adhesion, n m-1) increased as plaques aged ($F_{1,188}$= 80.86, $p < 0.001$; $F_{1,187}$ = 42.86, $p < 0.001$). Yellowing of plaques, consistent with quinone tanning, was also observed as plaques remained in seawater for longer periods of time (c-f; 1, 5, 12, and 20 days old respectively). Error bars represent 95% confidence intervals. Letters represent the result of Tukey HSD comparisons between groups.

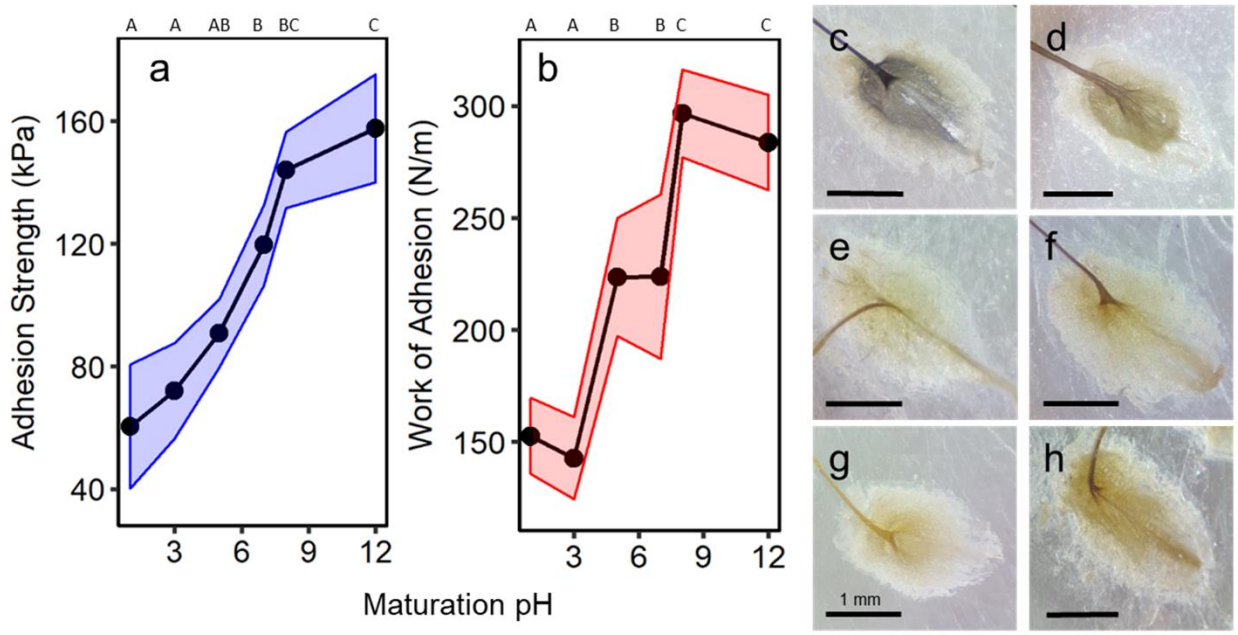

Figure 1.2. Strengthening characteristics of adhesive plaques aged to maturity (12 days) under different seawater pH conditions (pH = 1-12). The force required to remove plaques from a substrate normalized to the attachment area (a; adhesion strength) and the area under the force-extension curve (b; work of adhesion) increased with seawater pH ($F_{1,149} = 20.63$, $p < 0.001$; $F_{1,147} = 14.17$, $p<0.001$). Yellowing of plaques, consistent with quinone tanning, was observed in pH conditions above 5 (c-h; pH 1, 3, 5, 7, 8, and 12, respectively). Error bars represent 95% confidence intervals. Letters represent the result of Tukey HSD comparisons between groups.

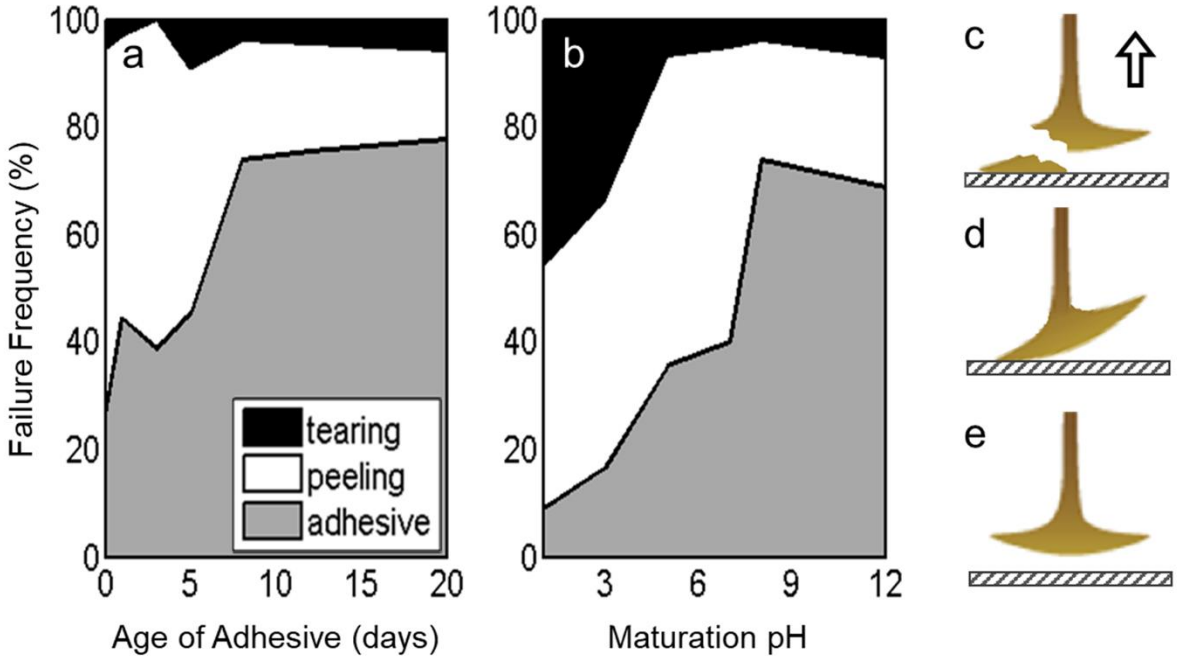

Figure 1.3. Frequency of each failure mode as adhesive plaques aged to maturity at standard seawater conditions (a, pH = 8.02 ± 0.03, T = 9.6 ± 1.1°C, Sal = 28 ± 1 PSU), and of mature adhesive plaques aged 12 days in different pH conditions (b, pH = 1-12). Tearing (a) occurred when the distal region of the thread dislodged from the adhesive or part of the adhesive remained attached to the substrate. Peeling failure (d) occurred when a plaque failed asymmetrically, while adhesive failure (e) was defined as the entire adhesive plaque failing as one unit.

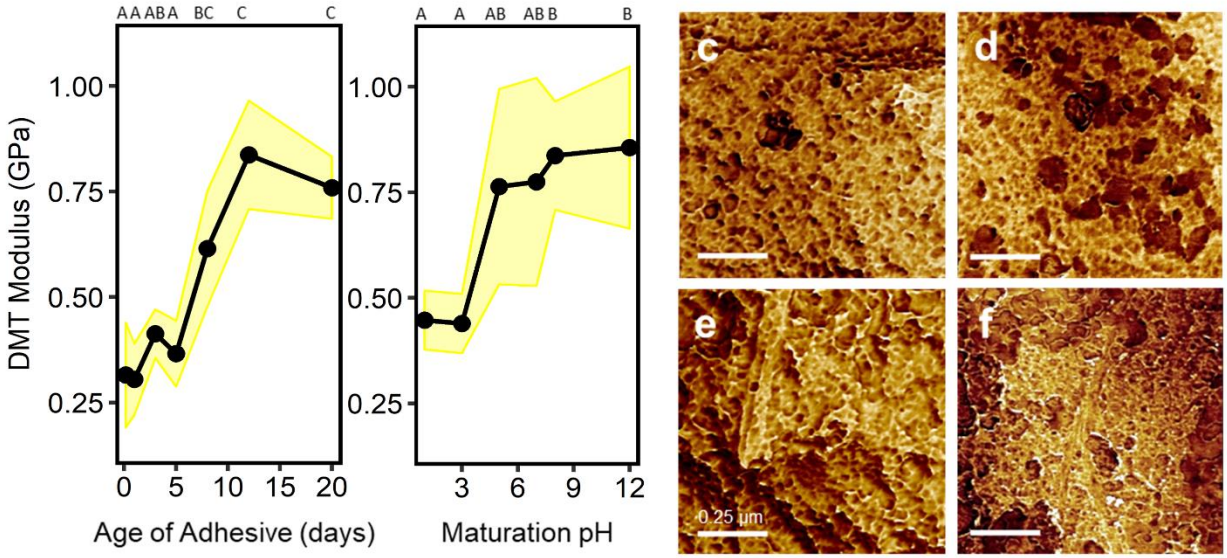

Figure 1.4. Material stiffness of the cuticle of adhesive plaques, measured as the mean DMT modulus of 10 nm^2 atomic force microscopy scans (AFM). Plaque stiffening occurred as the adhesive aged in standard seawater conditions (a, pH = 8.1 ± 0.2, T = 9 ± 2°C, Sal = 28 ± 1 PSU; $F_{1,57} = 30.10$; $p < 0.001$) and was prevented by increasing seawater acidity (b, pH = 1-12, T = 9 ± 2°C, Sal = 28 ± 1 PSU; $F_{1,42} = 9.15$, $p = 0.004$). Adhesion images of the cuticle outline the porous nature of the material during maturation at pH 8 (c, 4 hours; d, 12 days) and when held in acidic (e, pH 1) and basic (f, pH 12) environments during solidification for 12 days. Error bars represent 95% confidence intervals. Letters represent the result of Tukey HSD comparisons between groups.

1.13. Supplemental Material

Table S1.1. Body size and condition metrics for mussels that produced adhesive plaques included in tensometer measurements in experiment 1, investigating the effect of adhesive age on adhesion strength (kPa) and the work of adhesion (N m^{-1}). Values are means ± 1 s.d. Statistics are the result of linear regressions of metrics across treatment groups.

Age (days)	n	Shell Length (cm)	Plaque Area (mm^2)	Gonad Index	Condition Index ($x10^{-3}$ g cm^{-3})
0.17	38	4.9 ± 0.5	2.19 ± 0.72	0.11 ± 0.02	4.0 ± 0.6
1	36	4.8 ± 0.6	2.06 ± 0.76	0.12 ± 0.03	3.8 ± 0.6
3	18	4.9 ± 0.6	2.22 ± 0.73	0.11 ± 0.02	3.7 ± 0.5
5	11	5.0 ± 0.5	2.18 ± 0.36	0.11 ± 0.01	4.3 ± 0.7
8	27	5.0 ± 0.5	2.26 ± 0.80	0.11 ± 0.02	3.9 ± 0.5
12	45	5.4 ± 0.5	2.24 ± 0.46	0.11 ± 0.02	4.0 ± 0.5
20	18	4.8 ± 0.5	2.20 ± 0.48	0.12 ± 0.04	3.8 ± 0.6
	R^2	0.03	0.003	0.005	0.005
	p value	0.16	0.45	0.35	0.35

Table S1.2. Body size and condition metrics for mussels that produced adhesive plaques included in AFM measurements in experiment 1, investigating the effect of adhesive age on material stiffness (MPa). Values are means ± 1 s.d. Statistics are the result of linear regressions of metrics across treatment groups.

Age (days)	n	Shell Length (cm)	Plaque Area (mm^2)	Gonad Index	Condition Index ($x10^{-3}$ g cm^{-3})
0.17	9	4.4 ± 0.5	1.63 ± 0.26	0.12 ± 0.02	3.9 ± 0.4
1	8	4.8 ± 0.6	2.31 ± 0.70	0.12 ± 0.04	3.7 ± 0.6
3	8	5.1 ± 0.5	2.59 ± 0.79	0.11 ± 0.02	3.5 ± 0.5
5	7	5.0 ± 0.5	2.29 ± 0.39	0.11 ± 0.03	4.5 ± 0.7
8	11	4.9 ± 0.7	2.25 ± 0.73	0.11 ± 0.02	3.8 ± 0.5
12	10	5.5 ± 0.3	2.60 ± 0.54	0.11 ± 0.03	3.9 ± 0.5
20	10	4.8 ± 0.5	2.27 ± 0.58	0.11 ± 0.02	3.9 ± 0.6
	R^2	0.02	0.03	0.008	0.005
	p value	0.24	0.21	0.49	0.59

Table S1.3. Body size and condition metrics for mussels that produced adhesive plaques included in tensometer measurements in experiment 2, investigating the effect of seawater pH on adhesion strength (kPa) and the work of adhesion (N m^{-1}). Values are means ± 1 s.d. Statistics are the result of linear regressions of metrics across treatment groups.

pH	n	Shell Length (cm)	Plaque Area (mm^2)	Gonad Index	Condition Index ($x10^{-3}$ g cm^{-3})
1	11	4.9 ± 0.4	2.64 ± 0.40	0.11 ± 0.02	3.8 ± 0.8
3	18	4.4 ± 0.7	2.12 ± 0.71	0.12 ± 0.04	3.9 ± 0.7
5	31	5.0 ± 0.6	2.18 ± 0.40	0.11 ± 0.02	4.0 ± 0.7
7	20	4.6 ± 0.7	2.11 ± 0.54	0.12 ± 0.03	4.2 ± 0.8
8	45	5.4 ± 0.5	2.24 ± 0.46	0.11 ± 0.02	4.0 ± 0.5
12	29	4.8 ± 0.8	2.11 ± 0.59	0.11 ± 0.02	4.1 ± 0.7
	R^2	0.01	0.02	0.002	0.007
	p value	0.17	0.11	0.55	0.30

Table S1.4. Body size and condition metrics for mussels that produced adhesive plaques included in AFM measurements in experiment 2, investigating the effect of seawater pH on material stiffness (MPa). Values are means ± 1 s.d. Statistics are the result of linear regressions of metrics across treatment groups.

pH	n	Shell Length (cm)	Plaque Area (mm^2)	Gonad Index	Condition Index ($x10^{-3}$ g cm^{-3})
1	8	5.0 ± 0.5	2.48 ± 0.48	0.13 ± 0.02	4.0 ± 0.5
3	7	4.5 ± 0.4	2.36 ± 0.87	0.11 ± 0.03	4.4 ± 1.1
5	7	4.5 ± 0.5	2.05 ± 0.79	0.13 ± 0.01	4.2 ± 0.6
7	7	4.6 ± 0.6	1.98 ± 0.69	0.13 ± 0.02	3.7 ± 0.6
8	10	4.8 ± 0.2	2.16 ± 0.48	0.11 ± 0.02	3.9 ± 0.9
12	9	4.9 ± 0.4	1.99 ± 0.47	0.11 ± 0.01	3.8 ± 0.5
	R^2	0.006	0.06	0.04	0.04
	p value	0.58	0.09	0.17	0.28

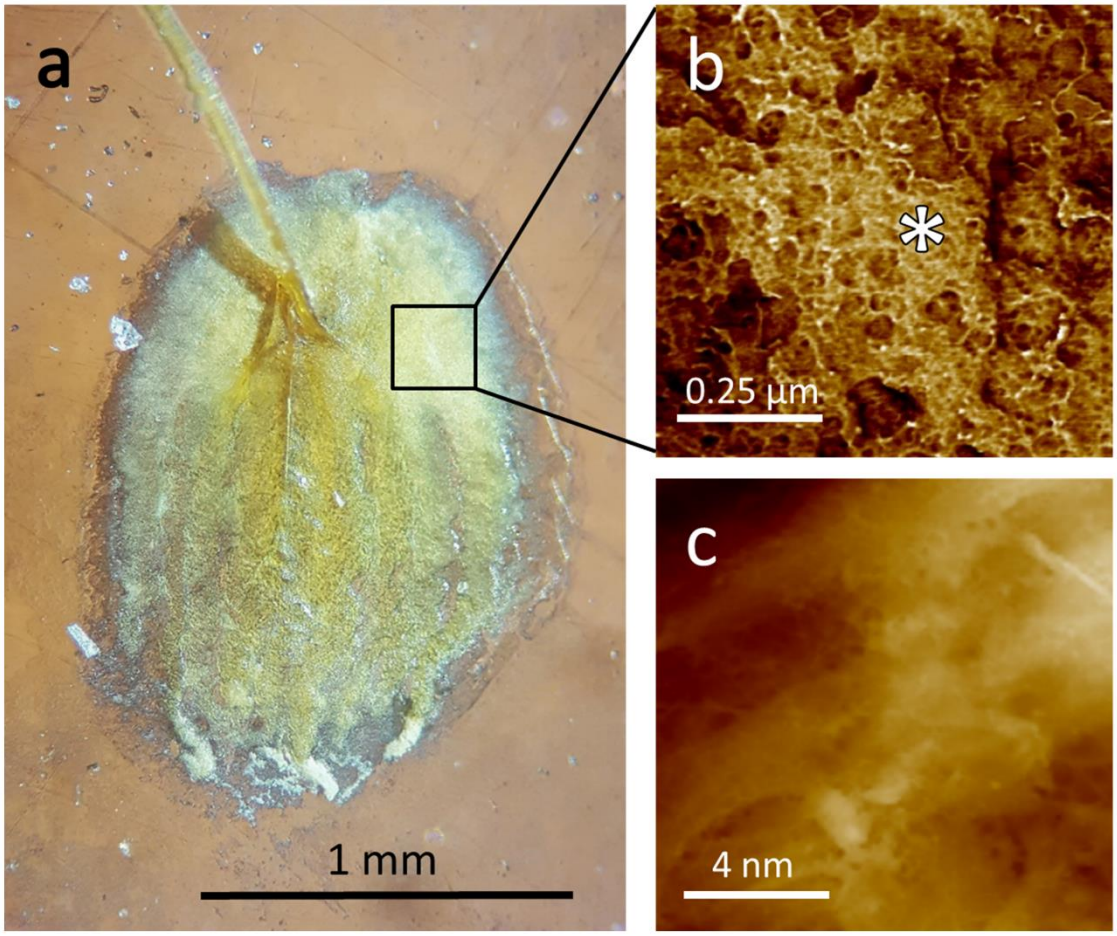

Figure S1.1. Location of atomic force microscopy (AFM) measurements on the cuticle of each plaque. Efforts were taken to avoid the innervating roots of the thread, opting for smooth patches away from the thread-plaque junction (black box in panel a). Adhesion images provided in Figure 1.4 are 1 μm^2 scans of the plaque cuticle in order to display the local topography (b). 10 nm^2 scans (taken at the starred location in panel b) produced DMT modulus maps with a resolution of 512 x 512 (c), that were then averaged to get a representative stiffness of the cuticle.

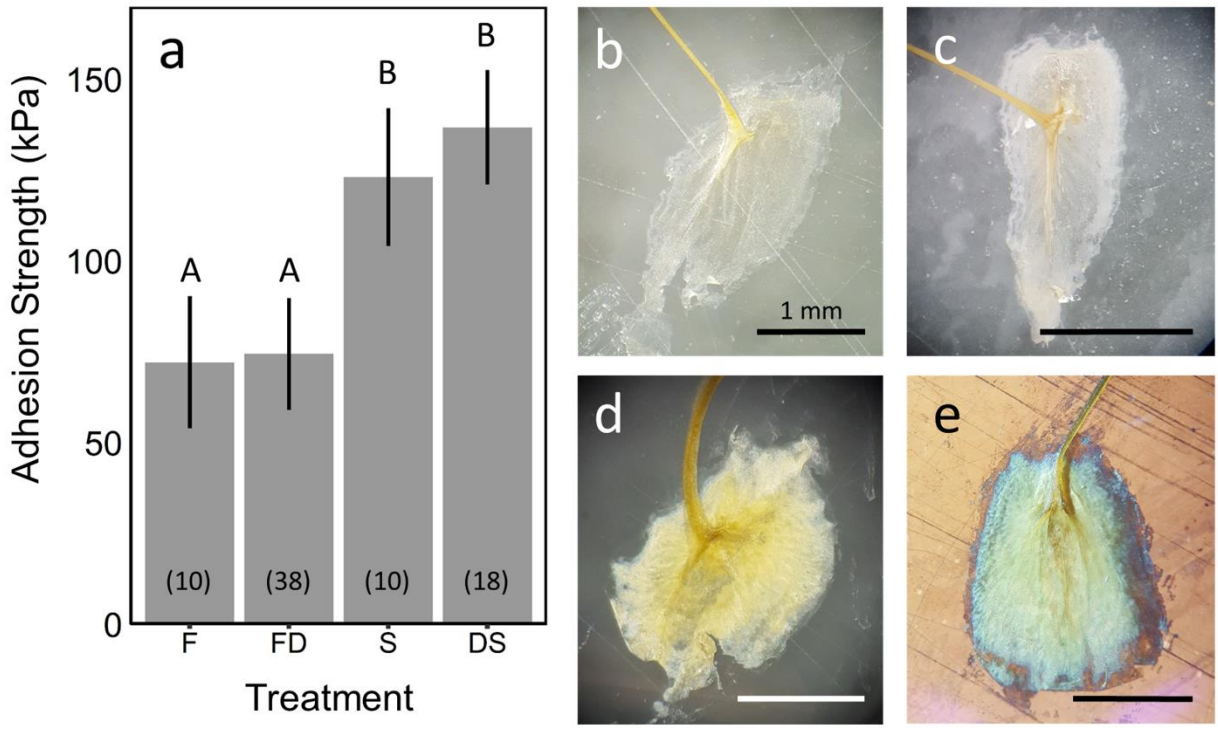

Figure S1.2. The effect of dry storage on plaque maturation and adhesion strength (kPa). Mussels were allowed to attach to mica plates over the course of 4 hours, then adhesive plaques were collected. A portion of the freshly secreted plaques were tested immediately (panel a, F; b), while others were allowed to mature in seawater (T = 8.02 ± 0.03, T = 9.6 ± 1.1°C, Sal = 28 ± 1 PSU) for 20 days (a, S; d). A second subset of freshly made plaques were stored in air (T = ~21°C; RH = 30-40%) for approximately two weeks, and either rehydrated and tested (a, FD; c), or returned to seawater and aged for 20 days (a, DS; e). Plaques stored in seawater for 20 days were significantly stronger than those that were 4 hours old ($p<0.001$) and stored in air for two weeks ($p<0.001$), and were markedly more yellow in color (d). Plaques that were stored in air for two weeks and then matured in seawater for 20 days were not significantly different in strength from those that were never exposed to air ($p=0.84$) and were similar in color (e). Error bars represent 95% confidence intervals. Letters represent the result of Tukey HSD comparisons between treatments. Numbers within each bar are the sample size for each treatment.

Chapter 2

Hypoxia weakens mussel attachment by interrupting DOPA cross-linking during adhesive plaque curing

Matthew N. George[1,2], Benjamin Pedigo[1], and Emily Carrington[1,2]

1 – University of Washington, Department of Biology, BOX 358100, Seattle, WA 98195

2 – Friday Harbor Laboratories, 620 University Rd., Friday Harbor, WA 98250

Keywords: Underwater adhesion; mussel foot protein (Mfp); *Mytilus trossulus*; amino acid analysis

2.1. Abstract

Marine mussels (*Mytilus spp.*) attach to a wide variety of surfaces underwater using a network of byssal threads, each tipped with a protein-based adhesive plaque that uses the surrounding seawater environment as a curing agent. Plaques undergo extensive environmental post-processing, requiring a basic seawater pH be maintained for up to 8 days in order for the adhesive to strengthen completely. Given the sensitivity of plaques to local pH conditions long after deposition, we investigated the effect of over aspects of the seawater environment that are known to vary in nearshore habitats on plaque curing. The effect of seawater temperature, salinity, and dissolved oxygen concentration were investigated using tensile testing, atomic force microscopy, and amino acid compositional analysis. High temperature (30^{o}C) and low salinity (1 PSU) had no effect on adhesion strength, while incubation in hypoxia (0.9 mg L^{-1}) left plaques with a mottled coloration, prematurely peeled from substrates before the thread could be loaded, and led to a 51% decrease in adhesion strength. AFM imaging of the plaque cuticle found that plaques cured in hypoxia had regions of lower stiffness throughout, indicative of reductions in DOPA crosslinking between adhesive proteins. A better understanding of the mechanisms underlying oxygen's role in plaque curing could aid in the design of better medical adhesives for use in body cavities, as well as help mussel growers predict the frequency of mussel fall-off.

2.2. Introduction

Marine mussels (*Mytilus spp.*) have mastered the art of underwater adhesion, producing a holdfast comprised of proteinaceous fibers known as byssal threads. Attaching to rocks in the intertidal zone, byssal threads are capable of adhering to a wide variety of substrates with different surface chemistries, hydrophobicities, and physical properties [1–3], all while contending with the presence of water, salts, and organic films [3]. The mechanisms underlying byssal thread adhesion have therefore inspired the synthesis of several anti-fouling coatings for use in the maritime industry, novel polymers with applications in wet environments, and bio-compatible medical adhesives for the repair of sensitive tissues within the human body [4–8].

Each byssal thread is part of a network, extending outwards radially from within the shell, and making contact with a surface at an adhesive plaque [9]. The plaque is made up of adhesive proteins (Mfps) that contain 3,4-dihydroxyphenly-L-alanine (DOPA) residues, relatively rare post-translationally modified amino acids with adhesion properties [10,11]. Plaques are produced when a mussel extends its foot from the shell, pressing a small depression at the distal end (distal depression) against a surface [12,13]. Once contact is made, the chemical environment within the distal depression is adjusted, producing an acidic micro-environment (pH 1-3) [14] that is also heavily reduced and nearly free of ionic molecules [15–17]. After these conditions are established, Mfps are secreted into the cavity as complex coacervates, electrostatically neutral mixtures of polyelectrolytes that form fluid-fluid phase separations [18,19]. Under these conditions, DOPA residues preferentially form interfacial interactions with surfaces (hydrogen bonding, coordination, etc.), rather than interacting with one another [20,21].

Byssal thread formation takes approximately five minutes, after which the foot is removed and the newly formed plaque is exposed to seawater. The chemistry of typical open-

ocean seawater, with a pH of 8.1, oxygen saturation of ~100%, and ionic concentration of 0.7M, is drastically different than the microenvironment that a mussel creates during Mfp secretion. Contact with seawater causes the coacervate to collapse and form a bulk solid, oxidizing DOPA residues to form DOPA-quinone through a process called quinone tanning [22]. This switch in environment turns out to be an essential part of the adhesive formation process, as DOPA-quinone preferentially forms covalent crosslinks between like proteins at a basic pH [2,23] while also establishing increasingly stable (DOPA)Fe^{3+} complexes within the cuticle of the plaque [24,25].

While the properties of seawater act as a molecular trigger to initiate a phase change during plaque solidification, the local seawater environment continues to be important well after the plaque is deposited. In seawater, plaque adhesion strength doubles over a 8-12 days, changing from a milky white to dark tan color [26]. but this maturation process is arrested when plaques are held at a pH below 5.0. Together, these findings show that environmental post-processing is essential for the adhesive to form correctly and that plaque strengthening requires access to favorable conditions for significantly longer than would be predicted from the cross-linking rates of individual Mfps [27].

With such a long cure window, it is possible that plaques are sensitive plaques to other aspects of the seawater environment that typically vary in nearshore environments. In addition to fluctuations in pH, mussels regularly experience a broad range of seawater temperatures, salinities, and dissolved oxygen concentrations, with daily or seasonal variability exceeding even the most extreme values seen in the open-ocean [28–31]. Such extremes in these parameters have the potential to impact plaque curing positively or negatively. For example, high temperatures could accelerate the kinetics of DOPA-quinone cross-linking, speed up the curing process [32],

and/or break hydrogen bonds and cause protein unfolding and plaque weakening. Similarly, a hyposaline environment could reduce Mfp stability due to a reduction in charge-balancing counter-ions, causing the adhesive cuticle to weaken [33,34]. DOPA-quinone formation is dependent on oxygen absorption from the surrounding seawater environment; [35] oxygen limitation during the curing process could either slow down DOPA conversion or lead to a reduction in cross-linking densities all together, reducing the cohesive strength of the plaque [36]. Therefore, the aim of this study is to determine the sensitivity of adhesive plaque curing to extreme seawater temperature, salinity, or dissolved oxygen concentration.

Freshly made byssal threads were incubated in seawater treatments (warm, hyposaline or hypoxic) for 12 days and then pulled from the substrate with a tensile testing machine. In addition to adhesion strength, the failure mode of each plaque was also recorded in order to determine how molecular changes the material affected the mechanics of the structure under tension. For the subset of these seawater parameters that were found to significantly affect adhesion, changes in plaque structure and composition were characterized using atomic force microscopy and amino acid analysis. To provide real-world context for these laboratory treatments, seawater conditions (temperature, salinity, and dissolved oxygen concentration) were measured continuously at a mussel farm in Washington State for over two years, in an effort to quantify seasonal trends across depth. By identifying which aspects of the multivariate seawater environment have post-processing effects on adhesive plaques, this study suggests a mechanism by which environmental variability influences mussel attachment in nature, while also informing the design of better medical adhesives that employ DOPA-mediated adhesion to persist in wet and ionically complex environments in the human body [37].

2.3. Materials and methods

2.3.1. Byssal thread experiments

Adult mussels (*Mytilus trossulus*, Gould 1850; ~4-6 cm shell length) were collected from aquaculture lines at Penn Cove Shellfish's mussel aquaculture operation located in Quilcene Bay, Quilcene, Washington, USA (47°47'42.0" N, 122°51"10.8" W) during the winter of 2016 (December-February). Mussel were kept in 50 L aquaria for up to two weeks, filled with 0.2 µm filtered seawater and fed Shellfish Diet 1800 (Reed Mariculture, Campbell, CA) up to 5% of wet tissue mass day^{-1} at an algal concentration of 2000 cells ml^{-1}. Upon collection the shell length (±0.1 cm) of each mussel was determined using a vernier caliper, while the reproductive condition (Gonad Index), and physiological condition (Condition Index) were determined for a subset of the collected population. Gonad index (GI) was calculated as the ratio of dried gonadal to total tissue mass [38], while the condition index (CI) was calculated as the total dry tissue mass divided by shell $length^3$ [39]. Gonadal tissue was dissected from somatic tissue and subsequently dried at 60°C to a constant dry weight (~3 days). The remaining mussels were haphazardly assigned to treatment groups and at the end of the experiment the GI and CI for each mussel was determined.

Mussels were secured to mica plates with rubber bands and allowed to produce byssal threads for up to four hours in typical open-ocean seawater conditions (pH ~ 8.1, T ~ 10°C, Sal ~ 31 PSU, O_2 = ~8 mg L^{-1}), after which threads were cut away from the animal in the proximal region of the thread (at the shell margin). Only mussels that produced three or more attachments were included in a treatment group. A subset of threads was tested immediately, serving as a 4 hour, 'freshly made' control. The remainder of mica plates with attached threads were placed in

one of four treatments (Control, N_2, 30°C, and DI water) and allowed to mature for 12 days, removing a subset of plates at 3, 5, 8, and 12 days.

Seawater treatments were designed to mimic open-ocean conditions in all ways but one, pushing either temperature, dissolved oxygen, or salinity to the most extreme values seen in estuarine systems that are metabolically driven by the local biota [40]. A hypoxia treatment (O_2 <2 mg L^{-1}) was achieved through the injection of N_2 gas into a 3 L container, using an aerator. The dissolved oxygen concentration of seawater treatments was monitored in real-time with a DirectLine DL5000 equilibrium probe (accuracy ± 1%) attached to a UDA2182 analyzer (Honeywell, Fort Washington, PA), which controlled the injection of N_2 by dynamically opening a solenoid valve in-line with a nitrogen gas cylinder. A high temperature treatment (30°C) was achieved using a 500 Watt titanium aquarium heater and accompanying PID controller (Aquatop Aquatic Supplies, Brea, CA). A low salinity treatment (<1 PSU) was achieved by placing plaques in deionized water. Seawater pH and temperature were monitored in each treatment with a Honeywell Durafet III pH electrode ([41]; accuracy ± 0.01), while salinity was monitored with a DL4000 conductivity cell (accuracy ± 1 PSU). Treatment means (± s.d.) for seawater pH (NBS scale), temperature (°C), salinity (PSU), and dissolved oxygen (mg L^{-1}) are reported in Table 2.1.

2.3.2. Mechanical testing and atomic force microscopy

The adhesion strength of individual plaques was determined by gripping each byssal thread in the distal region, 1 mm away from the adhesive plaque, and pulling perpendicular to the substrate until failure using a tensometer [42]. Adhesion strength (kPa) was calculated as the maximum of the force extension curve (N), normalized by the planform area of the attachment plaque measured in mm^2 [43]. The adhesion strength for 3-5 plaques were averaged and reported

as a single value for each mussel. During mechanical testing, the failure mode of each plaque was also visually scored as an adhesive, peeling, or tearing failure, as outlined by Young and Crisp [44]. Adhesive failure occurred when a plaque disengaged from a surface uniformly at the adhesive-substrate interface, while a peeling failure characteristically began at a single point along the outer edge of the plaque, propagating to the rest of the structure. A tearing failure was evident when a portion of the adhesive remained attached to the surface after the test had completed.

The stiffness of the plaque cuticle was determined by following the protocol outlined by George and Carrington (2018) [42]. Briefly, stiffness (DMT modulus) was measured using a Dimension ICON atomic force microscope (AFM), fitted with a ScanAsyst-Air probe with a silicon-nitride tip (Bruker, Billerica, MA). Prior to testing, plaques were rinsed with DI water and allowed to dry for 5 minutes. Efforts were taken to probe smooth patches away from the thread-plaque junction, avoiding the innervating roots of the thread. DMT modulus (GPa) was calculated as the slope of the force curve during tip-sample separation [45]. To obtain a representative stiffness of the cuticle, DMT modulus was averaged over a 10 nm^2 scan area, with a sampling rate of 512 per line. DMT Modulus was calibrated against a fused silica standard (Veeco, Plainview, NY). Multiple locations (3-5) were scanned for each plaque and then averaged.

2.3.3. Biochemical characterization of adhesive plaques

In preparation for amino acid (AA) analysis, adhesive plaques were collected from three different seawater treatments (4 hours and 12 days in open-ocean conditions; 12 days in nitrogen infused seawater) and stored in nitrogen flushed microfuge tubes at -80^{o}C for up to 4 weeks.

Acid hydrolysis was then performed *in vacuo* at 110°C for 48 hours in 6M HCl, with 5% phenol added to preserve DOPA residues. The hydrolysate of each plaque was flash evaporated against DI water and methanol, dissolving the precipitate in 0.02 M HCl. 100 µl of the mixture was then analyzed using an amino acid analyzer system based on ninhydrin-based chemistry (Hitachi L-8900; Tokyo, Japan). A typical spectrum obtained from the analyzer with identified peaks is presented in Figure 2.6a. The integral of each amino acid peak was divided by the integral of all peaks to determine the relative molar concentration of each amino acid, normalizing against a background of 0.02 M HCl and subtracting the ammonia peak.

2.3.4 Seawater monitoring

Environmental monitoring took place from March, 2015 to September, 2017 at Penn Cove Shellfish's mussel aquaculture operation located in Quilcene Bay, Quilcene, Washington, USA (47°47'42.0" N, 122°51"10.8" W). Two YSI EXO2 water quality sondes (YSI #599502-00; Yellow Springs, OH, USA) were suspended from ropes in the center of a mussel raft, deployed at -1 and -7 meters below the surface. The mussel raft was approximately 15 x 18 m, supported ~1500 lines with ~20 kg of mussels per line. Sensors were deployed in the center of the raft, surrounded by mussel lines. Each sonde was equipped with an EXO pH smart sensor (accuracy ± 0.1 pH units; YSI #599701), an EXO optical dissolved oxygen smart sensor (accuracy ± 1%; YSI #599100-01), and an EXO conductivity and temperature smart sensor (accuracy ± 0.5%; YSI #599870). Water temperature (°C), salinity (PSU), and dissolve oxygen concentration (mg L^{-1}) were reported hourly, transmitting data to a logger onshore using radio telemetry. Electrodes were cleaned and calibrated monthly against NBS pH standards (YSI #3822), a 50,000 µS cm^{-1} conductivity standard (YSI #3169), and air-saturated DI water.

2.3.5 Statistical Analyses

2.3.5.1. Laboratory Experiments

All statistical analyses were performed in R (Version 3.4.1; http://www.r-project.org/) with the RStudio IDE (Version 1.0.153; http://www.rstudio.com/). When appropriate, datasets were transformed using the Johnson Transformations package (Version 1.4) to achieve normality. To control for any impact of mussel physiology on plaque strength within treatments, multiple linear regression models were used to investigate the effect of adhesive age (days), shell length (cm), gonad index (GI), condition index (CI, $x10^{-3}$ g cm^{-3}), and plaque planform area (mm^2) on adhesion strength (kPa). Across treatments, plaques sampled at 12 days were compared using ANOVA, listing seawater treatment, shell length, GI, CI, and plaque planform area as factors. For significant effects, a Tukey HSD test was performed to compare treatment groups. Adhesion strength is reported as the average of 3-5 plaque pulls per individual, while the failure mode of each plaque was pooled as part of a treatment. The effect of treatment on plaque failure mode was also evaluated using a Chi-Squared test, using the open-ocean control treatment as the expected distribution at each time point.

2.3.5.2. Seawater Conditions Under a Mussel Raft

Field measurements of seawater temperature (^{o}C), salinity (PSU), and dissolved oxygen (mg L^{-1}) were pooled across years into seasons (spring, summer, autumn, and winter), using the spring equinox, summer solstice, autumn equinox, and winter solstice of each year as the onset of each respective season. The time series for each parameter measured was transformed using the normal quantile transformation to achieve normality [46], and subsequently analyzed using a two-way ANOVA with depth and season as factors.

To determine how frequently mussels were exposed to periods of high temperature, hyposalinity, and hypoxia under a mussel raft, a threshold analysis was performed across all the time points available, grouped by depth. High temperature was defined as >20^{o}C, matching the induction temperature required for the production of heat-shock transcription factor 1 (HSF-1) for *Mytilus trossulus* living in subtidal conditions [47]. Salinities capable of causing hypoosomotic stress in *Mytilus galloprovincialis* (<10 PSU) were considered hyposaline [48], while hypoxia was defined by a dissolved oxygen concentration of <2 mg L^{-1}, representing conditions that are usually lethal for pelagic invertebrates and fishes [49], but have been shown to be tolerated by *Mytilus edulis* for up to 1000 hours [50,51] . The proportion of days that experienced at least one instance of heat stress, hyposalinity, or hypoxia was determined using the Quantmod package [52]. The mean, mode, and maximum excursion duration was also determined using the length of time each parameter remained below the threshold before returning.

2.4. Results

2.4.1. Plaques cured in open-ocean conditions

When held in typical open-ocean seawater conditions (control treatment; Table 2.1), freshly deposited plaques (4 hours) strengthened over time (Figure 2.1a), increasing in adhesion strength by 117% after 12 days ($p<0.001$; Table S2.2; Figure 2.1b). Strengthening was paired with a change in physical appearance, with fresh plaques changing from translucent white to yellow over time (Figure 2.1d,e). The length of time in seawater also influenced the mode of plaque failure under tension. Peeling failure was initially the most common failure mode observed (4 hours: 71%), but adhesive failure became more prevalent over time (12 days: 70%;

$p<0.001$; Figure 2.2). Strengthening was also observed at the nanometer scale, with AFM measurements of stiffness (DMT modulus) increasing 145% over 12 days ($p<0.001$; Figure 2.3e). This increase in strength and stiffness over time was accompanied by a decreased concentration of DOPA (mol%) within the plaque, from 3.2% in freshly made plaques and only 0.8% in the plaques aged in seawater for 12 days (Table 2.2; Figure 2.4). Plaques aged in the control treatment for 12 days were enriched in Glycine (18.1% to 19.6%) and Histidine (6.2% to 9.1%) relative to those that were freshly made, and also contained less Alanine (10.1% to 8.4%; Table 2.2). None of the physiological metrics measured affected plaque strength in the control treatment (Table S2.2).

2.4.2. Plaques cured under hypoxia

Plaques aged in hypoxic seawater conditions (0.9 ± 0.6 mg L^{-1}; Table 2.1) for 12 days failed to increase in strength over time ($p=0.86$; Table S2.2; Figure 2.1a), were 63% weaker than the 12-day control treatment ($p<0.001$; Figure 2.1b), and failed significantly more frequently by peeling (65%; $p<0.001$; Figure 2.2b). Physical differences were also evident, with plaques displaying a mottled coloration of yellow and white spots (Figure 2.1f; Figure 2.3a). Closer examination of the plaque cuticle using atomic force microscopy (AFM) demonstrated that the yellow regions were smooth in texture (Figure 2.3b), with a stiffness similar to plaques aged in open-ocean conditions for 12 days ($p<0.001$; Figure 2.3e). In contrast, the white regions were significantly softer than the yellow ($p<0.001$; Figure 2.3f) and had a porous architecture at the nanometer scale. Cracks in the cuticle were evident where a mottled coloration was observed (Figure 2.3c), with a stiffness that was not statistically different than regions that were yellow in color ($p=0.053$; Figure 2.3f). As with DMT modulus, the DOPA concentration of plaques aged

under hypoxia for 12 days were significantly higher (2.6%) than those aged in the control treatment for the same length of time (0.8%; Figure 2.4b). In contrast, the molar concentration of Glycine (18.0%) and Histidine (6.0%) were not significantly different from the 4-hour old control (18.1% and 6.2%), while Alanine (8.4%) was not significantly different than the 12-day control (8.4%; Table 2.2). None of the physiological metrics measured affected plaque strength in the hypoxia treatment (Table S2).

2.4.3. Plaques cured in high temperature and hyposalinity

The adhesion strength of plaques matured in high temperature (~30°C) and DI water (~1 PSU) were not significantly different from the 12-day control treatment ($p=0.06$ and $p=0.50$; Table S2.3; Figure 2.1c). The failure mode of plaques aged in DI water was similar to the 12-day control ($p=0.21$), while high temperature marginally increased the prevalence of peeling failure ($p=0.07$; Figure 2.2b). Incubating plaques at 30°C marginally slowed adhesive strengthening, with no significant difference observed at any time point when compared with the control treatment (Figure 2.1a). Plaques aged in either treatment did not appear different in color compared to the 12-day control, although high temperature caused uneven tanning in some cases (Figure 2.1g). There was no treatment level effect of mussel size, plaque area, or reproductive and physiological condition on adhesion strength. None of the physiological metrics measured affected plaque strength in either treatment (Table S2.2).

2.4.4. Seawater conditions under a mussel aquaculture raft

Field measurements of seawater temperature varied seasonally and with depth (Figure 2.5; Table S2.4; $p<0.001$), with a summer maximum of 24.1°C at the surface (-1 m) and a low of

5.3°C in autumn at depth (-7 m; Figure S2.1). Higher mean temperatures were observed at the surface during the spring and summer, while in the autumn and winter months the trend reversed, with cooler surface temperatures at the surface than at depth (Figure 2.5; Figure S2.1). High temperature excursions were only observed at the surface in the summer and spring, with 12% of days displaying at least one temperature spike above 20°C (Table 2.3). The average length of each high temperature excursion was 7.3 hours, with the longest excursion occurring over 18.1 days. Most commonly, excursions lasted for 2 hours. Although season and depth were both significant factors driving temperature in this system, the interaction between the two was also significant, indicating that the effect of one depends on the context of the other ($p<0.001$; Table S2.4).

Salinity also varied seasonally ($p<0.001$) and with depth ($p<0.001$), with excursions as low as 2.1 and 2.6 PSU occurring in autumn and winter at the surface (Table S2.4; Figure 2.5, Figure S2.1). Low salinity excursions were limited to the surface, and were relatively rare, with only 4% of the days where measurements were available displaying a salinity less than 10 PSU. The average length of a salinity excursion was 2.9 hours, with the longest bout of hyposalinity occurring in autumn and lasting 6.3 hours (Table 2.2). Salinity at depth (7 m) remained above 10 PSU year round (Figure S2.1; Table 2.3). As with temperature, the differences in salinity between depths depended on season (depth x season interaction, Table S2.4) and were most prominent in autumn and winter.

Variability in dissolved oxygen was observed in the spring and summer, with lower concentrations observed at depth (Figure 2.5; Figure S2.1). In contrast, less variation was seen in the autumn and winter, although the depth trend was maintained (Figure S2.1). As with temperature and salinity, dissolved oxygen varied significantly with depth ($p<0.001$), and season

($p<0.001$), with a significant interaction between the two factors ($p<0.001$; Table S2.4). Hypoxic excursions were routinely observed at both depths, with 3.7% of the days included in this study experiencing a hypoxic event at the surface, compared to 14% at depth (Table 2.3). The average length of an excursion was 3.3 hours for both depths, with the most common being 1 hour. The longest excursions observed lasted for 10 hours at the surface and 12 hours at depth (Table 2.3). The dissolved oxygen minima for each depth was 0.4 and 0.1 mg L^{-1} for the surface and at depth, respectively, with both conditions occurring during the summer (Figure S2.1, Figure 2.5).

2.5. Discussion

Of the three seawater parameters tested, dissolved oxygen was the only one that was required for environmental post-processing. Plaques deprived of oxygen were 51% weaker that those cured in open-ocean conditions for 12 days, and developed a mottled yellow coloration with translucent regions commonly found along the perimeter. While DOPA-quinone formation did occur under hypoxia, atomic force microscopy imaging of translucent patches pointed to cracks in the plaque cuticle and localized regions of low stiffness, causing plaques to prematurely peel from the substrate. These results show that, in addition to a basic pH, environmental oxygen must be available during the curing process for the complex protein structure of the plaque to form correctly, even long after the structure has transitioned from a fluid to a bulk solid.

Mussel plaques represent a special case where both the adhesive and cohesive properties of an adhesive are linked to a single functional group. DOPA-residues comprise between 2-30% of the molecular structure of adhesive proteins (Mfps) within the plaque [53], with the highest molecular concentrations of DOPA found in Mfps localized at the adhesive-substratum interface

[21,54] and in the cuticle [24,25]. While DOPA residues are initially responsible for substrate-level adhesion, the conversion of DOPA to DOPA-quinone after absorption can be just as important for overall adhesion strength [55]. In this way, adhesion strength is optimized when a balance is maintained between the adhesive and cohesive interactions within the plaque and the material distributes load evenly, leading to an adhesive failure due to bonds breaking at the adhesive-substrate interface [56,57].

Typically, temperature plays a pivotal role in modulating the balance between adhesive and cohesive interactions within adhesives by altering the kinetics of molecular interactions [32]. However, plaques cured in seawater heated to 30^{o}C, exceeding even the most extreme temperatures seen in surface waters in this study, failed to alter either the curing rate or adhesion strength of plaques after 12 days. This result is consistent with the crosslinking activity of DOPA functionalized synthetic polypeptide mimics of mussel adhesive, which was consistently achieved up to 60^{o}C [56]. Similar results were seen with hyposalinity, which also failed to affect plaque curing. This result may be due to ionic interactions in the plaque being limited mainly to Fe^{3+} in the cuticle [58,59], and Zn^{2+} and Cu^{2+} in the plaque-thread junction [60,61], which are supplied by the mussel during protein secretion [62].

In contrast, when separated from the mussel after deposition and aged to maturity under hypoxia, plaques displayed several indicators that cohesive interactions within the structure either did not form, or formed improperly during the curing process. Plaques incubated in hypoxia for 12 days lacked characteristic shifts in amino acid composition typical of biomaterials that undergo schlerotization. For example, plaques aged in open-ocean conditions for 12 days had a greater availability of covalent crosslinking partners for DOPA, such as Glycine and Histidine, a trend that is similar to the quinone tanning that is found in jumbo squid beaks

(*Dosidicus gigas*) [63]. Under hypoxia, the molar concentration of Glycine and DOPA residues were more similar to freshly made plaques (4 h) than to the 12-day control, indicating a lack of DOPA-quinone conversion.

Compositional similarities between plaques aged in hypoxia and those that were freshly made help to explain why their failure dynamics were also so similar. Peeling failure was the most common failure mode for both the 4 h control and hypoxia incubated plaques, while tearing failure occurred more frequently under hypoxic conditions than in any other treatment. On reason for this change could be a decrease in the integrity of the plaque structure when aged without oxygen readily available. AFM scans of the plaque cuticles matured under hypoxia identified numerous tears, through which the porous interior of the plaque was visible. Stiffness measurements of smooth, yellow regions near the plaque-thread junction were similar to those reported for the cuticle of *Mytilus galloprovincialis* (~1.5 GPa), while the white, porous regions had moduli consistent with the interior of the plaque (~400 MPa) [64]. These results intuitively make sense, as the cuticle of the plaque is made up of Mfp-1 (15% DOPA) and would have a greater crosslinking density than the core, comprised of Mfp-2 (5% DOPA) [65,66]. A reduction in the DOPA-quinone formation and the cohesive strength that comes with proper cuticle formation explains why plaques frequently peeled off of substrates under hypoxia, as areas of low stiffness acted as regions of concentrated stress while under tension.

While the crosslinking behavior of specific Mfps are well understood [27,36,67,68], the kinetics of cross-linking in a protein network as complex as the one in the plaque remains unclear. In this study, plaques were incubated in containers with constant aeration in the laboratory, without the addition of circulating pumps. It is therefore likely that curing window presented here approximates still or gently flowing water conditions found underneath mussel

rafts [69–71], rather than the turbulent, high flow conditions mussels may experience in the intertidal zone [72,73]. The increased flux of oxygen to the plaque in turbulent habitats may either speed up crosslinking or flush the local microenvironment, effectively rescuing adhesion stalled by localized regions of oxygen depletion [35]. Oxygen availability could explain why the tenacity of solitary mussels [74], and those located on the margins of mussel beds [75], are typically stronger than those in aggregations, although additional work in needed in order to separate this effect from any physiological response of mussels to flow or food availability [76,77].

The observed decrease in plaque adhesion strength with hypoxia is particularly relevant for mussels hanging from ropes in raft aquaculture, where robust adhesion is necessary for survival. Seasonal comparisons of byssal thread mechanics have found that threads decay in as little as two weeks in the summer [78], necessitating that mussels perpetually produce threads in order to remain attached. Even if mussels interrupt byssus production in response to disadvantageous conditions, closing their shells to reduce physiological stress [79,80], freshly made threads must contend with local seawater conditions during an 8-12 day curing period for quinone tanning to fully occur [42]. Given the sensitivity of the curing process to oxygen availability, further work is needed to tease apart whether the curing process is delayed or irrevocably altered. If delayed, tidal fluctuations in oxygen saturation could serve to rescue adhesion. Alternatively, if the ultimate cohesive strength of the plaque is determined by the rate of DOPA-quinone formation, then the curing process could have a window of time wherein crosslinking needs to occur in order to serve its function as a load bearing structure.

Mussels have adapted an adhesion strategy that circumvents the challenges of adhesion underwater, using the chemistry of their surroundings to their advantage. However, seawater

conditions in nearshore environments often vary dramatically from the basic, oxygen saturated conditions of the open-ocean that are conducive for adhesion [28,81–83]. For example, field observations outlining the prevalence of hypoxia excursions where mussels were collected in this study show that 14% of the days sampled experienced at least one hypoxic event (<2 mg L^{-1}), with the longest event lasting for 12 hours. Given the susceptibility of plaque curing to oxygen availability, experiments where the curing process is inundated by environmentally relevant excursions in dissolved oxygen are needed in order to determine whether hypoxia irrevocably damages the protein network or if adhesion strength can recover after favorable conditions return.

2.6. Competing Interests

The authors of the manuscript have no competing interests.

2.7. Authors' Contributions

MNG wrote the manuscript and conducted the majority of the research, including the monthly calibration of water sensors, tensometer testing, atomic force microscopy, and amino acid analysis. BP contributed to experimental design and performed mechanical testing for the temperature assays. EC and JHW helped to conceive of the study and edited drafts of the manuscript. All authors gave final approval for publication.

2.8. Acknowledgements

We thank MacKenzie Edelsward, Chandana Kulkarni, Chloe Peterschmidt, Benjamin Makhlouf, and Jonathan Huie for assistance with mechanical testing, Micah Glaz for support with AFM

analysis, Dr. Daniel DeMartini for assistance with amino acid analysis, and Dr. Herbert Waite for sharing his equipment, time, and expertise. We also thank Ian Jefferds, Dominic Pangelinan, and all of the mussel growers at Penn Cove Shellfish, without whom this project would not have been possible. Data are archived under project #2250 at www.bco-dmo.org.

2.9. Funding

This work was supported by an NSF GRFP fellowship [#DGE-1256082] to MNG, the Washington Research Foundation Benjamin Hall Fellowship to MNG, an Alan and Marian Kohn FHL Fellowship to MNG, a Mary Gates Fellowship to BP, and an NSF grant [#OCE-1041213] to EC. Part of this work was conducted at the Molecular Analysis Facility, a National Nanotechnology Coordinated Infrastructure site at the University of Washington which is supported in part by the National Science Foundation [#ECC-1542101], the University of Washington, the Molecular Engineering & Sciences Institute, the Clean Energy Institute, and the National Institutes of Health. The efforts of EC were supported while serving at the National Science Foundation. Any opinion, findings, and conclusions or recommendations expressed in this material are those of the author(s) and do not necessarily reflect the views of the National Science Foundation.

2.10. References

1. Lu Q, Danner E, Waite JH, Israelachvili JN, Zeng H, Hwang DS. 2013 Adhesion of mussel foot proteins to different substrate surfaces. *J. R. Soc. Interface* **10**, 20120759. (doi:10.1098/rsif.2012.0759)
2. Yu J, Wei W, Menyo MS, Masic A, Waite JH, Israelachvili JN. 2013 Adhesion of mussel foot protein-3 to TiO2 surfaces: the effect of pH. *Biomacromolecules* **14**, 1072–1077. (doi:10.1021/bm301908y)

3. Yu J *et al.* 2013 Adaptive hydrophobic and hydrophilic interactions of mussel foot proteins with organic thin films. *Proc. Natl. Acad. Sci.* **110**, 15680–15685. (doi:10.1073/pnas.1315015110)
4. Dalsin JL, Hu B-H, Lee BP, Messersmith PB. 2003 Mussel adhesive protein mimetic polymers for the preparation of nonfouling surfaces. *J. Am. Chem. Soc.* **125**, 4253–4258. (doi:10.1021/ja0284963)
5. Lee H, Lee BP, Messersmith PB. 2007 A reversible wet/dry adhesive inspired by mussels and geckos. *Nature* **448**, 338–341.
6. Holten-Andersen N, Waite J. 2008 Mussel-designed protective coatings for compliant substrates. *J. Dent. Res.* **87**, 701–709. (doi:10.1177/154405910808700808)
7. Lee BP, Messersmith PB, Israelachvili JN, Waite JH. 2011 Mussel-inspired adhesives and coatings. *Annu. Rev. Mater. Res.* **41**, 99. (doi:10.1146/annurev-matsci-062910-100429)
8. Barrett DG, Bushnell GG, Messersmith PB. 2013 Mechanically robust, negative-swelling, mussel-inspired tissue adhesives. *Adv. Healthc. Mater.* **2**, 745–755. (doi:10.1002/adhm.201200316)
9. Waite H. 1983 Adhesion in byssally attached bivalves. *Biol. Rev.* **58**, 209–231. (doi:10.1111/j.1469-185X.1983.tb00387.x)
10. Waite JH, Qin X. 2001 Polyphosphoprotein from the adhesive pads of *Mytilus edulis*. *Biochemistry (Mosc.)* **40**, 2887–2893. (doi:10.1021/bi002718x)
11. Zhao H, Robertson NB, Jewhurst SA, Waite JH. 2006 Probing the adhesive footprints of *Mytilus* californianus byssus. *J. Biol. Chem.* **281**, 11090–11096. (doi:10.1074/jbc.M510792200)
12. Waite JH. 1987 Nature's underwater adhesive specialist. *Int. J. Adhes. Adhes.* **7**, 9–14. (doi:10.1016/0143-7496(87)90048-0)
13. Waite JH. 1992 The formation of mussel byssus: anatomy of a natural manufacturing process. In *Structure, cellular synthesis and assembly of biopolymers*, pp. 27–54. Springer.
14. Martinez Rodriguez NR, Das S, Kaufman Y, Israelachvili JN, Waite JH. 2015 Interfacial pH during mussel adhesive plaque formation. *Biofouling* **31**, 221–227. (doi:10.1080/08927014.2015.1026337)
15. Yu J, Wei W, Danner E, Ashley RK, Israelachvili JN, Waite JH. 2011 Mussel protein adhesion depends on interprotein thiol-mediated redox modulation. *Nat. Chem. Biol.* **7**, 588–590. (doi:10.1038/nchembio.630)
16. Miller DR, Spahn JE, Waite JH. 2015 The staying power of adhesion-associated antioxidant activity in *Mytilus* californianus. *J. R. Soc. Interface* **12**, 20150614. (doi:10.1098/rsif.2015.0614)
17. Nicklisch SC, Spahn JE, Zhou H, Gruian CM, Waite JH. 2016 Redox capacity of an extracellular matrix protein associated with adhesion in *Mytilus* californianus. *Biochemistry (Mosc.)* **55**, 2022. (doi:10.1021/acs.biochem.6b00044)

18. Hwang DS, Zeng H, Srivastava A, Krogstad DV, Tirrell M, Israelachvili JN, Waite JH. 2010 Viscosity and interfacial properties in a mussel-inspired adhesive coacervate. *Soft Matter* **6**, 3232–3236.

19. Wei W, Tan Y, Rodriguez NRM, Yu J, Israelachvili JN, Waite JH. 2014 A mussel-derived one component adhesive coacervate. *Acta Biomater.* **10**, 1663–1670. (doi:10.1016/j.actbio.2013.09.007)

20. Anderson TH, Yu J, Estrada A, Hammer MU, Waite JH, Israelachvili JN. 2010 The contribution of DOPA to substrate–peptide adhesion and internal cohesion of mussel-inspired synthetic peptide films. *Adv. Funct. Mater.* **20**, 4196–4205. (doi:10.1002/adfm.201000932)

21. Danner EW, Kan Y, Hammer MU, Israelachvili JN, Waite JH. 2012 Adhesion of mussel foot protein mefp-5 to mica: an underwater superglue. *Biochemistry (Mosc.)* **51**, 6511–6518. (doi:10.1021/bi3002538)

22. Waite JH. 1983 Quinone-tanned scleroproteins. *The mollusca* **1**, 467–504.

23. Holten-Andersen N, Harrington MJ, Birkedal H, Lee BP, Messersmith PB, Lee KYC, Waite JH. 2011 pH-induced metal-ligand cross-links inspired by mussel yield self-healing polymer networks with near-covalent elastic moduli. *Proc. Natl. Acad. Sci.* **108**, 2651–2655. (doi:10.1073/pnas.1015862108)

24. Taylor SW, Chase DB, Emptage MH, Nelson MJ, Waite JH. 1996 Ferric ion complexes of a DOPA-containing adhesive protein from *Mytilus edulis*. *Inorg. Chem.* **35**, 7572–7577. (doi:10.1021/ic960514s)

25. Xu Z. 2013 Mechanics of metal-catecholate complexes: The roles of coordination state and metal types. *Sci. Rep.* **3**, 2914. (doi:10.1038/srep02914)

26. George MN, Carrington E. 2018 Environmental post-processing increases the adhesion strength of mussel byssus adhesive. *Biofouling* (doi:10.1080/08927014.2018.1453927)

27. Haemers S, Koper GJ, Frens G. 2003 Effect of oxidation rate on cross-linking of mussel adhesive proteins. *Biomacromolecules* **4**, 632–640. (doi:10.1021/bm025707n)

28. Baumann H, Wallace RB, Tagliaferri T, Gobler CJ. 2014 Large Natural pH, CO2 and O2 Fluctuations in a Temperate Tidal Salt Marsh on Diel, Seasonal, and Interannual Time Scales. *Estuaries Coasts* , 1–12.

29. Reum JC, Alin SR, Feely RA, Newton J, Warner M, McElhany P. 2014 Seasonal carbonate chemistry covariation with temperature, oxygen, and salinity in a fjord estuary: implications for the design of ocean acidification experiments. *PLoS One* **9**, e89619.

30. McGowan JA, Cayan DR, Dorman LM. 1998 Climate-Ocean Variability and Ecosystem Response in the Northeast Pacific. *Science* **281**, 210. (doi:10.1126/science.281.5374.210)

31. Feely RA, Alin SR, Newton J, Sabine CL, Warner M, Devol A, Krembs C, Maloy C. 2010 The combined effects of ocean acidification, mixing, and respiration on pH and carbonate saturation in an urbanized estuary. *Estuar. Coast. Shelf Sci.* **88**, 442–449.

32. Filippidi E, DeMartini DG, Malo de Molina P, Danner EW, Kim J, Helgeson ME, Waite JH, Valentine MT. 2015 The microscopic network structure of mussel (*Mytilus*) adhesive plaques. *J. R. Soc. Interface* **12**. (doi:10.1098/rsif.2015.0827)

33. Ibragimova GT, Wade RC. 1998 Importance of explicit salt ions for protein stability in molecular dynamics simulation. *Biophys. J.* **74**, 2906–2911.

34. Formaneck MS, Ma L, Cui Q. 2006 Effects of Temperature and Salt Concentration on the Structural Stability of Human Lymphotactin: Insights from Molecular Simulations. *J. Am. Chem. Soc.* **128**, 9506–9517. (doi:10.1021/ja061620o)

35. Sun C, Vaccaro E, Waite JH. 2001 Oxidative stress and the mechanical properties of naturally occurring chimeric collagen-containing fibers. *Biophys. J.* **81**, 3590–3595.

36. Haemers S, van der Leeden MC, Koper GJ, Frens G. 2002 Cross-linking and multilayer adsorption of mussel adhesive proteins. *Langmuir* **18**, 4903–4907. (doi:10.1021/la025626c)

37. Fan C, Fu J, Zhu W, Wang D-A. 2016 A mussel-inspired double-crosslinked tissue adhesive intended for internal medical use. *Acta Biomater.* **33**, 51–63. (doi:10.1016/j.actbio.2016.02.003)

38. Carrington E. 2002 Seasonal variation in the attachment strength of blue mussels: causes and consequences. *Limnol. Oceanogr.* **47**, 1723–1733. (doi:10.4319/lo.2002.47.6.1723)

39. Moeser GM, Leba H, Carrington E. 2006 Seasonal influence of wave action on thread production in *Mytilus edulis*. *J. Exp. Biol.* **209**, 881–890. (doi:10.1242/jeb.02050)

40. Baumann H, Smith EM. 2017 Quantifying metabolically driven pH and oxygen fluctuations in US nearshore habitats at diel to interannual time scales. *Estuaries Coasts* , 1–16.

41. Martz TR, Connery JG, Johnson KS. 2010 Testing the Honeywell Durafet® for seawater pH applications. *Limnol. Oceanogr. Methods* **8**, 172–184. (doi:10.4319/lom.2010.8.172)

42. George M, Carrington E. 2018 Environmental post-processing improves the adhesion strength of mussel byssus adhesive. *Biofouling* (doi:10.1080/08927014.2018.1453927)

43. Burkett JR, Wojtas JL, Cloud JL, Wilker JJ. 2009 A method for measuring the adhesion strength of marine mussels. *J. Adhes.* **85**, 601–615. (doi:10.1080/00218460902996903)

44. Young GA, Crisp D. 1982 Marine animals and adhesion. In *K.W. Allend (ed.) Adhesion*, pp. 19–39. Barking, England: Applied Science Publishers, Ltd.

45. Young TJ, Monclus MA, Burnett TL, Broughton WR, Ogin SL, Smith PA. 2011 The use of the PeakForce(TM) quantitative nanomechanical mapping AFM-based method for high-resolution Young's modulus measurement of polymers. *Meas. Sci. Technol.* **22**, 125703. (doi:10.1088/0957-0233/22/12/125703)

46. Bogner K, Pappenberger F, Cloke HL. 2012 The normal quantile transformation and its application in a flood forecasting system. *Hydrol. Earth Syst. Sci.* **16**, 1085–1094. (doi:10.5194/hess-16-1085-2012)

47. Buckley BA, Owen M-E, Hofmann GE. 2001 Adjusting the thermostat: the threshold induction temperature for the heat-shock response in intertidal mussels (genus *Mytilus*) changes as a function of thermal history. *J. Exp. Biol.* **204**, 3571–3579.

48. Hamer B *et al.* 2008 Effect of hypoosmotic stress by low salinity acclimation of Mediterranean mussels *Mytilus galloprovincialis* on biological parameters used for pollution assessment. *Aquat. Toxicol.* **89**, 137–151. (doi:10.1016/j.aquatox.2008.06.015)

49. Gray JS, Wu RS, Or YY. 2002 Effects of hypoxia and organic enrichment on the coastal marine environment. *Mar. Ecol. Prog. Ser.* **238**, 249–279. (doi:10.3354/meps238249)

50. Dries R-R, Theede H. 1974 Sauerstoffmangelresistenz mariner Bodenvertebraten aus der westlichen Ostsee. *Mar. Biol.* **25**, 327–333.

51. Rosenberg R. 1972 Benthic faunal recovery in a Swedish fjord following the closure of a sulphite pulp mill. *Oikos* , 92–108.

52. Ryan JA, Ulrich JM. 2017 *quantmod: Quantitative Financial Modelling Framework*. See https://CRAN.R-project.org/package=quantmod.

53. Waite JH. 2017 Mussel adhesion–essential footwork. *J. Exp. Biol.* **220**, 517–530. (doi:10.1242/jeb.134056)

54. Lin Q, Gourdon D, Sun C, Holten-Andersen N, Anderson TH, Waite JH, Israelachvili JN. 2007 Adhesion mechanisms of the mussel foot proteins mfp-1 and mfp-3. *Proc. Natl. Acad. Sci.* **104**, 3782–3786. (doi:10.1073/pnas.0607852104)

55. Yu M, Hwang J, Deming TJ. 1999 Role of L-3, 4-dihydroxyphenylalanine in mussel adhesive proteins. *J. Am. Chem. Soc.* **121**, 5825–5826.

56. Yu M, Deming T. 1998 Synthetic polypeptide mimics of marine adhesives. *Macromolecules* **31**, 4739–4745. (doi:10.1021/ma980268z)

57. Desmond KW, Zacchia NA, Waite JH, Valentine MT. 2015 Dynamics of mussel plaque detachment. *Soft Matter* **11**, 6832–6839. (doi:10.1039/C5SM01072A)

58. Holten-Andersen N, Fantner GE, Hohlbauch S, Waite JH, Zok FW. 2007 Protective coatings on extensible biofibres. *Nat. Mater.* **6**, 669.

59. Harrington MJ, Masic A, Holten-Andersen N, Waite JH, Fratzl P. 2010 Iron-clad fibers: a metal-based biological strategy for hard flexible coatings. *Science* **328**, 216–220.

60. Harrington MJ, Waite JH. 2007 Holdfast heroics: comparing the molecular and mechanical properties of *Mytilus* californianus byssal threads. *J. Exp. Biol.* **210**, 4307–4318.

61. Vaccaro E, Waite JH. 2001 Yield and post-yield behavior of mussel byssal thread: a self-healing biomolecular material. *Biomacromolecules* **2**, 906–911.

62. George SG, Pirie BJS, Coombs TL. 1976 The kinetics of accumulation and excretion of ferric hydroxide in *Mytilus edulis* (I.) and its distribution in the tissues. *J. Exp. Mar. Biol. Ecol.* **23**, 71–84.

63. Miserez A, Rubin D, Waite JH. 2010 Cross-linking chemistry of squid beak. *J. Biol. Chem.* **285**, 38115–38124. (doi:10.1074/jbc.M110.161174)

64. Holten-Andersen N, Zhao H, Waite JH. 2009 Stiff coatings on compliant biofibers: the cuticle of *Mytilus* californianus byssal threads. *Biochemistry (Mosc.)* **48**, 2752–2759. (doi:10.1021/bi900018m)

65. Waite JH. 1983 Evidence for a repeating 3, 4-dihydroxyphenylalanine-and hydroxyproline-containing decapeptide in the adhesive protein of the mussel, *Mytilus edulis* L. *J. Biol. Chem.* **258**, 2911–2915.

66. Inoue K, Waite JH, Matsuoka M, Odo S, Harayama S. 1995 Interspecific variations in adhesive protein sequences of *Mytilus edulis*, M. *galloprovincialis*, and M. *trossulus*. *Biol. Bull.* **189**, 370–375. (doi:10.2307/1542155)

67. Fant C, Sott K, Elwing H, Hook F. 2000 Adsorption behavior and enzymatically or chemically induced cross-linking of a mussel adhesive protein. *Biofouling* **16**, 119–132. (doi:10.1080/08927010009378437)

68. Fant C, Elwing H, Höök F. 2002 The influence of cross-linking on protein-protein interactions in a marine adhesive: the case of two byssus plaque proteins from the blue mussel. *Biomacromolecules* **3**, 732–741. (doi:10.1021/bm025506j)

69. Blanco J, Zapata M, Moro o A. 1996 Some aspects of the water flow through mussel rafts. *Sci. Mar.* **60**, 275–282.

70. Strohmeier T, Aure J, Duinker A, Castberg T, Svardal A, Strand Ø. 2005 Flow reduction, seston depletion, meat content and distribution of diarrhetic shellfish toxins in a long-line blue mussel (*Mytilus edulis*) farm. *J. Shellfish Res.* **24**, 15–23.

71. Grant J, Bacher C. 2001 A numerical model of flow modification induced by suspended aquaculture in a Chinese bay. *Can. J. Fish. Aquat. Sci.* **58**, 1003–1011. (doi:10.1139/f01-027)

72. Paine RT, Levin SA. 1981 Intertidal landscapes: disturbance and the dynamics of pattern. *Ecol. Monogr.* **51**, 145–178. (doi:10.2307/2937261)

73. Carrington E, Moeser GM, Thompson SB, Coutts LC, Craig CA. 2008 Mussel attachment on rocky shores: the effect of flow on byssus production. *Integr. Comp. Biol.* **48**, 801–807.

74. Bell E, Gosline J. 1997 Strategies for life in flow: tenacity, morphometry, and probability of dislodgment of two *Mytilus* species. *Mar. Ecol. Prog. Ser.* **159**, 197–208.

75. Witman JD, Suchanek TH. 1984 Mussels in flow: drag and dislodgement by epizoans. *Mar. Ecol. Prog. Ser.* , 259–268.

76. Dolmer P, Svane I. 1994 Attachment and orientation of *Mytilus edulis* L. in flowing water. *Ophelia* **40**, 63–74. (doi:10.1080/00785326.1994.10429551)

77. McDowell LM, Burzio LA, Waite JH, Schaefer J. 1999 Rotational echo double resonance detection of cross-links formed in mussel byssus under high-flow stress. *J. Biol. Chem.* **274**, 20293–20295. (doi:10.1074/jbc.274.29.20293)

78. Moeser GM, Carrington E. 2006 Seasonal variation in mussel byssal thread mechanics. *J. Exp. Biol.* **209**, 1996–2003. (doi:10.1242/jeb.02234)

79. García-March JR, Solsona MÁS, García-Carrascosa AM. 2008 Shell gaping behaviour of Pinna nobilis L., 1758: circadian and circalunar rhythms revealed by in situ monitoring. *Mar. Biol.* **153**, 689–698. (doi:10.1007/s00227-007-0842-6)

80. Robson A, Wilson R, de Leaniz CG. 2007 Mussels flexing their muscles: a new method for quantifying bivalve behaviour. *Mar. Biol.* **151**, 1195–1204. (doi:10.1007/s00227-006-0566-z)

81. Reum JC, Alin SR, Feely RA, Newton J, Warner M, McElhany P. 2014 Seasonal Carbonate Chemistry Covariation with Temperature, Oxygen, and Salinity in a Fjord Estuary: Implications for the Design of Ocean Acidification Experiments. *PloS One* **9**, e89619.

82. Booth JAT, McPhee-Shaw EE, Chua P, Kingsley E, Denny M, Phillips R, Bograd SJ, Zeidberg LD, Gilly WF. 2012 Natural intrusions of hypoxic, low pH water into nearshore marine environments on the California coast. *Cont. Shelf Res.* **45**, 108–115. (doi:10.1016/j.csr.2012.06.009)

83. Woźniak SB, Stramski D, Stramska M, Reynolds RA, Wright VM, Miksic EY, Cichocka M, Cieplak AM. 2010 Optical variability of seawater in relation to particle concentration, composition, and size distribution in the nearshore marine environment at Imperial Beach, California. *J. Geophys. Res. Oceans* **115**.

2.11. Tables

Table 2.1. Mean seawater conditions (± s.d.) in each treatment during 12-day exposures. pH, temperature (T), salinity (Sal), and dissolved oxygen (O_2) where recorded at 10 minute intervals.

Treatment	pH (NBS)	T (^{o}C)	Sal (PSU)	O_2 (mg L^{-1})
Control	8.01 ± 0.03	9.7 ± 1.4	29 ± 1	8.5 ± 0.5
N_2	8.00 ± 0.03	9.8 ± 1.0	28 ± 2	0.9 ± 0.6
30^{o}C	8.01 ± 0.04	29.7 ± 0.5	29 ± 1	8.7 ± 0.4
DI	7.22 ± 0.12	10.1 ± 0.6	1 ± 2	8.6 ± 0.3

Table 2.2. Mean amino acid (AA) composition (mol % ± se) of adhesive plaques that were freshly deposited (SW:4hrs), aged in seawater for 12 days (SW:12d), and matured in nitrogen infused seawater for 12 days (N_2:12d). The resulting p-values of ANOVA comparing the mol % of each AA across treatments are reported below, with letters representing the output of Tukey HSD comparisons (alpha=0.05).

AA	SW:4hrs	SW:12d	N_2:12d	p-value
Asx	9.1 ± 1.7^{a}	9.8 ± 1.8^{a}	10.7 ± 2.0^{b}	<0.001**
Thr	3.3 ± 0.6	3.2 ± 0.6	3.6 ± 0.7	0.249*
Ser	8.5 ± 1.6^{ab}	9.2 ± 1.7^{b}	8.0 ± 1.5^{a}	0.027*
Glx	5.3 ± 1.0	5.2 ± 1.0	5.1 ± 0.9	0.715*
Gly	18.1 ± 1.7^{b}	19.6 ± 3.6^{a}	18.0 ± 3.3^{b}	0.003*
Ala	10.1 ± 1.8^{a}	8.4 ± 1.6^{b}	8.4 ± 1.5^{b}	<0.001**
Cys	0	0	0	
Val	3.3 ± 0.6	3.6 ± 0.7	3.5 ± 0.6	0.587*
Met	0.8 ± 0.2^{a}	0.2 ± 0.1^{b}	0.2 ± 0.1^{b}	0.002*
Ile	1.6 ± 0.3^{a}	1.5 ± 0.3^{b}	2.1 ± 0.4^{b}	0.001*
Leu	4.8 ± 0.9	4.6 ± 0.8	4.9 ± 0.9	0.294*
DOPA	3.2 ± 0.6^{a}	0.8 ± 0.2^{b}	2.6 ± 0.6^{a}	<0.001**
Tyr	5.3 ± 1.0^{a}	6.3 ± 1.2^{b}	6.1 ± 1.1^{b}	0.016*
Phe	3.6 ± 0.7^{a}	4.3 ± 0.8^{b}	3.7 ± 0.7^{a}	0.045*
His	6.2 ± 1.1^{a}	9.1 ± 1.7^{b}	6.0 ± 1.4^{a}	<0.001**
Lys	4.7 ± 0.9^{a}	5.3 ± 1.0^{b}	5.4 ± 1.0^{b}	0.004*
Arg	6.3 ± 1.1	6.5 ± 1.2	6.7 ± 1.2	0.239*
Pro	4.1 ± 0.8^{ab}	3.7 ± 0.7^{a}	4.5 ± 0.8^{b}	0.031*
	n = 5	n = 5	n = 5	

Asx is Asp and/or Asn; Glx is Glu and/or Gln. DOPA is 3,4-dihydroxyphenyl-L-alanine.

Table 2.3. The frequency of extreme excursions in seawater temperature (ºC), salinity (PSU), and dissolved oxygen (mg L^{-1}) at two depths (1 and 7 meters) beneath a mussel aquaculture raft located in Quilcene Bay, Quilcene, Washington. Water conditions were monitored hourly from March, 2015 through September, 2017. Sample size (n) reflects the exclusion of data compromised by sensor fouling or communication error. The proportion of days that experienced at least one instance of heat stress (>20ºC), hyposalinity (<10 PSU), or hypoxia (<2 mg L^{-1}) is as n%. The mean, mode, and maximum excursion durations (hours) are also reported for each condition, at each depth.

				Excursion Duration (hours)		
Condition	**Depth (m)**	**n**	**n%**	**mean**	**mode**	**max**
T > 20ºC	-1	656	12.2	7.3	2	18
	-7	701	-	-	-	
Sal < 10 PSU	-1	506	4	2.9	2	6
	-7	528	-	-	-	
O_2 < 2 mg L^{-1}	-1	646	3.7	3.3	1	10
	-7	641	14	3.3	1	12

2.12. Figures

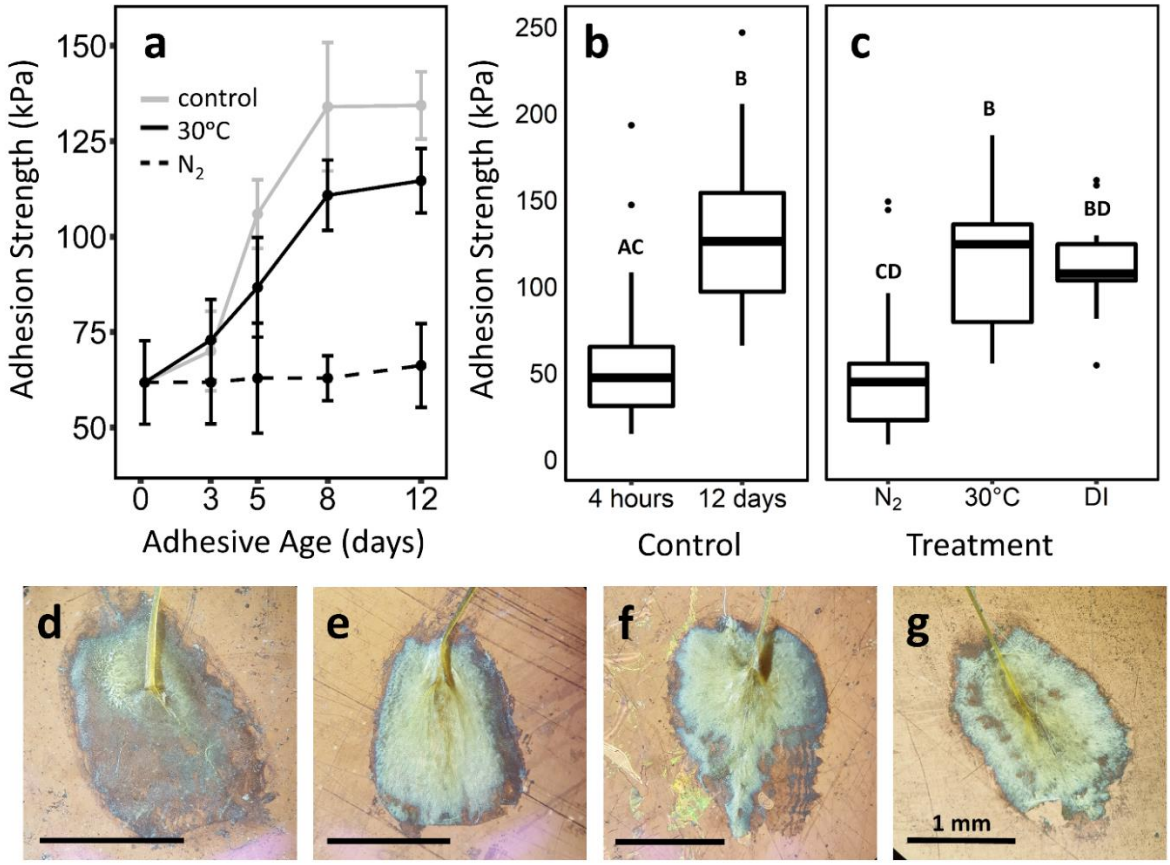

Figure 2.1. Adhesion strength (mean ± se; kPa) of adhesive plaques cured in different seawater conditions. Plaques aged under open-ocean seawater conditions (pH = 8.01 ± 0.03, T = 9.7 ± 1.4°C, Sal = 29 ± 1 PSU, O_2 = 8.5 ± 0.5 mgL^{-1}) were compared to plaques cured under high temperature (30°C; T = 29.7 ± 0.5°C), hyposaline (DI water; Sal = 1 ± 2 PSU), and hypoxic conditions (N_2 treated; O_2 = 0.9 ± 0.6 mg L^{-1}). Hypoxia arrested plaque strengthening, while high temperature and hyposalinity did not significantly affect adhesion strength at 12 days. Plaques changed color from translucent white (d, 4 hours old) to golden yellow (e, 12 days old) in open ocean conditions. Plaques aged in nitrogen treated seawater turned yellow around the thread-plaque junction, with noticeable gaps in colorations around the perimeter (f), while those held in the 30°C treatment turned yellow while retaining clear spots throughout (g). All full list of treatment conditions is available in Table 2.1. Letters represent the result of Tukey HSD comparisons.

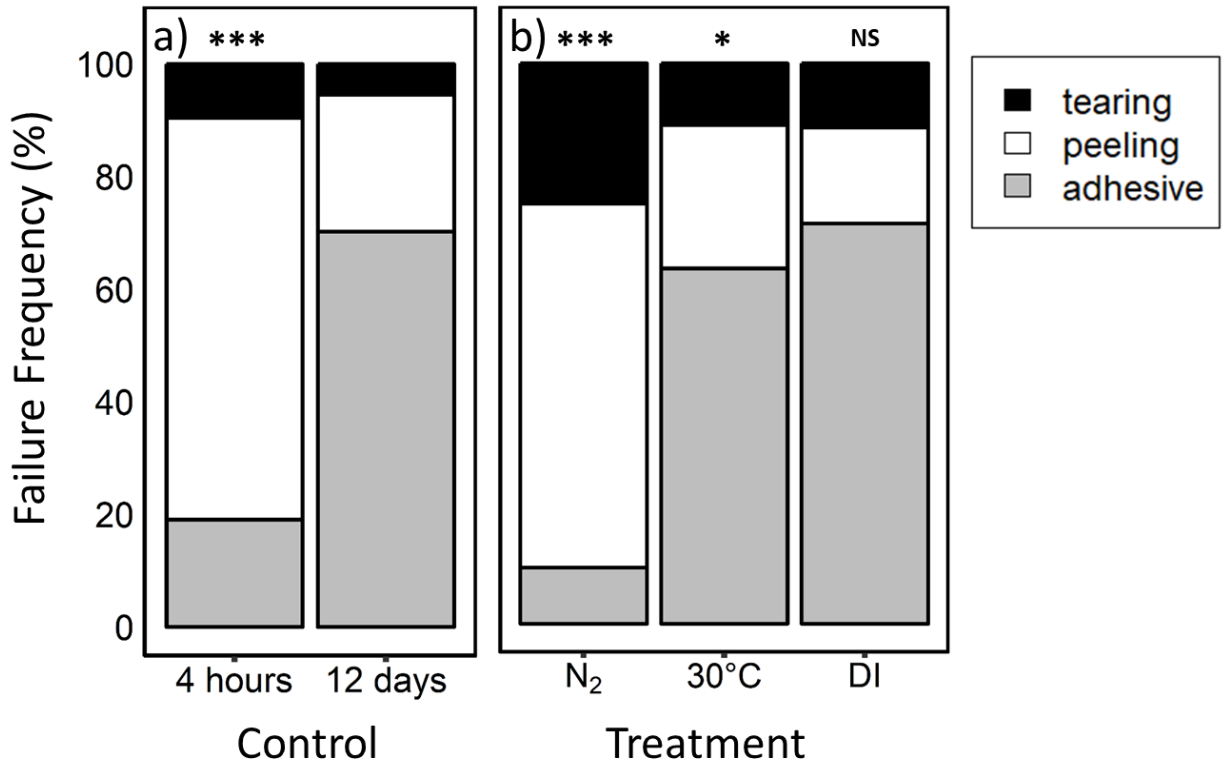

Figure 2.2. Failure mode frequency (%) of adhesive plaques aged to maturity (12 days) in different seawater conditions. In open-ocean conditions, the dominant mode of failure was peeling at 4 hours, and adhesive failure at 12 days (a, $p < 0.001$). Peeling was also the most prevalent failure mode in 12 day old plaques aged in hypoxic conditions (b, N_2), while those matured at high temperature (b, 30°C) and low salinity (b, DI) were not significantly different from 12 day old controls (30°C, $p = 0.07$; DI, $p = 0.21$). Stars represent the results of chi-squared tests comparing results to the 12-day control treatment (*** $p < 0.001$; ** $p < 0.01$; * $p < 0.1$).

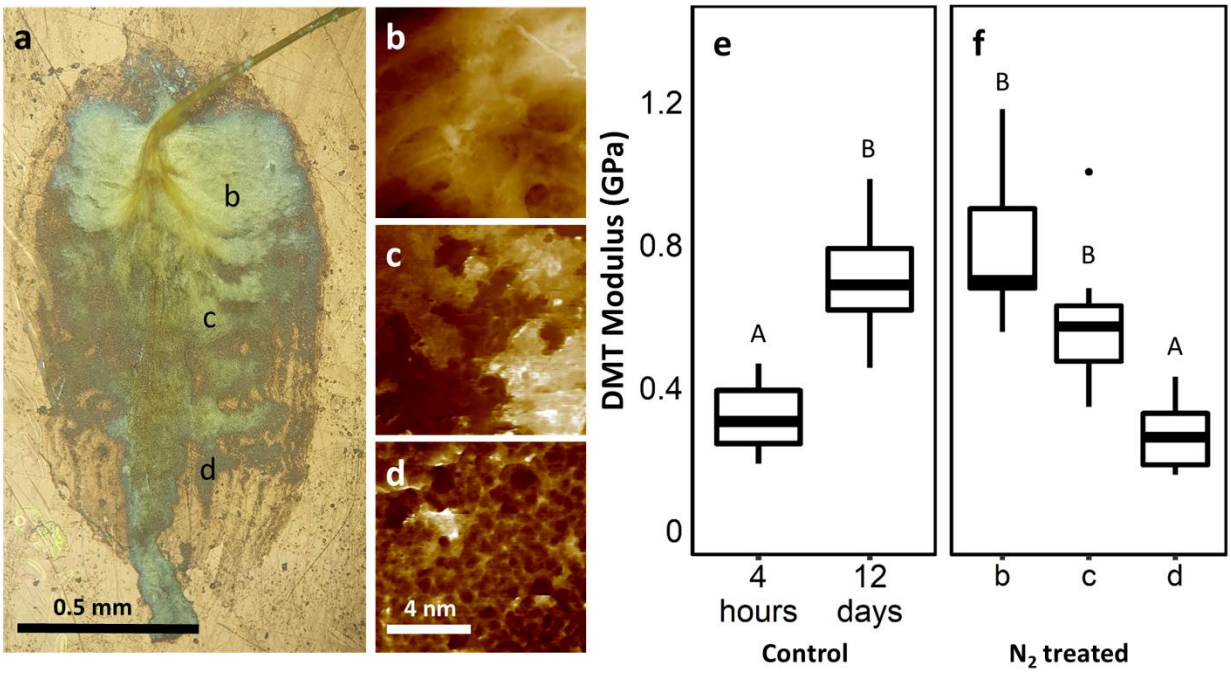

Figure 2.3. The effect of hypoxia on the cuticle of adhesive plaques. Plaques aged in nitrogen treated seawater (pH = 8.00 ± 0.03, T = 9.8 ± 1.0°C, Sal = 28 ± 2 PSU, O_2 = 0.9 ± 0.6 mg L^{-1}) displayed patchy cross-linking throughout, evident from disparate regions of yellow quinone tanning (a). AFM adhesion images of the plaque surface at three different positions (b-d) show that several regions lack a protective cuticle, exposing the porous inner core of the plaque to seawater. Reduced DOPA cross-linking is supported by localized stiffness measurements across the structure (f) when compared to surface measurements from plaques aged in typical seawater conditions (e; pH = 8.01 ± 0.03, T = 9.7 ± 1.4 °C, Sal = 29 ± 1 PSU, O_2 = 8.5 ± 0.5 mg L^{-1}). Letters above panels denote the results of Tukey HSD pairwise comparisons.

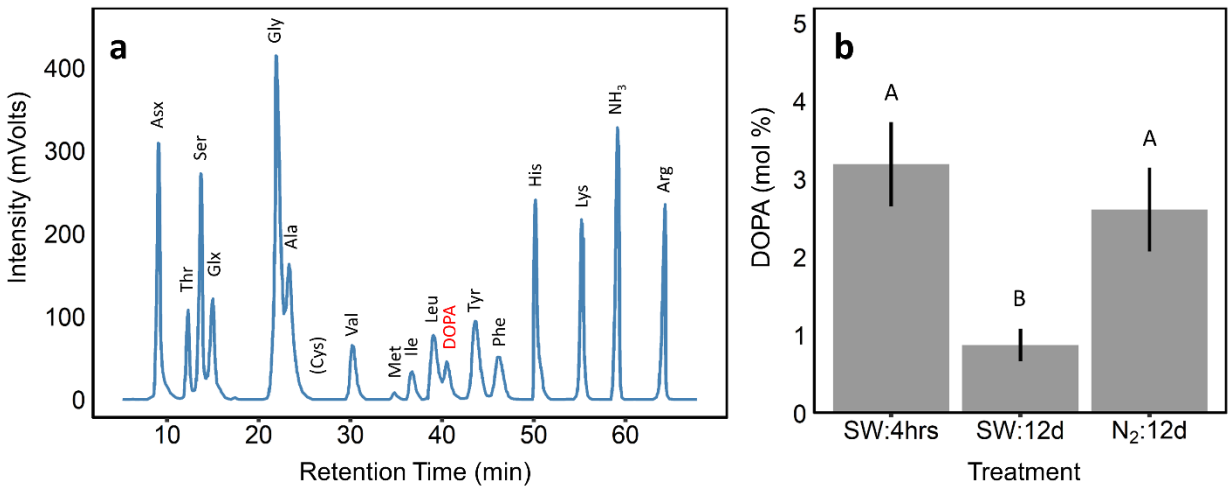

Figure 2.4. Amino acid composition analysis of adhesive plaques aged in control and nitrogen infused seawater treatments. Hydrolysate of individual plaques were run on an AA analyzer, producing characteristic peaks corresponding to each amino acid that were then integrated to determine molar concentration (a). The molecular concentration of DOPA (mean ± se, n=5 each) within the plaque was the greatest directly after plaques were deposited on surfaces (SW:4hrs) and decreased significantly after submersion in seawater for 12 days (b; SW:12d; $p<0.001$), due to the oxidation of DOPA to DOPA-quinone. Freshly made plaques aged in seawater infused with nitrogen gas for 12 days (N_2:12d) displayed DOPA concentrations that were not significantly different than freshly made plaques (b; $p=0.60$). Letters represent the result of Tukey HSD comparisons.

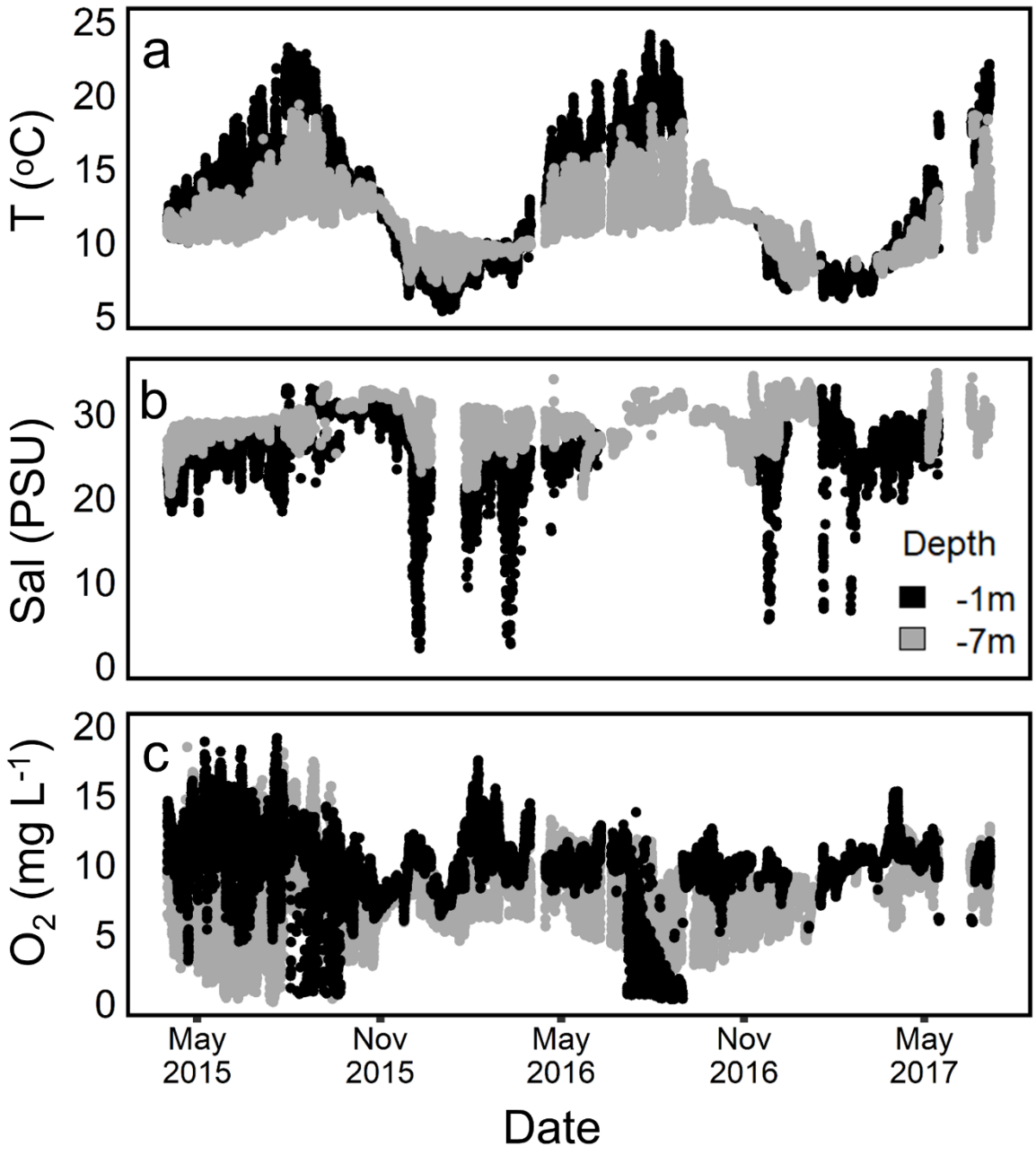

Figure 2.5. Water conditions measured under an aquaculture raft floating in Quilcene Bay, Washington, from April 2015 to September 2017. Temperature (°C, a), salinity (PSU, b), and dissolved oxygen (mg L^{-1}, c) were reported hourly for two depths below the surface (1 meter, black circles; 7 meters, gray circles).

2.13. Supplemental Material

Table S2.1. Body size and condition metrics for mussels that produced adhesive plaques included in tensometer measurements, grouped by treatment (mean ± s.d).

Treatment	n	Shell Length (cm)	Plaque Area (mm^2)	Gonad Index	Condition Index ($x10^{-3}$ g cm^{-3})
Control	78	4.9 ± 0.6	2.10 ± 0.53	0.11 ± 0.03	3.8 ± 0.9
N_2	64	4.6 ± 0.7	2.49 ± 0.38	0.11 ± 0.03	4.2 ± 0.7
30°C	66	4.9 ± 0.5	1.97 ± 0.54	0.11 ± 0.04	3.5 ± 0.9
DI	13	5.1 ± 0.6	2.4 ± 0.51	0.13 ± 0.03	3.3 ± 1.1

Table S2.2. Multiple linear regression results investigating the effect of adhesive age (days), mussel shell length (cm), gonad index (GI), condition index (CI), and planform plaque area (mm^2) on plaque adhesion strength (kPa). Results are reported for three, 12-day long exposure experiments where plaques were incubated in either control, high temperature (30°C), and hypoxia conditions. Seawater conditions are reported in Table 2.2. Asterisks represent significant results (alpha = 0.05).

Variable	Estimate	Std. Error	t value	p-value
Control (open-ocean)				
(Intercept)	73.11	59.23	1.23	0.22
Adhesive age	6.85	1.17	5.85	< 0.001*
Shell length	-5.74	9.50	-0.60	0.55
GI	207.68	168.51	1.23	0.22
CI	6857.73	6406.47	1.07	0.29
Plaque Area	-16.39	9.82	-1.67	0.10
Hypoxia (N_2 treated)				
(Intercept)	54.73	54.46	1.01	0.32
Adhesive age	0.27	1.57	0.17	0.86
Shell length	0.98	7.12	0.14	0.89
GI	-54.03	134.57	-0.40	0.69
CI	3290.46	5859.91	0.56	0.58
Plaque Area	-2.12	12.96	-0.16	0.87
High temperature (30°C)				
(Intercept)	12.88	65.42	0.20	0.84
Adhesive age	5.28	1.64	3.21	0.002*
Shell length	0.90	12.21	0.07	0.94
GI	51.53	144.70	0.36	0.72
CI	7317.28	8069.70	0.91	0.37
Plaque Area	3.34	11.39	0.29	0.77

Table S2.3. The effect of seawater treatment on plaque adhesion strength (kPa) after 12 days of exposure was analyzed using ANOVA, with the gonad index (GI), condition index (CI), shell length (cm), and planform plaque area (mm^2) for each mussel investigated as factors. Asterisks represent significant results (alpha = 0.05).

Source	d.f.	*SS*	F	p-value
Treatment	4	43.38	15.75	<0.001*
Shell Length	1	1.02	1.48	0.23
GI	1	2	2.91	0.09
CI	1	0	0.002	0.96
Plaque Area	1	0.33	0.48	0.49
Residuals	90	61.96	0.69	

Table S2.4. ANOVA results comparing temperature (°C), salinity (PSU), and dissolved oxygen (mg L^{-1}) from March, 2015 to September, 2017 underneath a mussel raft in Quilcene bay. Data were transformed using the normal quantile transformation, comparing the variance about the mean across season (spring, summer, autumn, and winter) and depth (1 and 7 meters below the surface).

Source	d.f.	*SS*	F	p-value
Temperature				
Season	3	204001	18014	<0.001*
Depth	1	19514	5458	<0.001*
Season x depth	3	39022	3637	<0.001*
Salinity				
Season	3	2625	875	<0.001*
Depth	1	2250	2250	<0.001*
Season x depth	3	1812	604	<0.001*
Dissolved Oxygen				
Season	3	3533	1368	<0.001*
Depth	1	739	858	<0.001*
Season x depth	3	1017	394	<0.001*

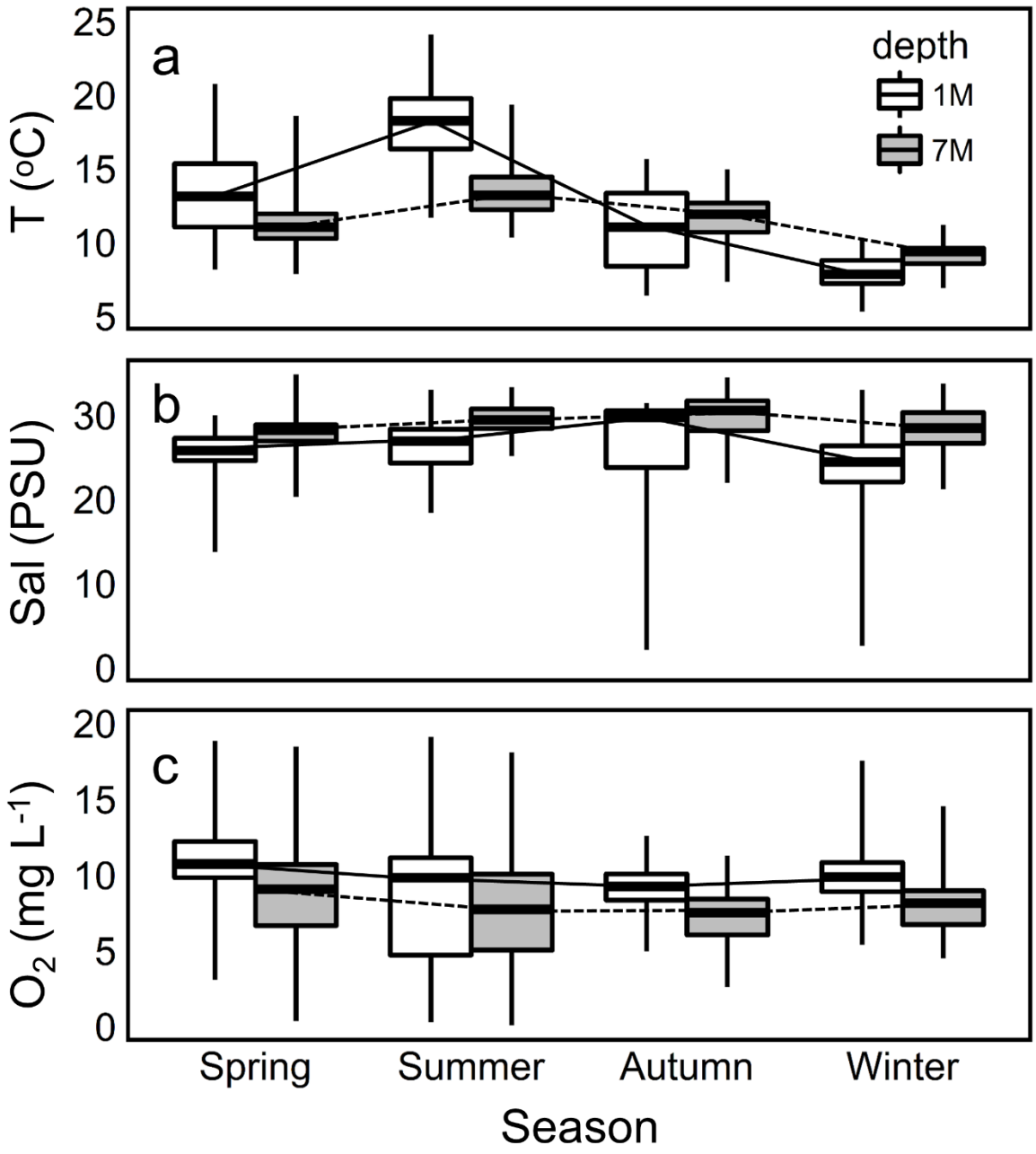

Figure S2.1. Seasonal variation in water conditions under a floating aquaculture raft in Quilcene Bay, WA, March 2015 – September 2017. Boxplots represent the mean, SD, and min and max for hourly measurements of temperature (^{o}C, a), salinity (PSU, b), and dissolved oxygen (mg L^{-1}, c) at two depths below the surface (1 meter, gray boxes; 7 meters, white boxes).

Chapter 3

Microscale pH and dissolved oxygen excursions within mussel raft aggregations: implications for byssus plaque curing and mussel attachment

Matthew N. George[1,2], Jessie Andino[1], Jonathan Huie[1], and Emily Carrington[1,2]

1 – University of Washington, Department of Biology, BOX 358100, Seattle, WA 98195

2 – Friday Harbor Laboratories, 620 University Rd., Friday Harbor, WA 98250

Keywords: Underwater adhesion; mussel foot protein (Mfp); *Mytilus trossulus*; mussel raft aquaculture

3.1. Abstract

Mussel mariculture relies on a mussel's ability to attach and grow on culture lines through the production of byssal threads, proteinaceous fibers that adhere to surfaces underwater using a powerful biological adhesive (adhesive plaque). After formation, the plaque uses the surrounding seawater as a molecular trigger to facilitate solidification and adhesive curing, a process that requires a pH above 7.0 and a high concentration of dissolved oxygen in order to progress. However, water quality monitoring outlined in this study from within mussel aggregations on culture lines from a mussel farm in Washington State demonstrate that mussels regularly experience acidic (pH < 5) and hypoxic excursions (O_2 < 2 mg L^{-1}) in the summer, near the seafloor. When exposed to fluctuations of this magnitude in laboratory experiments, pH excursions delayed plaque strengthening when applied early in the curing process, while hypoxia decreased adhesion strength after the adhesive had fully matured. In both cases, adhesion strength was rescued after re-immersion in open-ocean seawater conditions. The susceptibility of the plaque to environmental conditions during and after curing could explain why fall-off events occur at mussel farms, and could help to inform management strategies that promote the recovery of attachment strength during times of the year when fall-off is common.

3.2. Introduction

Bivalve mariculture is a rapidly growing industry, with worldwide harvests exceeding a value of 27 Million USD in 2016 (FAO 2017). As part of this global trend, suspended raft culture of marine mussels is becoming increasingly popular, in large part as a result of farming practices that are efficient, sustainable, and require limited investment after seed cultivation (Shumway et al. 2003, Lindahl et al. 2005, Whitmarsh et al. 2006, Troell et al. 2009, Lozano et al. 2010). However, mussel growers must contend with one particularly troublesome aspect of farming near coastlines that fisheries off-shore do not. Unlike the open-ocean, nearshore environments can experience large oscillations in seawater chemistry as a result of riverine inputs (Rysgaard et al. 2012), industrial pollution (van Dam et al. 2011, Förstner and Wittmann 2012), coastal upwelling (Wang et al. 2015), and agricultural runoff (Shaw et al. 2010), all of which can directly influence the growth and survival of marine organisms (Doney et al. 2011, Vernberg and Vernberg 2013, Bakun et al. 2015). Given these challenges, the identification of environmental parameters that impact mussel settlement, growth, and attachment will be of paramount importance for growers going forward, especially as global ocean conditions continue to change due to human activities (Levin et al. 2009, Doney et al. 2009).

During the production process, shellfish growers commonly leverage the underwater attachment strategies of marine bivalves, enabling them to adhere to manmade structures that promote rapid production and efficient harvest. In the case of marine mussels, attachment is made possible by a network of proteinaceous fibers called byssal threads, each of which is tipped with a powerful biological adhesive. Byssal threads are an important feature of a mussel's functional morphology, preventing dislodgement through the absorption of wave energy (Bell and Gosline 1996), while anchoring each thread to the substrate with an adhesive plaque

(Tamarin et al. 1976). In fact, the mussel's ability to adhere underwater has captured the interest of the synthetic adhesive industry (Kamino 2008, Lee et al. 2011); several adhesive proteins in the plaque have been identified, many of which have a high abundance of 3,4-dihydroxyphenly-L-alanine (DOPA) residues that are capable of forming interfacial interactions (i.e. hydrogen bonding, hydrophobic, coordination, etc.) with both hydrophobic and hydrophilic surfaces (Waite 1983, Waite and Qin 2001, Anderson et al. 2010, Danner et al. 2012).

In suspended raft culture, post-larval mussels are applied to hanging culture lines made from braided plastics or natural fibers (Brenner and Buck 2010). Once mussels are attached, culture lines are hung *en masse* from rafts that float off-shore, protecting mussels from predators on the seafloor and allowing them to feed freely on microalgae in the water column. Under this method, mussels must remain attached to culture lines anywhere between 12-18 months before reaching a marketable size (>6 cm, Ian Jefferds personal communication). In order to remain attached, mussel must continually make new byssal threads throughout this period as older threads decay and fall away (Moeser and Carrington 2006). In this way, mussel attachment strength plays an integral role in the survival of the organism throughout its lifecycle, while also ultimately determining farm yield at the end of a growing season.

Mussels manufacture byssal threads by secreting protein precursors into a specialized groove that runs along the length of their foot, with each fiber imbedded in an adhesive plaque that is deposited on a surface. Plaque production begins when a small depression at the tip of the foot (the distal depression) is pressed against a surface and the resulting cavity is filled with adhesive proteins (mussel foot proteins, hereafter referred to as Mfps). During protein secretion, mussels control the chemistry within the distal depression, maintaining a highly acidic (Martinez Rodriguez et al. 2015), anoxic (Nicklisch et al. 2016), and ionically sparse (Yu et al. 2011, Miller

et al. 2015) environment. Under these conditions DOPA residues on Mfps preferentially interact with the surface rather than with each other (Anderson et al. 2010, Danner et al. 2012), while protein side chain oxidation is also minimized (Xu et al. 2012, Miller et al. 2015). After approximately five minutes, the foot is removed and seawater infiltrates the cavity, drastically changing the conditions around the adhesive (pH~8.0, O_2~8 mg L^{-1}, and salinity ~31 PSU). Through this process, seawater acts as a molecular trigger, 'curing' the newly formed adhesive. The result is a transition from a fluidic state during protein secretion, to a porous solid over the course of a few seconds (Hwang et al. 2010, Lim et al. 2010, Wei et al. 2014).

Seawater is responsible for the initial phase change that forms the adhesive plaque, with recent work demonstrating that the curing process continues long after solidification (George and Carrington 2018). When held in open-open conditions (pH ~8.0, O_2 ~8.5 mg L^{-1}) the adhesion strength of plaques doubles over the course of 8 days, with plaques shifting from translucent white to dark tan in color. In contrast, holding plaques in low pH (<5.0) and hypoxic (<2 mg L^{-1}) seawater conditions effectively stopped strengthening all together, causing the adhesive to peel from the substrate before the material could be fully loaded during tensile testing. High temperature (30^{o}C) and hyposalinity (1 PSU), however, did not affect adhesive strengthening (George et al. unpublished, George and Carrington 2018). These results show that plaques require continued access to basic pH conditions and a high availability of dissolved oxygen long after protein deposition. Under these conditions, covalent cross-links between Mfps are formed as DOPA residues are oxidized to DOPA-quinone (McDowell et al. 1999, Haemers et al. 2003, Xu et al. 2012), a process that is mediated by the pH-sensitive enzyme catechol oxidase (Waite 1985).

While incorporating seawater into the curing process may have negated one of the greatest challenges of underwater adhesion (Comyn 1981), the instability of seawater conditions in nearshore environments may ultimately pose a problem for mussel attachment (Waite and Broomell 2012, Carrington et al. 2015). In estuaries, large diel fluctuations in seawater pH and dissolved oxygen saturation can be metabolically driven by the local biology, with ranges as large as 2 pH units and over 100% swings in oxygen saturation reported at sites throughout the United States (Baumann and Smith 2017). To make matters worse, these ranges almost surely underestimate the variability seen in mussel mariculture, as the largescale addition of biomass on culture lines has been found to drastically change the biogeochemistry of the local environment (Christensen et al. 2003, Lozano et al. 2010). In addition, the high stocking density of mussels on culture lines could lead to localized regions of hypoxia and acidification within mussel aggregations; a likely consequence of observed flow reductions of up to 70% underneath mariculture rafts (Grant and Bacher 2001, Strohmeier et al. 2005). Given that mussels can't protect threads from environmental conditions of this kind after they are made, the sensitivity of the curing process to environmental fluctuations after adhesive formation may influence the timing and magnitude of mussel fall-off.

The microenvironment mussels experience on rope lines during suspended raft culture has the potential to dramatically affect attachment strength, by either (1) preventing plaque curing, (2) damaging mature threads, or (3) decreasing thread production. However, the magnitude and duration of pH and dissolved oxygen excursions within mussel aggregations remains unknown. In this study, water quality measurements were taken underneath a suspended culture raft deployed within Puget Sound, in an effort to quantify the spatial (depth) and temporal (season) variation in water conditions that mussels experience throughout the year. Additionally,

microscale modifications to seawater pH and dissolved oxygen at the site of plaque adhesion were measured by imbedding sensors directly in mussel aggregations. The effect of temporal dynamics on adhesive curing was then investigated in the laboratory, replicating extreme excursions in pH and oxygen either early or late in the curing process. Here we are able to show that extreme excursions in pH and dissolved oxygen that are capable of decreasing thread production and interrupting plaque curing occur underneath rafts and are amplified in mussel aggregations, a result that could contribute to holdfast weakening.

3.3. Materials and Methods

3.3.1. Seawater monitoring

3.3.1.1. Seawater conditions under a mussel aquaculture raft

Water conditions were monitored underneath a mussel raft over the course of three years (April 1, 2015 – March 3, 2018) at Penn Cove Shellfish's mussel aquaculture operation in Quilcene Bay, Quilcene, Washington, USA (47°47'48.0" N, 122°51"16.6" W). The mussel raft chosen was closest to the inlet and was approximately 15 x 18 m in size, supported ~1500 mussel lines, with a typical yield of ~20 kg mussels per line (Dominic Pangelinan, personal communication). Water quality sondes (YSI EXO2 #599502-00; Yellow Springs, OH, USA), hereafter referred to as 'raft sensors', were suspended from ropes in the center the raft, deployed at 1 and 7 meters below the surface (Figure 3.1).

Each sonde was equipped with an EXO pH sensor (accuracy ± 0.1 pH units; YSI #599701), optical dissolved oxygen sensor (accuracy ± 1%; YSI #599100-01), conductivity and temperature sensor (accuracy ± 0.5%; YSI #599870), and an EXO total algae PE sensor (precision: 0-100 µg L^{-1}; YSI # 599103-01). Water temperature (°C), salinity (PSU), dissolved

oxygen concentration (mg L^{-1}), and chlorophyll concentration (µg L^{-1}) were recorded as the average of 10-minute samples, taken every hour, and transmitted to a database using a radio transmitter. Sensors were calibrated monthly against NBS pH standards (YSI #3822), a 50,000 µS cm^{-1} conductivity standard (YSI #3169), and air-saturated DI water. Total algae sensors were calibrated against a 0.625 mg L^{-1} Rhodamine FWT red dye solution (Kingscote Chemicals, Miamisburg, OH, USA; #106023).

The effect of seasonality and depth on each measured seawater parameter was investigated using a two-way ANOVA. Seasons were defined by the spring equinox, summer solstice, autumn equinox, and winter solstice of each year. Each parameter was rank transformed to achieve normality with the normal quantile transformation (Ryan and Ulrich 2017). The Pearson's correlation test was employed to determine the degree to which seawater parameters co-varied. All statistical analyses were performed in R (Version 3.4.1; http://www.r-project.org/) with the RStudio IDE (Version 1.0.153; http://www.rstudio.com/).

3.3.1.2 Seawater conditions in mussel aggregations

The pH and oxygen conditions mussels experience within aggregations was measured during different seasons as follows. Nylon mesh bags filled with mussels (~5 kg total weight) were hung from rope lines and positioned adjacent to the 1m and 7m sondes (Figure 3.1). An 'aggregation sensor' was place in the center of each bag, comprising a Durafet III pH electrode (Honeywell, Fort Washington, PA, USA; accuracy ± 0.01; Martz et al. 2010) and a Honeywell DirectLine DL5000 equilibrium probe (accuracy ± 0.1 mg L^{-1}) and recorded 10 minutes of measurements every hour. Measurements of pH (NBS) and oxygen concentration (mg L^{-1}) were monitored using a Honeywell UDA2182 analyzer, powered by a 12-volt AGM battery

(Universal Power Group, Coppell, TX, USA; #UB12900), and logged using 4-20 mA data loggers (Lascar Electronics, Erie, PA, USA; #EL-USB-4). Aggregation sensors and sondes were calibrated at the same time and were temporally synced to record at the top of every hour. Bags were deployed four times during both the summer (June-September) and winter (December-March) of 2015-2016, for up to three weeks at a time, cleaning sensors between deployments to limit any effects of fouling.

3.3.2. Laboratory experiments

Adult mussels (*Mytilus trossulus*, Gould 1850) used in laboratory experiments were collected from the top of aquaculture rope lines from November, 2015 to February, 2016 and kept in 50 L aquaria, filled with 0.2 µm filtered, UV-sterilized seawater. Mussels were kept in aquaria for no longer than three weeks at a time, and were fed Shellfish Diet 1800 (Reed Mariculture, Campbell, CA) up to 5% of their wet tissue mass day^{-1}, dispensed at a concentration of 2000 algal cells ml^{-1}. After collection, the shell length (±0.1 cm) of each mussel was determined using Vernier calipers, while the reproductive condition (Gonad Index, GI), and physiological condition (Condition Index, CI) were determined for a subset of the population. Gonadal tissue was excised from each animal by prying apart the valves of the shell, peeling back the gill flaps, and removing the underlying tissue with a scalpel. The remaining somatic tissue was then removed and dried separately from the gonads at 60°C until a constant dry weight was achieved (~3 days). GI was calculated as the ratio of dried gonadal tissue to total tissue mass for each individual following the protocol of Carrington (2002), and was calculated as the total dry tissue mass, normalized to the shell length cubed (Moeser and Carrington 2006). This procedure was repeated for each mussel after its inclusion in an experiment, comparing the GI

and CI to mussels that were sacrificed immediately upon collection in order to control for the effects of cohort, treatment, and captivity.

Byssal threads were collected in the laboratory by securing mussels to mica plates with rubber bands, orienting the valve opening towards the substrate and allowing them to attach under seawater conditions that mimicked those found in the open-ocean (pH ~ 8, O_2~ 8.5 mg L^{-1}, Sal ~ 30 PSU, T ~ 9^{o}C). After four hours, threads were separated from each animal at the shell margin by cutting the proximal region of each thread, preserving the attachment plaque's connection with each plate. Plates with attached threads were then incubated in seawater treatments, with only mussels that made three or more attachments included in a treatment group. After incubation, plates were removed from seawater, dried, and stored for up to two weeks before mechanical testing was performed. Storage in air for up to two weeks arrests the curing process, which can then be resumed upon resubmission in seawater, effectively preventing adhesive plaque curing during storage without adversely affecting adhesion strength (George and Carrington 2018).

For each experiment described below, linear mixed-effects models and ANOVA were used to identify any effect of mussel condition on either thread production or plaque adhesion strength (nlme package; Pinheiro et al. 2017), transforming data to achieve linearity when necessary (Johnson Transformations package; Fernandez 2014). A combination factors such as shell length (cm), plaque planform area (mm^2), GI, CI; and adhesive age (days) were included as fixed effects, while each mussel was incorporated as a random effect. For each significant effect, a one-way ANOVA and Tukey HSD test was performed to determine differences between treatment groups.

3.3.3. The effect of seawater excursions on adhesive plaque curing

To determine whether pH and oxygen excursions can directly affect the plaque curing process, plaques were aged in fluctuating seawater treatments for up to 20 days after being separated from the mussels that made them. Mica plates with freshly made (~4hrs after deposition) attached threads were haphazardly assigned to one of five experimental treatments, controlled using the pH and oxygen-stat system described above. Threads aged in the first two experiments experienced constant oxygen (~8 mg L^{-1}), temperature (~9^{o}C), and salinity conditions (~29), while also being subjected to an excursion in seawater pH (pH~5.0) after either 1 (Exp. 1) or 8 (Exp. 2) days. The second two experiments mimicked the conditions of the first, except that seawater pH was maintained at ~8.0 throughout and threads were exposed to hypoxia excursions (O_2 < 2 mg L^{-1}) either at 1 (Exp. 3) or 8 (Exp. 4) days into the experiment. pH and oxygen excursions were maintained for 5 days, after which conditions returned to a baseline that represented open-ocean conditions (pH ~8.0, O_2 ~8.5, T ~9^{o}C, Sal ~29 PSU). A subset of plates was removed within each experiment after either 3, 5, 8, 12, or 20 days and stored dry for up to two weeks before mechanical testing was performed. A control treatment wherein open-ocean conditions were maintained for 20 days was also performed with the same sampling regime.

3.3.4. Byssal thread production during seawater excursions

The behavioral response of mussels to reductions in pH and oxygen dissolved was investigated by placing mussels secured to mica plates in one of five pH treatments (pH target = 5.0, 6.0, 7.0, 7.5, or 8.0) or one of two dissolved oxygen treatments (O_2 target = < 2.0 or > 8.0 mg L^{-1}) for seven days. pH treatments were maintained using a pH-stat system similar to the one described in O'Donnell et al. (2013). Briefly, seawater pH (NBS) and temperature (^{o}C) were

measured with a Honeywell Durafet III pH electrode and monitored with a Honeywell UDA2182 analyzer that controlled the operation of a solenoid valve. The solenoid value regulated the flow of CO_2 into the aerator of each tank. Using a PID loop, the analyzer tailored a CO_2:air mixture by controlling the proportional operation of the valve, using pH as the response variable. Dissolved oxygen treatments were accomplished in a similar way by equipping the analyzer with a Honeywell DL5000 equilibrium oxygen probe (accuracy ± 0.1) and replacing the CO_2 cylinder with N_2 gas. The salinity (PSU) in each treatment was monitored with a Honeywell DL4000 conductivity cell (accuracy ± 1 PSU), which was also monitored by the analyzer. pH, oxygen, temperature, and salinity were logged every 10 minutes using a 4-20 mA data logger. Any pre-existing byssal threads were removed from each mussel, by cutting threads in the proximal region at the shell margin, prior to being placed in a treatment. Once in a treatment, a subset of mussels (~20) were removed at 1, 3, 5, and 7 days, counting the number of new threads each mussel produced before determining the CI and GI for each animal. Linear mixed-effects models were constructed to investigate the effect of pH, dissolved oxygen, shell length, GI, and CI on thread production.

3.3.5. Mechanical testing

Plaque attachment strength was determined by gripping the distal region of each byssal thread and pulling perpendicular (90^{o}) to the substrate until failure, following the protocol of George and Carrington (2018). This testing angle was chosen for its reproducibility; it should be noted that the contact angle of the thread with the plaque varies and threads are rarely brought into tension fully perpendicular to the substrate (Desmond et al. 2015). Plaques were rehydrated in their respective seawater treatments prior to mechanical testing for more than 5 minutes. The

distal region was gripped with a hemostat ~1 mm above the plaque-thread junction, and force was recorded using a 10 N digital force gauge (OMEGA, Stamford, CT, USA; accuracy ± 0.01 N) attached to a motor-driven testing frame. Threads were pulled at an extension of 10 mm min^{-1}, recording force (N) and extension (mm) at 20 Hz. The adhesion strength (kPa) of each plaque was determined by normalizing the maximum force required to dislodge each plaque by the attachment planform area (mm^2), measured by tracing the outline of each plaque from above using a dissection scope with accompanying AmScope MU1000 camera (Irvine, CA, USA) and AmScope X imaging software (Burkett et al. 2009). The mean adhesion strength of 3-5 plaques is reported for each mussel.

In an effort to link observed differences in plaque adhesion with the failure mechanics of the adhesive, the failure mode of each plaque was also scored visually during mechanical testing following Young & Crisp (1982) and George & Carrington (2018). Briefly, plaques were binned within three failure types: adhesive, peeling, or tearing. In the case of adhesive failure, plaques detached from the substrate in a single, swift, plunger like motion. Peeling failure was characterized by a detachment beginning at one location along the perimeter of the plaque, propagating from one side of the structure to the other. Tearing failure was evident when a portion of the plaque remained attached to the substrate after the test was completed, or the thread became dislodged from the attachment plaque at the thread-plaque junction. The failure mode of plaques at each time point were pooled and compared with an open-ocean control treatment (expected values) using a Chi-Squared test.

3.4. Results

3.4.1. Seawater conditions under a mussel aquaculture raft

Raft sensor measurements of seawater temperature, salinity, dissolved oxygen concentration, pH, and chlorophyll concentration varied as a result of the interaction between seasonality and depth ($p<0.001$; Table S3.2; Figure 3.2). Over the three years measured, seawater temperature was typically higher at the surface (1 m) in the spring and summer than at depth (7 m), with the trend reversing in the autumn and winter (Table S3.1; Figure 3.2a). Salinity excursions (<10 PSU) were observed exclusively at the surface, and were isolated to the autumn and winter months (Table S3.1; Figure 3.2b). The dissolved oxygen concentration and seawater pH remained higher at the surface, regardless of season (Table S3.1; Figure 3.2c), with the same trend observed with seawater pH (Figure 3.2d). Chlorophyll concentration varied widely between seasons and years, with spikes frequently observed in the autumn and winter at the surface (Figure 3.2e). Out of the five parameters measured, seawater pH and dissolved oxygen concentration were most strongly correlated (1 m: slope = 5.13, R = 0.68; 7 m: slope = 9.31, R = 0.82; Figure 3.3a), with excursions commonly co-occurring in the summer and spring at both depths (Figure 3.3b,c).

A summary of the mean, standard deviation, minimum, and maximum seawater conditions, grouped by season and depth, are reported in Table S3.1 in the supplemental material. ANOVA results comparing seasons and depth for each parameter measured are reported in Table S3.2.

3.4.2. pH and oxygen excursions in mussel aggregations

pH and dissolved oxygen measurements from within mussel aggregations were tightly correlated with raft sensor recordings between mussel lines during the winter months, at both the surface (pH: slope = 1.15; R = 0.77; O_2: slope = 0.88; R = 0.94; Figure 3.4a) and at depth (pH: slope = 0.90; R = 0.64; O_2: slope = 0.85; R = 0.92; Figure 3.4c). The same was true for pH during the summer at the surface (slope = 0.80; R = 0.82), but not at depth (slope = 1.71; R = 0.52) where measurements from within aggregations often fell well below values recorded by raft sensors hanging less than a meter away (Figure 3.4b). Excursions in dissolved oxygen concentration commonly accompanied pH excursions within aggregations (slope = 1.6, R = 0.46, $p < 0.001$), particularly in the summer at depth (slope = 0.52, R = 0.65, $p < 0.001$; Figure 3.4d). Excursions at depth in the summer, when defined as a pH<7.0 and dissolved oxygen concentration less than 5 mg L^{-1}, were usually short lived, with 42% of all excursions lasting for less than 2 hours, while the longest was maintained for 5.2 days. During these excursions, aggregation sensors readings were, on average, 1.49 pH units and 1.98 mg L^{-1} below readings recorded by raft sensors. An example of an excursion that took place during July of 2015 is presented in panels e and f of Figure 3.4.

3.4.3. Adhesive plaque curing during seawater excursions

Plaque adhesion strength increased over time, more than doubling in strength after 8 days in the control condition (+117%; Figure 3.5). When pH was held below 5.0 during days 1-6 of the curing process, plaque strengthening was delayed, leading to weaker attachments at 5 (-64%; p=0.004) and 8 days after deposition (-56%; p=0.02; Figure 3.5a). During this period, plaques also peeled more frequently from the substrate during tensile tests, failing before the thread could

be loaded (5 days: $p<0.001$; 8 days: $p=0.03$; Figure 3.5e). However, at day 6 when conditions returned to the baseline, plaques resumed strengthening, and were not significantly weaker than the control at day 12 (-8%; $p=0.53$). In contrast, a low pH excursion (pH<5) after 8 days did not significantly affect adhesion strength when compared with the control (-19%; $p=0.28$; Figure 3.5b).

Plaques exposed to hypoxia during the beginning of the curing window (day 1-5) showed no sign of delayed strengthening (Figure 3.5c). However, when plaques were exposed to hypoxia after the curing process was complete (day 8-13), plaques were significantly weaker than the control treatment (-74%; $p=0.003$; Figure 3.5d). Plaque adhesion strength then recovered after oxygen returned to baseline levels and plaques were tested at 20 days (-17%; $p=0.37$; Figure 3.5d). While weakened, the proportion of plaques that failed by peeling from the substrate drastically increased to 61% of those tested, leading to a significantly different failure distribution than the control ($p<0.001$; Figure 3.5h).

Across all plaque curing experiments, mussel size (shell length), reproductive condition (GI), physiological condition (CI), and plaque attachment area (mm^2) was consistent across treatments and time points (Table S3.3) and did not influence plaque adhesion strength (Table S3.4). Plaque adhesion strength increased as a function of plaque age in all experiments ($p<0.001$). A summary of seawater conditions for each treatment is presented in Table 3.1.

3.4.4. Byssal thread production during seawater excursions

Seawater pH ($p<0.001$) and dissolved oxygen concentration ($p<0.001$) had a significant effect on the rate and number of byssal threads produced after seven days (Figure 3.6a,b; Table S3.6). Mussels held at a pH less than 7.0 and dissolved oxygen concentration less than 2 mg L^{-1}

neglected to produce threads for up to 3 days and manufactured an average of less than 10 per individual thereafter. A summary of seawater conditions for each treatment is presented in Table 3.2. Mussel shell length, gonad index, and condition index were consistent across treatments (Table S3.5) and did not negatively affect thread production (Table S3.6).

3.5. Discussion

The temperature, salinity, pH, and dissolved oxygen conditions measured underneath a mussel raft in this study varied drastically from typical open-ocean conditions, with mussels frequently experiencing pH and oxygen excursions within aggregations that form on culture lines. Excursions, defined as any period of time that seawater pH dropped below 7.0 or dissolved oxygen decreased to less than 5.0 mg L^{-1}, typically only lasted for a few hours, while the longest was sustained for over 5 days. When exposed to these excursions, the maturation state of the plaque determined whether adhesion strength was negatively affected. An acidic excursion (pH 5.0) early in the curing process (day 1-6) caused a delay in plaque strengthening, while sustained hypoxic conditions (~1 mg L^{-1}) after the curing window had passed (day 8-13), was sufficient to cause plaque weakening. However, any negative affect of acidification or hypoxia was reversible, given that the material was allowed time to recover under favorable conditions. These results stress that, while environmental variability in the nearshore can affect the adhesion mechanism that mussels use to attach to surfaces, the timing and duration of these harmful conditions may modulate their ultimate impact on mussel attachment.

Hypoxic and acidic conditions have been shown previously to arrest the curing process of byssus plaques, causing the material to peel from surfaces at lower forces than when fully matured (George et al. unpublished, George and Carrington 2018). Both a basic pH and high

oxygen availability are needed for the conversion of DOPA residues to DOPA-quinone (Haemers et al. 2002, 2003), a post-translationally modified amino acid that is responsible for the formation of covalent cross-links between Mfps in the adhesive (McDowell et al. 1999, Zhao and Waite 2006, Miserez et al. 2010). While the cross-linking behavior of specific Mfps is well understood (Fant et al. 2000, 2002), the cross-linking kinetics of the entire network of Mfps present within the plaque is not, particularly in the context of variability in the surrounding seawater environment (Waite and Broomell 2012). In light of the fact that plaques are constantly inundated with unfavorable conditions during the curing process, it remains unclear from the molecular mechanics of Mfp cross-linking whether plaque strengthening is irrevocably damaged by environmental conditions or just delayed, two possibilities that could have very different outcomes for a mussel that depends on strong attachment for survival.

To test these two hypotheses, plaques in this study were exposed to hypoxic and acidic excursions during either early in the curing process (day 1-5) or after they were fully mature (day 8-13). Matching the worst case scenario from our field surveys, plaques were exposed to excursions for 5 days, after which conditions returned to that of the open-ocean and plaques continued to age until they were 20 days old. Early exposure to acidic conditions (pH=5) during plaque curing effectively delayed strengthening, causing the material to be weaker at 5 and 8 days, while exposure following the curing period did not cause significant weakening. The opposite was true for hypoxia (O_2 < 2 mg L^{-1}), with plaque curing proceeding normally when exposure occurred during the curing window, but then decreasing in adhesion strength when deprived of oxygen after maturation. However, in both of the cases where plaque weakening was observed, adhesion strength increased when affected plaques were allowed to continue curing in

open-ocean conditions, effectively recovering from any negative impact of the local seawater environment.

The dynamic response of the plaque to pH and oxygen excursions in this study confirm that, while basic pH and dissolved oxygen are required for plaque strengthening, the curing process can start and stop based on the presence or absence of these conditions. Additionally, there was no evidence that plaques were permanently damaged by unfavorable conditions; mature plaques weakened by hypoxia in this study were able to recover when incubated in sufficiently high oxygen concentrations for 8 days. Placed in the context of DOPA-quinone cross-linking, these results mimic those found in the distal region of the thread, a material that is known for reforming sacrificial His-metal coordinate cross-links after they are broken during the extension of the thread (Harrington and Waite 2007, Harrington et al. 2009). While the role of metal-coordination within the protein network of the plaque remains to be explored, the plaque cuticle (Mfp-1) is known to form increasingly stable mono-, bis-, and tris-(DOPA)Fe^{3+} complexes as pH increases above a pH of 5.5, increasing the cohesive strength of the structure (Taylor et al. 1996, Xu 2013, Yang et al. 2016).

Over three years of measurements from underneath a mussel raft indicate that the vertical position in the water column can influence the type of environmental variation that mussels experience. For mussels at the surface, the temperature (5.3-24.1^{o}C) and salinity (2.1-33.0 PSU) of seawater flowing through culture lines were the most variable, while mussels living just 6 m deeper experienced a broader range of pH (7.14-8.58) and dissolved oxygen concentrations (0.1-18.5 mg L^{-1}). However, a positive correlation of pH and dissolved oxygen was universal, leading to the co-occurrence of hypoxia and acidification at both depths, particularly during the summer months. The timing of these events implies that, rather than being driven by the upwelling of

oxygen depleted waters from off-shore that typically occur in the winter months (Peterson et al. 1988), the net effect of biological processes (respiration, photosynthesis, etc.) could be responsible for moderating the carbonate chemistry in this nearshore habitat (Feely et al. 2010, Baumann and Smith 2017). This is highly likely within mussel aquaculture rafts due to the large biomass of mussels that support dense epifaunal communities, often comprising hundreds of other species (Tenore and Gonzalez 1976).

While the seawater between culture lines represented a significant departure from conditions found in the open-ocean, even the most extreme values of pH and oxygen observed within these spaces were overshadowed by the mean conditions within mussel aggregations. At depth during the summer, seawater pH routinely fell 2-4 units below values recorded by raft sensors placed less than one meter away, while dissolved oxygen decreased by 2-6 mg L^{-1}. These kinds of excursions typically lasted only a few hours, with the longest lasting just over five days, exposing threads to both pH and oxygen conditions that have been deemed to be harmful to the curing process (George et al. unpublished, George and Carrington 2018). While not directly measured in this study, one possible explanation that could account for such a dramatic decrease in pH and oxygen is the formation of a thick diffusive boundary layers (DBL) around aggregations. Given a sufficient flow reduction through culture lines, a DBL would limit the diffusion of CO_2 away from the organisms, effectively trapping conditions along the rope line. As a point of reference, increases in DBL thickness have been shown to decrease oxygen availability surrounding corals (Shashar et al. 1993), decreasing the respiration rate and primary production of reefs (Patterson et al. 1991), while the efflux of O_2 away from seagrasses has been found to be reliant on the hydrodynamic thinning of the DBL (Larkum et al. 1989, Koch 1994), ultimately leading to an increase in photosynthetic rate (Mass et al. 2010).

While a promising explanation for hourly pH and oxygen excursions, increased thickness of the DBL surrounding aggregations is unlikely to result in the persistent hypoxia and acidification observed in this study. Within mussel aggregations, excursions in pH (<7.0) and oxygen (<5.0) were maintained for more than 5 days in the summer at depth, necessitating a flow reduction over a timescale that is not typically seen underneath aquaculture rafts (Blanco et al. 1996, Grant and Bacher 2001, Aguiar et al. 2017) or in tidally driven nearshore systems (Cahalan et al. 1989, Leonard et al. 1998). Alternatively, the fact that pH and oxygen excursions of this magnitude almost exclusively occurred at 7 meters during the late summer could be explained by an accelerated accumulation of particulate organic matter (POM), driven by an increase in primary productivity (Wieters et al. 2003). When feeding on phytoplankton blooms near the surface (Winter et al. 1975), mussel feces and pseudofeces can also accumulate on the seafloor, forming a layer of 'mussel mud' that can be several meters thick at the end of a growing season (Davies et al. 1980, Chamberlain et al. 2001). Without adequate flow to remove sediments, high summer seawater temperatures at depth can accelerate the decomposition of mussel mud, promoting the growth of bacterial communities (Dahlbäck and Gunnarsson 1981), and eventually leading to hypoxic and acidic conditions (Pearson and Rosenberg 1978). Further investigations in the bacterial community structure and flow environment present within mussel aggregations are needed to identify whether the environmental variation observed in this study is the result of geophysical or biological forces.

Regardless of their cause, when exposed to excursions in seawater pH and dissolved oxygen directly, mussels refrained from making threads as conditions got progressively worse. Thread production stopped for the first three days of exposure at a pH of 6.0, with almost no mussels producing threads at pH 5.0 over the entire 7-day exposure. A similar result was seen

under hypoxia, with mussels refraining from making threads for the first day, and producing minimal threads thereafter. Likely a behavioral response to stressful physiological conditions (Gudimov 2006), intertidal mussels routinely remain closed for extended periods of time during low tide in order to lower predation risk and water loss (Lent 1968). In subtidal habitats, mussels close the valves of their shell when the chemical conditions of the ocean are physiologically harmful (Gleason et al. 2017), perhaps as an attempt wait out stressful conditions before reopening. However, there is evidence that this strategy may not be effective long term, as the functionality of the abductor muscle actually diminishing after high temperature stress (Dowd and Somero 2013), decreasing a mussel's ability to resist damage from further excursions. Either way, mussels cannot protect byssal threads from unfavorable conditions after they are made, or predict when conditions will be bad in order to protect them from exposure. As a result, threads that are made under favorable pH and oxygen conditions are vulnerable to excursions while they proceed through their cure window (1-8 days after deposition).

Although seawater pH and dissolved oxygen had a significant effect on plaque adhesion strength and thread production in this study, additional work is needed in order to link environmental conditions to the fall-off events that are commonly seen in mussel mariculture. Higher resolution measurements of pH and oxygen conditions in mussel aggregations are needed in order to show that conditions truly remain unfavorable for plaque adhesion for days at a time without occasional increases back to baseline conditions. Given the ability of the plaque to recover and continue strengthening after the curing process is arrested, even intermittent changes in flow through rafts could serve to rescue mussel attachment by increasing the flux of oxygen to the byssus. This process may occur naturally, as mussel in high densities often undergo processes such as self-thinning where competition-driven mortality causes mussels to fall-off of when

conditions are too stagnant, increasing the space between individuals (Fréchette and Lefaivre 1995, Lachance-Bernard et al. 2010). Although not yet shown experimentally, evidence for the relationship between oxygen flux and attachment strength can be seen in mussel beds where animals at the perimeter have a higher attachment strength than those in the interior (Witman and Suchanek 1984) and when comparing the superior strength of solitary mussels to those in aggregations (Bell and Gosline 1997).

This study demonstrates that the pH and dissolved oxygen variability that mussels currently experience on culture lines can (1) prevent plaque curing, (2) weaken mature plaques, and (3) decrease thread production. In light of this finding, the challenge for shellfish growers going forward is to adopt farming practices that ensure mussels attach under favorable seawater conditions, particularly as the frequency and magnitude of excursions in seawater temperature (Roemmich et al. 2015, Wijffels et al. 2016), pH (Woosley et al. 2016), and dissolved oxygen (Stramma et al. 2010, Gobler and Baumann 2016) continue to increase. The results presented here suggest that growers can promote adequate strengthening and adhesion recovery by ensuring an adequate flux of dissolved oxygen to the site of adhesion, either through regular thinning of culture lines, increasing line spacing, or by reducing stocking densities.

3.6. Competing interests

The authors of the manuscript have no competing interests.

3.7. Author's contributions

MNG designed the study, calibrated water quality sensors, conducted laboratory experiments, performed mechanical testing, and wrote the manuscript. JA and JH preformed tensometer

testing and aided in experimental design of fluctuating pH and oxygen experiment. EC conceived of the study, aided in data analysis, and edited the manuscript. All authors gave final approval for publication.

3.8. Acknowledgements

We thank Dominic Pangelinan, Ian Jefferds, and all the mussel growers of Penn Cove Shellfish for their assistance with transportation, organism collection, and sensor maintenance. We also thank Laura Marsh and Molly Roberts for contributing artwork and images included in figures. Data are archived under project #2250 at www.bco-dmo.org.

3.9. Funding

This work was supported, in part, by an NSF GFRP fellowship to MNG [#DGE-1256082], NSF award to EC [#OCE-1041213], and a Royalty Research Fund award to EC [#A97940]. Water quality monitoring at Penn Cove Shellfish was made possible by a Washington Sea Grant award to EC and Carolyn Friedman. The efforts of EC were supported while serving at the National Science Foundation. Any opinion, findings, and conclusions or recommendations expressed in this material are those of the author(s) and do not necessarily reflect the views of the National Science Foundation.

3.10. References

Aguiar, E., Piedracoba, S., Álvarez-Salgado, X.A., and Labarta, U. 2017. Circulation of water through a mussel raft: clearance area vs. idealized linear flows. Rev. Aquac. 9(1): 3–22. doi:10.1111/raq.12099.

Anderson, T.H., Yu, J., Estrada, A., Hammer, M.U., Waite, J.H., and Israelachvili, J.N. 2010. The contribution of DOPA to substrate–peptide adhesion and internal cohesion of mussel-inspired synthetic peptide films. Adv. Funct. Mater. 20(23): 4196–4205. doi:10.1002/adfm.201000932.

Bakun, A., Black, B.A., Bograd, S.J., Garcia-Reyes, M., Miller, A.J., Rykaczewski, R.R., and Sydeman, W.J. 2015. Anticipated effects of climate change on coastal upwelling ecosystems. Curr. Clim. Change Rep. 1(2): 85–93.

Baumann, H., and Smith, E.M. 2017. Quantifying metabolically driven pH and oxygen fluctuations in US nearshore habitats at diel to interannual time scales. Estuaries Coasts: 1–16.

Bell, E., and Gosline, J. 1996. Mechanical design of mussel byssus: material yield enhances attachment strength. J. Exp. Biol. 199(4): 1005–1017.

Bell, E., and Gosline, J. 1997. Strategies for life in flow: tenacity, morphometry, and probability of dislodgment of two Mytilus species. Mar. Ecol. Prog. Ser. 159: 197–208.

Blanco, J., Zapata, M., and Moro o, A. 1996. Some aspects of the water flow through mussel rafts. Sci. Mar. 60: 275–282.

Brenner, M., and Buck, B.H. 2010. Attachment properties of blue mussel (Mytilus edulis L.) byssus threads on culture-based artificial collector substrates. Aquac. Eng. 42(3): 128–139. doi:10.1016/j.aquaeng.2010.02.001.

Burkett, J.R., Wojtas, J.L., Cloud, J.L., and Wilker, J.J. 2009. A method for measuring the adhesion strength of marine mussels. J. Adhes. 85(9): 601–615. doi:10.1080/00218460902996903.

Cahalan, J.A., Siddall, S.E., and Luckenbach, M.W. 1989. Effects of flow velocity, food concentration and particle flux on growth rates of juvenile bay scallops< i> Argopecten irradians. J. Exp. Mar. Biol. Ecol. 129(1): 45–60.

Carrington, E. 2002. Seasonal variation in the attachment strength of blue mussels: causes and consequences. Limnol. Oceanogr. 47(6): 1723–1733. doi:10.4319/lo.2002.47.6.1723.

Carrington, E., Waite, J.H., Sarà, G., and Sebens, K.P. 2015. Mussels as a model system for integrative ecomechanics. Annu. Rev. Mar. Sci. 7(1): 443–469. doi:10.1146/annurev-marine-010213-135049.

Chamberlain, J., Fernandes, T.F., Read, P., Nickell, T.D., and Davies, I.M. 2001. Impacts of biodeposits from suspended mussel (Mytilus edulis L.) culture on the surrounding surficial sediments. ICES J. Mar. Sci. 58(2): 411–416.

Christensen, P.B., Glud, R.N., Dalsgaard, T., and Gillespie, P. 2003. Impacts of longline mussel farming on oxygen and nitrogen dynamics and biological communities of coastal sediments. Aquaculture 218(1–4): 567–588.

Comyn, J. 1981. The relationship between joint durability and water diffusion. In Developments in Adhesives. ed AJ Kinloch. Applied Science Publishers, Barking, UK. pp. 279–313.

Dahlbäck, B., and Gunnarsson, L. 1981. Sedimentation and sulfate reduction under a mussel culture. Mar. Biol. 63(3): 269–275.

van Dam, J.W., Negri, A.P., Uthicke, S., and Mueller, J.F. 2011. Chemical pollution on coral reefs: exposure and ecological effects. Ecol. Impacts Toxic Chem.: 187–211.

Danner, E.W., Kan, Y., Hammer, M.U., Israelachvili, J.N., and Waite, J.H. 2012. Adhesion of mussel foot protein Mefp-5 to mica: an underwater superglue. Biochemistry (Mosc.) 51(33): 6511–6518.

Davies, G., Dare, P.J., and Edwards, D.B. 1980. Fenced enclosures for the protection of seed mussels (Mytilus edulis L.) from predation by shore crabs (Carcinus maenas L.). Ministry of Agriculture, Fisheries and Food. Directorate of Fisheries Research.

Desmond, K.W., Zacchia, N.A., Waite, J.H., and Valentine, M.T. 2015. Dynamics of mussel plaque detachment. Soft Matter 11(34): 6832–6839. doi:10.1039/C5SM01072A.

Doney, S.C., Fabry, V.J., Feely, R.A., and Kleypas, J.A. 2009. Ocean Acidification: The Other CO2 Problem. Annu. Rev. Mar. Sci. 1(1): 169–192. doi:10.1146/annurev.marine.010908.163834.

Doney, S.C., Ruckelshaus, M., Duffy, J.E., Barry, J.P., Chan, F., English, C.A., Galindo, H.M., Grebmeier, J.M., Hollowed, A.B., and Knowlton, N. 2011. Climate change impacts on marine ecosystems. Annu. Rev. Mar. Sci. 4: 11–37. doi:10.1146/annurev-marine-041911-111611.

Dowd, W.W., and Somero, G.N. 2013. Behavior and survival of Mytilus congeners following episodes of elevated body temperature in air and seawater. J. Exp. Biol. 216(3): 502–514.

Edgar Santos Fernandez. 2014. Johnson: Johnson Transformation. R package version 1.4. Available from https://CRAN.R-project.org/package=Johnson.

Fant, C., Elwing, H., and Höök, F. 2002. The influence of cross-linking on protein-protein interactions in a marine adhesive: the case of two byssus plaque proteins from the blue mussel. Biomacromolecules 3(4): 732–741. doi:10.1021/bm025506j.

Fant, C., Sott, K., Elwing, H., and Hook, F. 2000. Adsorption behavior and enzymatically or chemically induced cross-linking of a mussel adhesive protein. Biofouling 16(2–4): 119–132. doi:10.1080/08927010009378437.

FAO. 2017. FAO Yearbook. Fishery and Aquaculture Statistics. 2015.

Feely, R.A., Alin, S.R., Newton, J., Sabine, C.L., Warner, M., Devol, A., Krembs, C., and Maloy, C. 2010. The combined effects of ocean acidification, mixing, and respiration on pH and carbonate saturation in an urbanized estuary. Estuar. Coast. Shelf Sci. 88(4): 442–449.

Förstner, U., and Wittmann, G.T. 2012. Metal pollution in the aquatic environment. Springer Science & Business Media.

Fréchette, M., and Lefaivre, D. 1995. On self-thinning in animals. Oikos: 425–428.

George, M.N., and Carrington, E. 2018. Environmental post-processing increases the adhesion strength of mussel byssus adhesive. Biofouling. doi:10.1080/08927014.2018.1453927.

Gleason, L.U., Miller, L.P., Winnikoff, J.R., Somero, G.N., Yancey, P.H., Bratz, D., and Dowd, W.W. 2017. Thermal history and gape of individual Mytilus californianus correlate with oxidative damage and thermoprotective osmolytes. J. Exp. Biol. 220(22): 4292–4304.

Gobler, C.J., and Baumann, H. 2016. Hypoxia and acidification in ocean ecosystems: coupled dynamics and effects on marine life. Biol. Lett. 12(5): 20150976.

Grant, J., and Bacher, C. 2001. A numerical model of flow modification induced by suspended aquaculture in a Chinese bay. Can. J. Fish. Aquat. Sci. 58(5): 1003–1011. doi:10.1139/f01-027.

Gudimov, A.V. 2006. Behavior of blue mussels (Mytilus edulis L.) under the fluctuating environmental conditions. In Doklady Biological Sciences. Springer. pp. 314–316.

Haemers, S., Koper, G.J., and Frens, G. 2003. Effect of oxidation rate on cross-linking of mussel adhesive proteins. Biomacromolecules 4(3): 632–640. doi:10.1021/bm025707n.

Haemers, S., van der Leeden, M.C., Koper, G.J., and Frens, G. 2002. Cross-linking and multilayer adsorption of mussel adhesive proteins. Langmuir 18(12): 4903–4907. doi:10.1021/la025626c.

Harrington, M.J., Gupta, H.S., Fratzl, P., and Waite, J.H. 2009. Collagen insulated from tensile damage by domains that unfold reversibly:< i> In situ X-ray investigation of mechanical yield and damage repair in the mussel byssus. J. Struct. Biol. 167(1): 47–54.

Harrington, M.J., and Waite, J.H. 2007. Holdfast heroics: comparing the molecular and mechanical properties of Mytilus californianus byssal threads. J. Exp. Biol. 210(24): 4307–4318.

Hwang, D.S., Zeng, H., Srivastava, A., Krogstad, D.V., Tirrell, M., Israelachvili, J.N., and Waite, J.H. 2010. Viscosity and interfacial properties in a mussel-inspired adhesive coacervate. Soft Matter 6(14): 3232–3236.

Kamino, K. 2008. Underwater adhesive of marine organisms as the vital link between biological science and material science. Mar. Biotechnol. 10(2): 111–121. doi:10.1007/s10126-007-9076-3.

Koch, E.W. 1994. Hydrodynamics, diffusion-boundary layers and photosynthesis of the seagrasses Thalassia testudinum and Cymodocea nodosa. Mar. Biol. 118(4): 767–776.

Lachance-Bernard, M., Daigle, G., Himmelman, J.H., and Fréchette, M. 2010. Biomass–density relationships and self-thinning of blue mussels (Mytilus spp.) reared on self-regulated longlines. Aquaculture 308(1–2): 34–43.

Larkum, A.W., Roberts, G., Kuo, J., and Strother, S. 1989. Gaseous movement in seagrasses. In Biology of seagrasses: a treatise on the biology of seagrasses with special reference to the Australian region. Edited by A.W. Larkum, A.J. McComb, and S.A. Shephard. Elsevier Science Pub., New York. pp. 686–722.

Lee, B.P., Messersmith, P.B., Israelachvili, J.N., and Waite, J.H. 2011. Mussel-inspired adhesives and coatings. Annu. Rev. Mater. Res. 41: 99. doi:10.1146/annurev-matsci-062910-100429.

Lent, C.M. 1968. Air-gaping by the ribbed mussel, Modiolus demissus (Dillwyn): effects and adaptive significance. Biol. Bull. 134(1): 60–73.

Leonard, G.H., Levine, J.M., Schmidt, P.R., and Bertness, M.D. 1998. Flow-driven variation in intertidal community structure in a Maine estuary. Ecology 79(4): 1395–1411. doi:10.1890/0012-9658(1998)079[1395:FDVIIC]2.0.CO;2.

Levin, L., Ekau, W., Gooday, A., Jorissen, F., Middelburg, J., Naqvi, S., Neira, C., Rabalais, N., and Zhang, J. 2009. Effects of natural and human-induced hypoxia on coastal benthos. Biogeosciences 6(10): 2063–2098.

Lim, S., Choi, Y.S., Kang, D.G., Song, Y.H., and Cha, H.J. 2010. The adhesive properties of coacervated recombinant hybrid mussel adhesive proteins. Biomaterials 31(13): 3715–3722.

Lindahl, O., Hart, R., Hernroth, B., Kollberg, S., Loo, L.-O., Olrog, L., Rehnstam-Holm, A.-S., Svensson, J., Svensson, S., and Syversen, U. 2005. Improving marine water quality by mussel farming: a profitable solution for Swedish society. AMBIO J. Hum. Environ. 34(2): 131–138. doi:10.1579/0044-7447-34.2.131.

Lozano, S., Iribarren, D., Moreira, M.T., and Feijoo, G. 2010. Environmental impact efficiency in mussel cultivation. Resour. Conserv. Recycl. 54(12): 1269–1277.

Martinez Rodriguez, N.R., Das, S., Kaufman, Y., Israelachvili, J.N., and Waite, J.H. 2015. Interfacial pH during mussel adhesive plaque formation. Biofouling 31(2): 221–227. doi:10.1080/08927014.2015.1026337.

Martz, T.R., Connery, J.G., and Johnson, K.S. 2010. Testing the Honeywell Durafet® for seawater pH applications. Limnol. Oceanogr. Methods 8: 172–184. doi:10.4319/lom.2010.8.172.

Mass, T., Genin, A., Shavit, U., Grinstein, M., and Tchernov, D. 2010. Flow enhances photosynthesis in marine benthic autotrophs by increasing the efflux of oxygen from the organism to the water. Proc. Natl. Acad. Sci. 107(6): 2527–2531.

McDowell, L.M., Burzio, L.A., Waite, J.H., and Schaefer, J. 1999. Rotational echo double resonance detection of cross-links formed in mussel byssus under high-flow stress. J. Biol. Chem. 274(29): 20293–20295. doi:10.1074/jbc.274.29.20293.

Miller, D.R., Spahn, J.E., and Waite, J.H. 2015. The staying power of adhesion-associated antioxidant activity in Mytilus californianus. J. R. Soc. Interface 12(111): 20150614. doi:10.1098/rsif.2015.0614.

Miserez, A., Rubin, D., and Waite, J.H. 2010. Cross-linking chemistry of squid beak. J. Biol. Chem. 285(49): 38115–38124. doi:10.1074/jbc.M110.161174.

Moeser, G.M., and Carrington, E. 2006. Seasonal variation in mussel byssal thread mechanics. J. Exp. Biol. 209(10): 1996–2003. doi:10.1242/jeb.02234.

Nicklisch, S.C., Spahn, J.E., Zhou, H., Gruian, C.M., and Waite, J.H. 2016. Redox capacity of an extracellular matrix protein associated with adhesion in Mytilus californianus. Biochemistry (Mosc.) 55(13): 2022. doi:10.1021/acs.biochem.6b00044.

O'Donnell, M.J., George, M.N., and Carrington, E. 2013. Mussel byssus attachment weakened by ocean acidification. Nat. Clim. Change 3(6): 587–590. doi:10.1038/nclimate1846.

Patterson, M.R., Sebens, K.P., and Olson, R.R. 1991. In situ measurements of flow effects on primary production and dark respiration in reef corals. Limnol. Oceanogr. 36(5): 936–948.

Pearson, T.H., and Rosenberg, R. 1978. Macrobenthic succession in relation to organic enrichment and pollution of the marine environment. Ocean. Mar Biol Ann Rev 16: 229–311.

Peterson, W.T., Arcos, D.F., McMANuS, G.B., Dam, H., Bellantoni, D., Johnson, T., and Tiselius, P. 1988. The nearshore zone during coastal upwelling: daily variability and coupling between primary and secondary production off central Chile. Prog. Oceanogr. 20(1): 1–40.

Pinheiro, J., Bates, D., DebRoy, S., Sarkar, D., and R Core Team. 2017. nlme: Linear and Nonlinear Mixed Effects Models. R package version 3.1-131. Available from https://CRAN.R-project.org/package=nlme.

Roemmich, D., Church, J., Gilson, J., Monselesan, D., Sutton, P., and Wijffels, S. 2015. Unabated planetary warming and its ocean structure since 2006. Nat. Clim. Change 5(3): 240.

Ryan, J.A., and Ulrich, J.M. 2017. quantmod: Quantitative Financial Modelling Framework. Available from https://CRAN.R-project.org/package=quantmod.

Rysgaard, S., Mortensen, J., Juul-Pedersen, T., Sørensen, L.L., Lennert, K., Søgaard, D.H., Arendt, K.E., Blicher, M.E., Sejr, M.K., and Bendtsen, J. 2012. High air–sea CO2 uptake rates in nearshore and shelf areas of Southern Greenland: Temporal and spatial variability. Mar. Chem. 128: 26–33. doi:10.1016/j.marchem.2011.11.002.

Shashar, N., Cohen, Y., and Loya, Y. 1993. Extreme diel fluctuations of oxygen in diffusive boundary layers surrounding stony corals. Biol. Bull. 185(3): 455–461.

Shaw, M., Furnas, M.J., Fabricius, K., Haynes, D., Carter, S., Eaglesham, G., and Mueller, J.F. 2010. Monitoring pesticides in the great barrier reef. Mar. Pollut. Bull. 60(1): 113–122. doi:10.1016/j.marpolbul.2009.08.026.

Shumway, S.E., Davis, C., Downey, R., Karney, R., Kraeuter, J., Parsons, J., Rheault, R., and Wikfors, G. 2003. Shellfish aquaculture–in praise of sustainable economies and environments. World Aquac. 34(4): 8–10.

Stramma, L., Schmidtko, S., Levin, L.A., and Johnson, G.C. 2010. Ocean oxygen minima expansions and their biological impacts. Deep Sea Res. Part Oceanogr. Res. Pap. 57(4): 587–595.

Strohmeier, T., Aure, J., Duinker, A., Castberg, T., Svardal, A., and Strand, Ø. 2005. Flow reduction, seston depletion, meat content and distribution of diarrhetic shellfish toxins in a long-line blue mussel (Mytilus edulis) farm. J. Shellfish Res. 24(1): 15–23.

Tamarin, A., Lewis, P., and Askey, J. 1976. The structure and formation of the byssus attachment plaque in Mytilus. J. Morphol. 149(2): 199–221.

Taylor, S.W., Chase, D.B., Emptage, M.H., Nelson, M.J., and Waite, J.H. 1996. Ferric ion complexes of a DOPA-containing adhesive protein from Mytilus edulis. Inorg. Chem. 35(26): 7572–7577. doi:10.1021/ic960514s.

Tenore, K.R., and Gonzalez, N. 1976. Food chain patterns in the Ria de Arosa, Spain: an area of intense mussel aquaculture. In Population dynamics. G. Persoone and E. Jaspers, Ostend, Belgium. pp. 601–609.

Troell, M., Joyce, A., Chopin, T., Neori, A., Buschmann, A.H., and Fang, J.-G. 2009. Ecological engineering in aquaculture—potential for integrated multi-trophic aquaculture (IMTA) in marine offshore systems. Aquaculture 297(1–4): 1–9.

Vernberg, F.J., and Vernberg, W.B. 2013. Pollution and physiology of marine organisms. Elsevier.

Waite, H. 1983. Adhesion in byssally attached bivalves. Biol. Rev. 58(2): 209–231. doi:10.1111/j.1469-185X.1983.tb00387.x.

Waite, J.H. 1985. Catechol oxidase in the byssus of the common mussel, Mytilus edulis L. J. Mar. Biol. Assoc. U. K. 65(2): 359–371. doi:10.1017/S0025315400050487.

Waite, J.H., and Broomell, C.C. 2012. Changing environments and structure–property relationships in marine biomaterials. J. Exp. Biol. 215(6): 873–883. doi:10.1242/jeb.058925.

Waite, J.H., and Qin, X. 2001. Polyphosphoprotein from the adhesive pads of Mytilus edulis. Biochemistry (Mosc.) 40(9): 2887–2893. doi:10.1021/bi002718x.

Wang, D., Gouhier, T.C., Menge, B.A., and Ganguly, A.R. 2015. Intensification and spatial homogenization of coastal upwelling under climate change. Nature 518(7539): 390. doi:10.1038/nature14235.

Wei, W., Tan, Y., Rodriguez, N.R.M., Yu, J., Israelachvili, J.N., and Waite, J.H. 2014. A mussel-derived one component adhesive coacervate. Acta Biomater. 10(4): 1663–1670. doi:10.1016/j.actbio.2013.09.007.

Whitmarsh, D.J., Cook, E.J., and Black, K.D. 2006. Searching for sustainability in aquaculture: an investigation into the economic prospects for an integrated salmon–mussel production system. Mar. Policy 30(3): 293–298.

Wieters, E.A., Kaplan, D.M., Navarrete, S.A., Sotomayor, A., Largier, J., Nielsen, K.J., and Veliz, F. 2003. Alongshore and temporal variability in chlorophyll a concentration in Chilean nearshore waters. Mar. Ecol. Prog. Ser. 249: 93–105.

Wijffels, S., Roemmich, D., Monselesan, D., Church, J., and Gilson, J. 2016. Ocean temperatures chronicle the ongoing warming of Earth. Nat. Clim. Change 6(2): 116.

Winter, D.F., Banse, K., and Anderson, G.C. 1975. The dynamics of phytoplankton blooms in puget sound a fjord in the northwestern united states. Mar. Biol. 29(2): 139–176.

Witman, J.D., and Suchanek, T.H. 1984. Mussels in flow: drag and dislodgement by epizoans. Mar. Ecol. Prog. Ser.: 259–268.

Woosley, R.J., Millero, F.J., and Wanninkhof, R. 2016. Rapid anthropogenic changes in CO2 and pH in the Atlantic Ocean: 2003–2014. Glob. Biogeochem. Cycles 30(1): 70–90.

Xu, H., Nishida, J., Ma, W., Wu, H., Kobayashi, M., Otsuka, H., and Takahara, A. 2012. Competition between oxidation and coordination in cross-linking of polystyrene copolymer containing catechol groups. ACS Macro Lett. 1(4): 457–460.

Xu, Z. 2013. Mechanics of metal-catecholate complexes: The roles of coordination state and metal types. Sci. Rep. 3: 2914. doi:10.1038/srep02914.

Yang, B., Lim, C., Hwang, D.S., and Cha, H.J. 2016. Switch of Surface Adhesion to Cohesion by Dopa-Fe3+ Complexation, in Response to Microenvironment at the Mussel Plaque/Substrate Interface. Chem. Mater. 28(21): 7982–7989. doi:10.1021/acs.chemmater.6b03676.

Young, G.A., and Crisp, D. 1982. Marine animals and adhesion. In K.W. Allend (ed.) Adhesion. Applied Science Publishers, Ltd., Barking, England. pp. 19–39.

Yu, J., Wei, W., Danner, E., Ashley, R.K., Israelachvili, J.N., and Waite, J.H. 2011. Mussel protein adhesion depends on interprotein thiol-mediated redox modulation. Nat. Chem. Biol. 7(9): 588–590. doi:10.1038/nchembio.630.

Zhao, H., and Waite, J.H. 2006. Linking adhesive and structural proteins in the attachment plaque of Mytilus californianus. J. Biol. Chem. 281(36): 26150–26158. doi:10.1074/jbc.M604357200.

3.11. Tables

Table 3.1. Seawater conditions (mean ± SD) during laboratory experiments wherein freshly made plaques cured in fluctuating pH and dissolved oxygen treatments. During each experiment, a baseline was set for both pH and oxygen approximating conditions found in the open ocean (control). For pH excursion experiments, pH (NBS) was reduced through the addition of CO_2, either 1 day after plaque deposition (Exp. 1), or 8 days (Exp. 2). For oxygen excursion experiments, dissolved oxygen (O_2) was reduced through the addition of N_2, either 1 (Exp. 3) or 8 days (Exp. 4) after deposition. In both cases, excursions lasted 5 days, after which variables returned to the stated baseline. Salinity (Sal) and seawater temperature (T) remained stable across all treatments.

Exp.	**Excursion (day)**		**pH (NBS)**		**O_2 (mg L^{-1})**		**Sal (PSU)**	**T (°C)**
	start	**end**	**baseline**	**excursion**	**baseline**	**excursion**		
Control			8.03 ± 0.04		8.54 ± 0.25		29 ± 1	8.8 ± 0.4
Exp. 1	1	6	8.01 ± 0.09	4.96 ± 0.03	8.33 ± 0.19		28 ± 2	9.1 ± 0.3
Exp. 2	8	13	8.04 ± 0.06	4.94 ± 0.06	8.36 ± 0.22		29 ± 1	9.1 ± 0.4
Exp. 3	1	6	7.98 ± 0.04		8.31 ± 0.37	1.13 ± 0.32	28 ± 2	8.8 ± 0.3
Exp. 4	8	13	7.98 ± 0.06		8.28 ± 0.26	1.59 ± 0.63	29 ± 2	9.2 ± 0.4

Table 3.2. Seawater conditions (mean ± SD) during laboratory experiments that investigated the effect of pH and oxygen excursions on thread production. Mussels were placed in each treatment condition for seven days, recording seawater pH, dissolved oxygen (O_2), temperature (T), and salinity (Sal) at 10 minute intervals.

Exp.	target	pH (NBS)	O_2 (mg L^{-1})	T (^oC)	Sal (PSU)
pH	8.0	8.15 ± 0.06	8.44 ± 0.88	8.9 ± 1.4	30 ± 2
	7.5	7.48 ± 0.09	8.48 ± 1.22	8.8 ± 0.9	29 ± 2
	7.0	6.83 ± 0.06	8.83 ± 0.81	9.2 ± 1.1	28 ± 1
	6.0	6.01 ± 0.02	8.70 ± 0.50	9.3 ± 0.6	29 ± 2
	5.0	5.03 ± 0.03	8.91 ± 0.73	9.1 ± 0.4	28 ± 1
O_2	> 8.0	8.10 ± 0.04	8.87 ± 0.45	8.8 ± 0.7	28 ± 1
	< 2.0	8.06 ± 0.05	0.93 ± 1.86	9.3 ± 0.9	28 ± 1

3.12. Figures

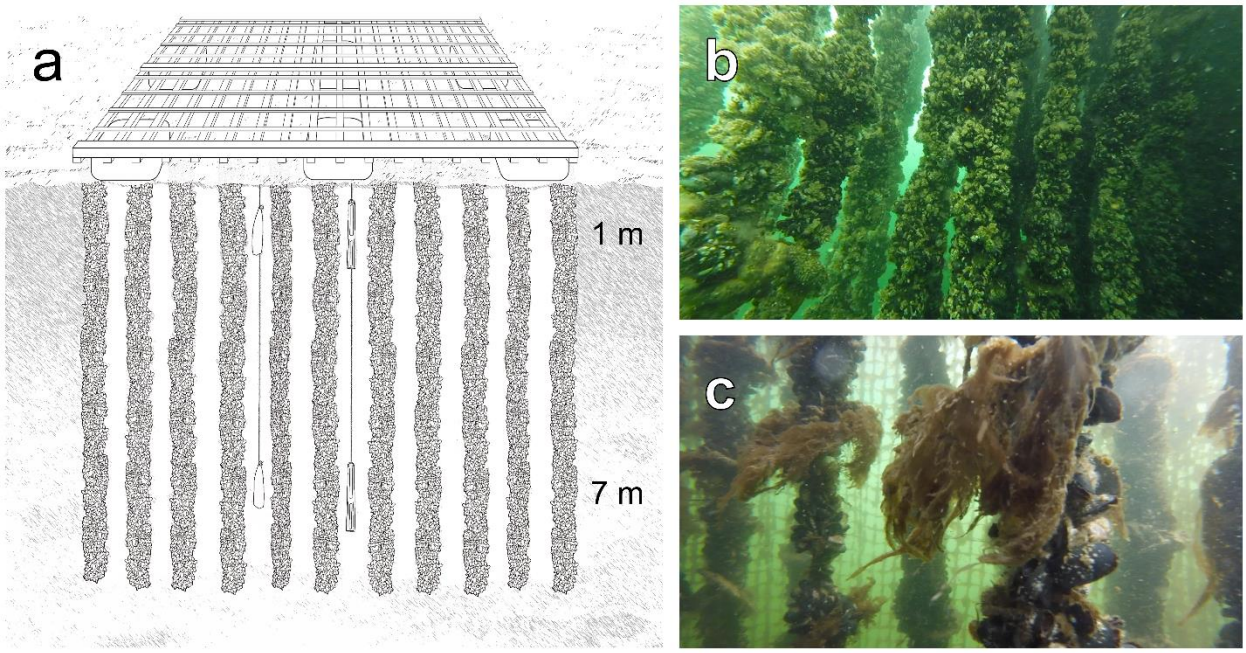

Figure 3.1. Simplified diagram of a mussel aquaculture raft with hanging rope lines (a), describing the position of hanging bags ('aggregation sensors', left) and YSI water quality sondes ('raft sensors', right). Rope lines were approximately 0.3 meters apart. Hanging bags were filled with mussels (~5 kg), with a pH and oxygen sensor embedded in the center of each bag. Aggregation and raft sensors recorded conditions every hour at two depths (1 and 7 meters below the surface). Mussel density on rope lines varied seasonally, with noticeable differences observed between spring (b) and late autumn (c), presumably due to fall-off events.

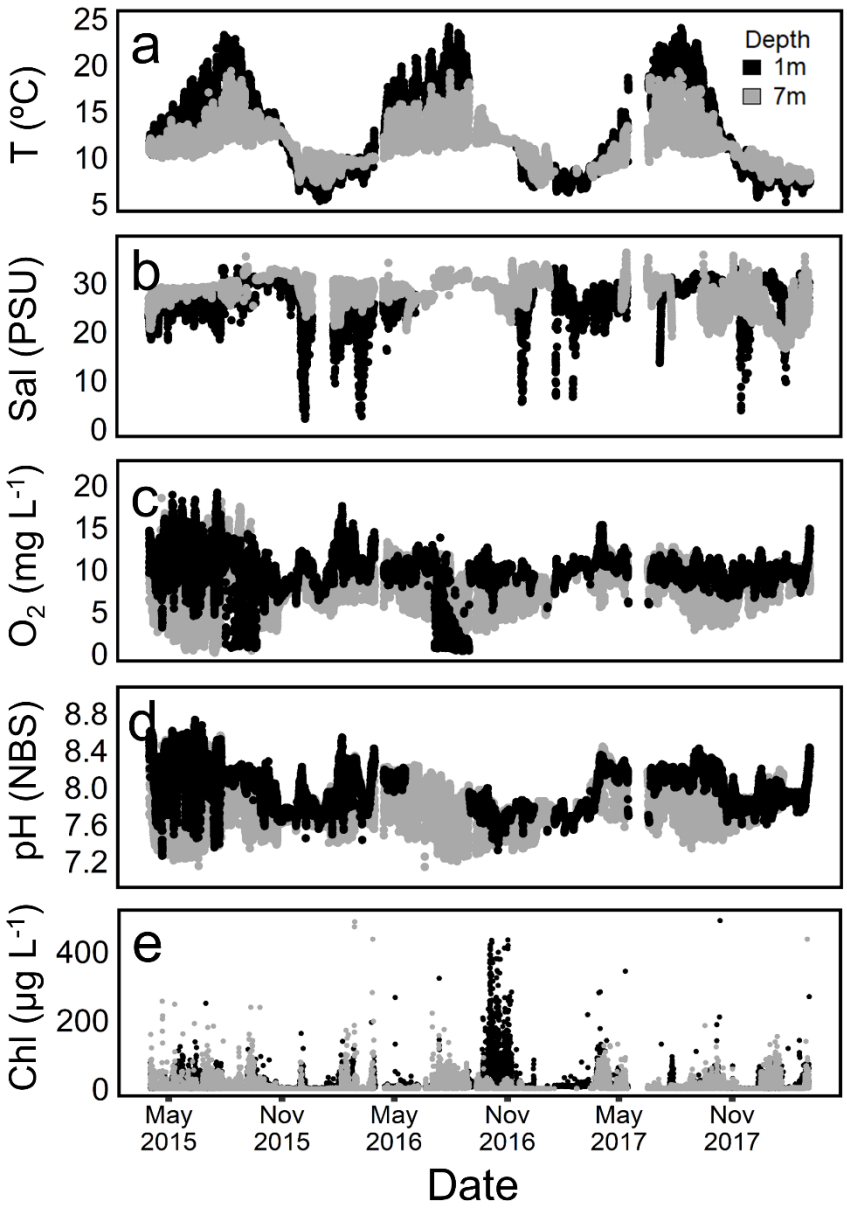

Figure 3.2. Seawater conditions underneath a mussel aquaculture raft in Quilcene bay, Quilcene, WA, from March, 2015 through March, 2018. Seawater temperature (a, ºC), salinity (b, PSU), dissolved oxygen concentration (c, mg L^{-1}), pH (d, NBS scale), and chlorophyll concentration (e, µg L^{-1}), were measured at two depths (1 and 7 meters) below the surface hanging two raft sensors between mussel lines. A summary of conditions by season is presented in Table S3.1.

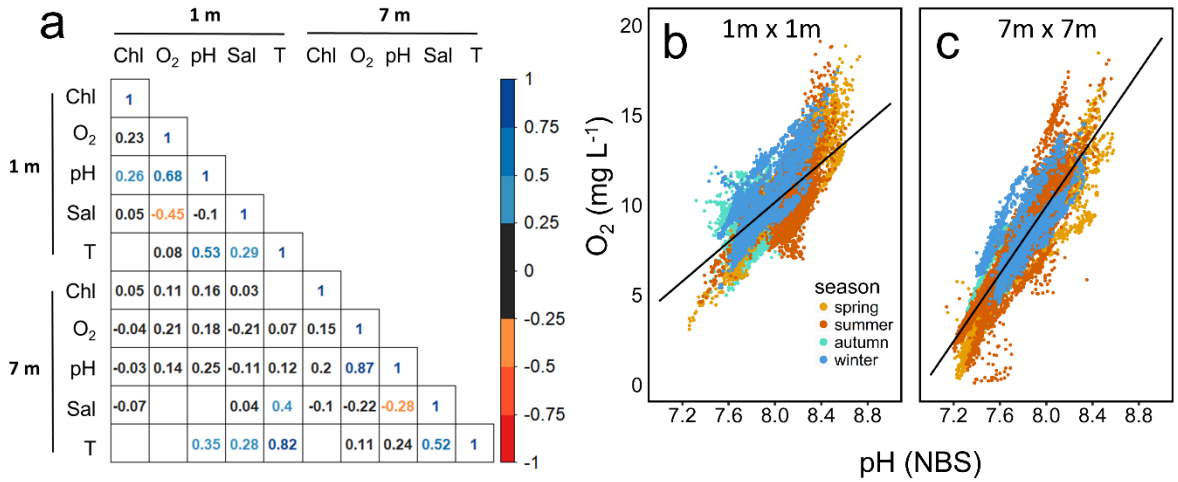

Figure 3.3. Seawater conditions recorded by raft sensors, at two depths below the surface (1 and 7 meters), were measured from March, 2015 through March, 2018. The pairwise Pearson's correlation test was used to generate a matrix of correlation coefficients for all parameters measured (a, alpha = 0.001). Dissolved oxygen (mg L^{-1}) was positively correlated with pH at 1 (b; slope = 5.13, R = 0.68) and 7 meters (c; slope = 9.31, R = 0.87). Datasets were color coded by season (spring = orange; summer = red; autumn = teal; winter = blue). A summary of all conditions measured, grouped by season is presented in Table S3.1.

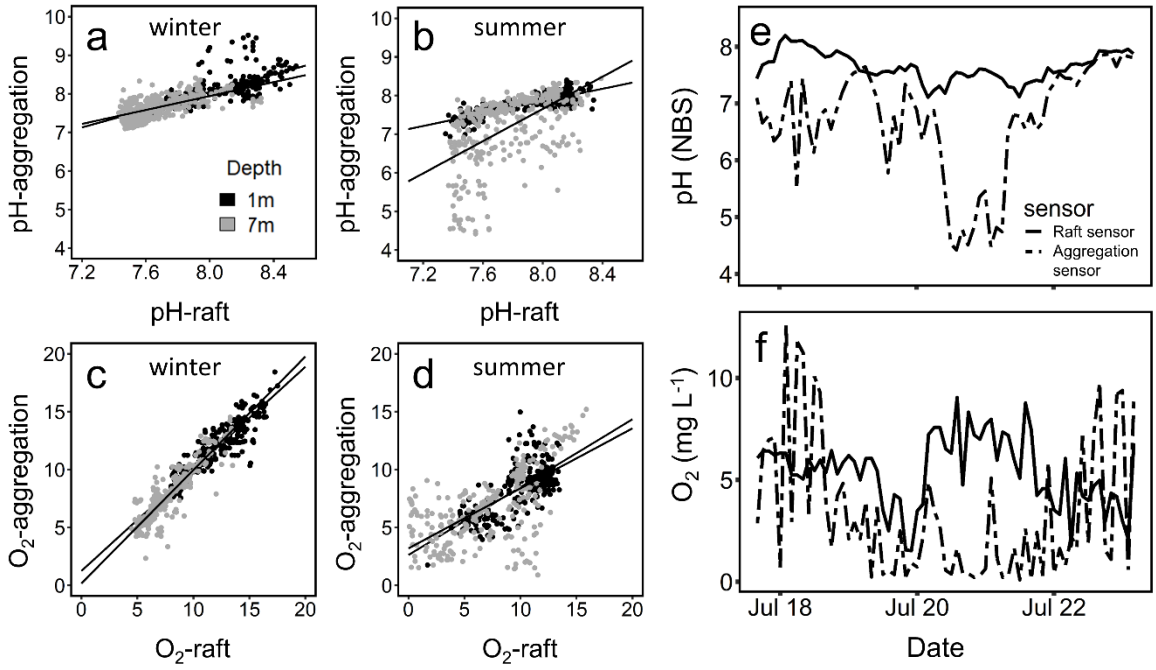

Figure 3.4. A comparison of seawater conditions (pH, dissolved oxygen concentration) found in mussel aggregation sensors and raft sensors. Measurements were taken during the summer and winter months of 2015, at two depths below the surface (1m, black; 7m, gray circles). Seawater pH (NBS) within mussel aggregations was tightly correlated with raft sensor measurements in the winter at both depths (a,c). In the summer, low pH and oxygen excursions were recorded at depth (b,d). A typical pH/oxygen excursion (7m; summer) that resulted in a mismatch between mussel aggregation and raft sensors is depicted in panels e and f.

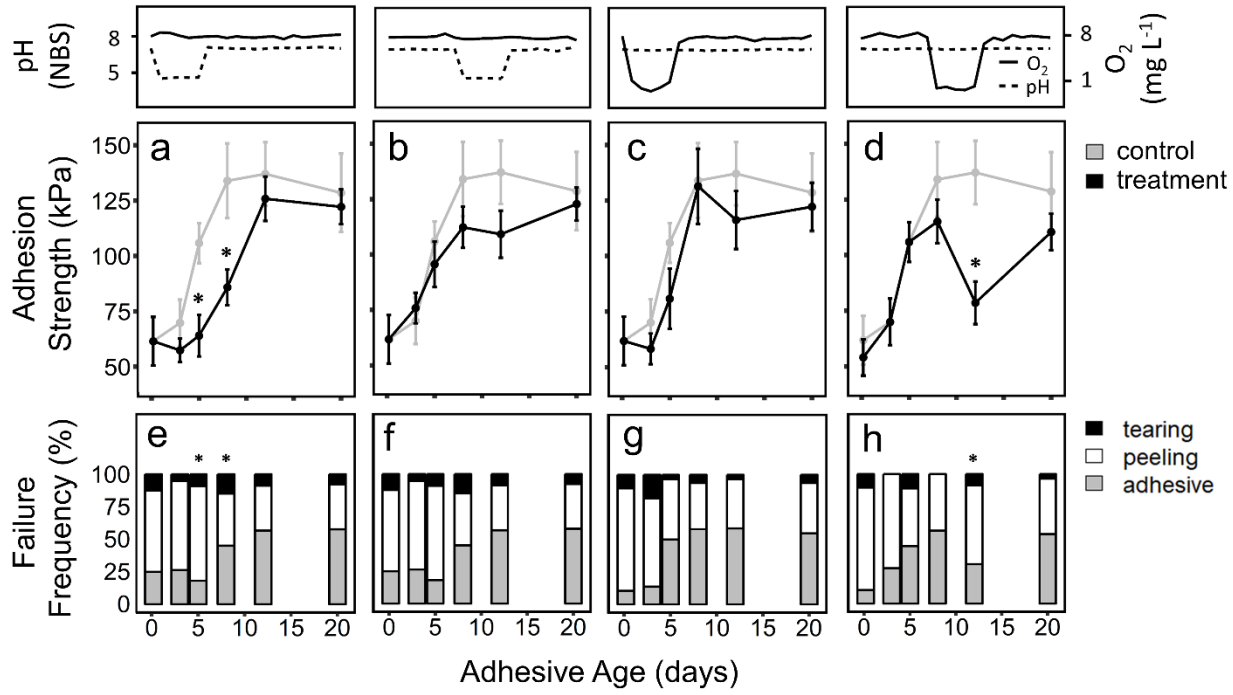

Figure 3.5. The effect of low pH and hypoxia excursions on adhesive plaque curing. The top panels represent schematic representations of the laboratory seawater treatments that freshly made plaques were exposed to after being deposited by a mussel. The adhesion strength (kPa) of plaques (a-d), along with the frequency of each failure mode (e-f; tearing, peeling, or adhesive failure) are reported underneath the schematic of each treatment. A control treatment wherein pH and oxygen remained at a baseline (pH = ~8.0, O_2 = ~8.5 mg L^{-1}) for 20 days is included in panels a-d, represented in gray. Error bars represent the standard error about the mean for each time point. Asterisks indicate either a significantly different (alpha = 0.05) adhesion strength between treatments and the control (a-d), or a significantly different failure mode distribution at a given time point (e-h), as determined by a chi squared test using the open ocean control as the expected values.

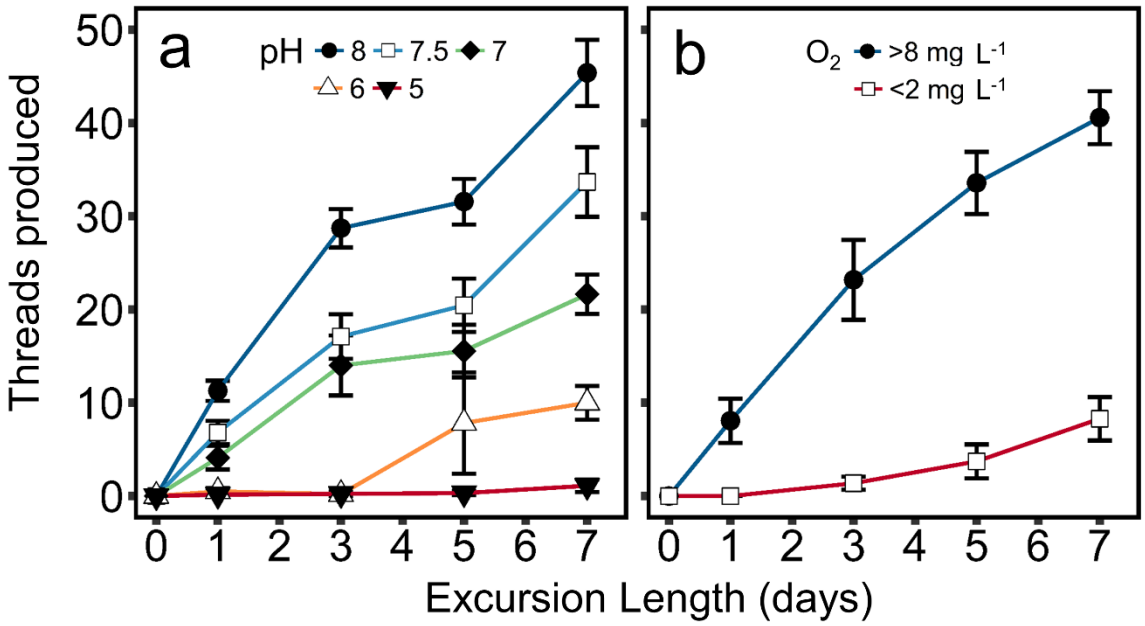

Figure 3.6. Byssal thread production during pH (a; pH targets = 8.0, 7.5, 7.0, 6.0, 5.0) and oxygen (b; O2 targets = >8.0, <2.0 mg L-1) excursions. Mussels were sampled after 1, 3, 5, or 7 days, counting the number of threads produced by each individual and averaging (± se) by treatment. At pH 5, 6, and a dissolved oxygen concentration of <2 mg L-1, the majority of mussels remained closed for the first three days of exposure.

3.13. Supplementary Material

Table S3.1. Water conditions (temperature, salinity, dissolved oxygen, pH, and chlorophyll concentration, measured hourly) recorded by raft sensors in Quilcene Bay, from April 2015 to March 2018. Reported values are aggregated season means ± S.D, recorded at 1 and 7 meters below the surface. The minimum and maximum values observed for each seawater parameter, at a given depth and season, are listed in parentheses.

Season	Depth	n	T (°C)	n	Sal (PSU)	n	O_2 (mg L^{-1})	n	pH (NBS)	n	Chl (µg L^{-1})
Spring	1m	4897	13.2 ± 2.6 (8.1-20.7)	4731	25.7 ± 2.1 (13.7-30.0)	4871	11.0 ± 2.1 (3.1-18.9)	4342	8.15 ± 0.21 (7.26-8.73)	4871	9 ± 16 (0-342)
	7m	4895	11.0 ± 1.2 (7.8-18.6)	3864	27.8 ± 1.7 (20.3-36.2)	4895	8.5 ± 2.9 (0.4-18.5)	4885	7.89 ± 0.29 (7.15-8.58)	4843	7 ± 18 (0-435)
Summer	1m	4355	18.0 ± 2.3 (11.7-24.1)	1246	26.6 ± 3.3 (13.5-33.0)	4833	8.3 ± 4.1 (0.3-19.1)	3108	8.08 ± 0.18 (7.35-8.67)	4861	6 ± 10 (0-321)
	7m	4435	13.2 ± 1.6 (10.3-19.3)	3354	29.4 ± 1.6 (25.1-35.4)	4435	7.7 ± 3.4 (0.1-18.1)	4435	7.77 ± 0.28 (7.14-8.56)	4457	10 ± 18 (0-238)
Autumn	1m	2641	10.9 ± 2.5 (6.4-15.7)	2642	26.9 ± 5.4 (2.1-31.4)	3783	9.2 ± 1.2 (5.0-12.6)	3783	7.80 ± 0.14 (7.32-8.28)	3783	27 ± 56 (0-433)
	7m	4049	11.4 ± 4.3 (7.3-15.0)	4049	29.7 ± 2.5 (21.9-34.5)	4049	7.2 ± 1.7 (2.6-11.3)	4049	7.66 ± 0.15 (7.32-8.07)	4029	2 ± 6 (0-237)
Winter	1m	3514	7.9 ± 1.0 (5.3-10.1)	2639	23.8 ± 4.1 (2.6-33.0)	3514	10.1 ± 1.8 (5.4-17.5)	3514	7.85 ± 0.19 (7.43-8.54)	3513	6 ± 10 (0-215)
	7m	2712	9.4 ± 2.5 (6.9-11.2)	1767	28.4 ± 2.4 (21.2-33.7)	2712	8.2 ± 1.9 (4.5-14.5)	2712	7.77 ± 0.19 (7.40-8.34)	2691	3 ± 18 (0-486)

Table S3.2. ANOVA results comparing raft sensor measurements of temperature (°C), salinity (PSU), and dissolved oxygen (mg L^{-1}), seawater pH (NBS), and chlorophyll concentration (µg L^{-1}) from April, 2015 to March, 2018. Data were transformed using the normal quantile transformation, comparing the variance about the mean across season (spring, summer, autumn, and winter) and depth (1 and 7 meters below the surface).

Source	d.f.	*SS*	F	p-value
Temperature				
Season	3	112617	33378	<0.001*
Depth	1	31128	9226	<0.004*
Season x depth	3	68282	6746	<0.001*
Salinity				
Season	3	3585	1377	<0.001*
Depth	1	1293	1490	<0.001*
Season x depth	3	1664	639	<0.001*
Dissolved Oxygen				
Season	3	4469	1749	<0.001*
Depth	1	1639	1924	<0.001*
Season x depth	3	1249	489	<0.001*
pH				
Season	3	4825	2130	<0.001*
Depth	1	2208	2924	<0.001*
Season x depth	3	5113	2257	<0.001*
Chlorophyll				
Season	3	232	85	<0.001*
Depth	1	769	849	<0.001*
Season x depth	3	1232	453	<0.001*

Table S3.3. Body size and condition metrics for mussels that produced adhesive plaques included in tensometer tests. Results are presented for five laboratory experiments, within which plaques were incubated in open-ocean conditions (control), fluctuating seawater pH (Exp. 1 and 2) and dissolved oxygen (Exp. 3 and 4) conditions, sampled over the course of 20 days.

Age (days)	n	Shell Length (cm)	Plaque Area (mm^2)	Gonad Index	Condition Index ($x10^{-3}$ g cm^{-3})
Control					
0.17	18	4.6 ± 0.5	1.99 ± 0.65	0.11 ± 0.02	4.1 ± 0.5
3	11	4.9 ± 0.6	2.17 ± 0.88	0.11 ± 0.02	3.5 ± 0.4
5	9	4.9 ± 0.3	2.14 ± 0.37	0.11 ± 0.01	4.1 ± 0.4
8	10	5.0 ± 0.5	2.16 ± 0.32	0.11 ± 0.03	4.0 ± 0.9
12	12	5.2 ± 0.6	2.35 ± 0.43	0.12 ± 0.02	4.0 ± 0.5
20	10	4.8 ± 0.5	2.07 ± 0.44	0.11 ± 0.02	3.9 ± 0.6
Experiment 1					
3	12	5.0 ± 0.3	2.15 ± 0.37	0.11 ± 0.03	3.8 ± 0.8
5	12	4.4 ± 0.4	2.30 ± 1.07	0.10 ± 0.03	4.1 ± 1.0
8	11	4.5 ± 0.2	2.27 ± 0.42	0.08 ± 0.03	4.3 ± 0.5
12	12	4.6 ± 0.3	2.33 ± 0.37	0.10 ± 0.04	4.1 ± 0.8
20	13	4.8 ± 0.4	2.19 ± 0.44	0.12 ± 0.03	4.2 ± 0.5
Experiment 2					
3	15	4.4 ± 0.4	2.19 ± 0.37	0.09 ± 0.03	3.8 ± 1.3
5	15	4.5 ± 0.4	2.41 ± 0.50	0.10 ± 0.04	3.9 ± 1.2
8	16	4.3 ± 0.7	2.05 ± 0.62	0.11 ± 0.03	3.4 ± 0.8
12	12	4.5 ± 0.5	2.29 ± 0.68	0.10 ± 0.02	3.5 ± 1.4
20	14	4.6 ± 0.4	2.14 ± 0.40	0.11 ± 0.04	3.4 ± 1.2
Experiment 3					
3	11	4.9 ± 0.6	1.90 ± 0.43	0.11 ± 0.02	3.5 ± 0.4
5	9	4.9 ± 0.3	2.14 ± 0.37	0.11 ± 0.01	4.1 ± 0.4
8	11	5.0 ± 0.5	2.38 ± 0.34	0.11 ± 0.03	4.1 ± 0.9
12	10	4.9 ± 0.6	2.48 ± 0.45	0.11 ± 0.03	3.5 ± 1.4
20	10	4.9 ± 0.5	2.41 ± 0.32	0.11 ± 0.04	4.2 ± 1.2
Experiment 4					
3	11	4.6 ± 0.7	2.23 ± 0.32	0.14 ± 0.20	4.8 ± 0.8
5	10	4.8 ± 0.4	2.17 ± 0.35	0.11 ± 0.03	4.6 ± 1.8
8	10	4.6 ± 0.5	2.30 ± 0.60	0.11 ± 0.03	4.4 ± 1.0
12	9	4.5 ± 0.6	2.67 ± 0.38	0.12 ± 0.03	4.0 ± 1.0
20	10	4.8 ± 0.4	2.33 ± 0.43	0.11 ± 0.03	4.8 ± 1.5

Table S3.4. ANOVA results of linear mixed-effects models investigating the effect of mussel physiology on adhesive plaque adhesion strength (kPa), including adhesive age (days), mussel shell length (cm), gonad index (GI), condition index (CI, $x10^{-3}$ g cm^{-3}), and plaque planform area (mm^2) as factors, grouped within each mussel as a random effect. Results are presented for four laboratory experiments, within which plaques were incubated in fluctuating pH (Exp. 1 and 2) and dissolved oxygen (Exp. 3 and 4) conditions. Asterisks represent significant results (alpha = 0.05).

Source	DF_{num}	DF_{den}	F	P-value
Control				
Adhesive Age	1	64	20.50	<0.001*
Shell length	1	64	0.08	0.78
GI	1	64	0.19	0.67
CI	1	64	0.41	0.53
Plaque area	1	64	2.24	0.14
Experiment 1				
Adhesive Age	1	72	25.25	<0.001*
Shell length	1	72	0.44	0.51
GI	1	72	2.11	0.15
CI	1	72	0.36	0.55
Plaque area	1	72	0.06	0.81
Experiment 2				
Adhesive Age	1	84	42.09	<0.001*
Shell length	1	84	0.29	0.59
GI	1	84	0.32	0.58
CI	1	84	0.89	0.35
Plaque area	1	84	0.86	0.36
Experiment 3				
Adhesive Age	1	62	13.83	0.004*
Shell length	1	62	0.14	0.71
GI	1	62	0.002	0.97
CI	1	62	0.28	0.60
Plaque area	1	62	2.91	0.09
Experiment 4				
Adhesive Age	1	62	27.39	<0.001*
Shell length	1	62	0.12	0.73
GI	1	62	0.37	0.54
CI	1	62	0.003	0.96
Plaque area	1	62	0.42	0.52

Table S3.5. Body size and condition metrics for mussels that were included in thread production assays, grouped by treatment and collection time point (mean ± s.d).

Trt	Target	Time	n	Shell Length (cm)	Gonad Index	Condition Index ($x10^{-3}$ g cm^{-3})
pH	8.0	1	14	4.7 ± 0.3	0.11 ± 0.03	4.2 ± 0.8
		3	14	5.0 ± 0.4	0.12 ± 0.03	4.2 ± 0.4
		5	36	5.0 ± 0.6	0.11 ± 0.03	4.1 ± 0.4
		7	22	5.1 ± 0.5	0.11 ± 0.03	3.9 ± 0.5
	7.5	1	22	5.3 ± 0.6	0.11 ± 0.03	3.9 ± 0.5
		3	20	5.2 ± 0.4	0.10 ± 0.03	3.9 ± 0.6
		5	20	5.1 ± 0.5	0.12 ± 0.03	3.9 ± 0.7
		7	21	4.9 ± 0.4	0.10 ± 0.03	3.7 ± 0.6
	7.0	1	18	5.5 ± 0.5	0.13 ± 0.04	4.1 ± 0.6
		3	20	5.1 ± 0.9	0.09 ± 0.03	3.9 ± 0.7
		5	20	4.9 ± 0.4	0.11 ± 0.04	3.7 ± 0.8
		7	19	4.7 ± 0.6	0.11 ± 0.03	4.1 ± 0.7
	6.0	1	14	5.7 ± 0.6	0.09 ± 0.04	3.2 ± 1.2
		3	15	5.2 ± 0.6	0.06 ± 0.04	4.3 ± 1.3
		5	12	5.4 ± 0.6	0.09 ± 0.04	4.0 ± 1.4
		7	20	4.9 ± 0.6	0.08 ± 0.03	4.1 ± 0.7
	5.0	1	20	5.0 ± 0.6	0.07 ± 0.03	5.0 ± 1.0
		3	13	5.3 ± 0.6	0.09 ± 0.05	4.3 ± 1.9
		5	22	4.9 ± 0.4	0.08 ± 0.04	3.7 ± 0.8
		7	19	5.1 ± 0.4	0.08 ± 0.04	3.8 ± 0.6
O_2	> 8.0	1	15	4.5 ± 0.5	0.12 ± 0.03	3.8 ± 0.8
		3	17	4.8 ± 0.6	0.11 ± 0.04	4.0 ± 0.6
		5	16	4.8 ± 0.4	0.12 ± 0.03	3.6 ± 0.7
		7	18	4.6 ± 0.7	0.1 ± 0.03	3.8 ± 0.4
	< 2.0	1	11	4.8 ± 0.6	0.11 ± 0.03	3.9 ± 0.6
		3	21	5.0 ± 0.7	0.09 ± 0.04	4.1 ± 1.3
		5	21	5.2 ± 0.9	0.07 ± 0.04	4.0 ± 1.1
		7	14	4.6 ± 0.5	0.09 ± 0.02	3.6 ± 0.5

Table S3.6. ANOVA results of linear mixed-effects models investigating the effect of pH or oxygen treatment, gonad index (GI), condition index (CI), and shell length (cm) on the number of threads produced after seven day excursions, using each mussel as a random effect. Asterisks represent significant results (alpha = 0.05).

Source	DF_{num}	DF_{den}	F	P-value
pH Experiment				
pH	1	96	154.5	<0.001*
Shell length	1	96	0.23	0.64
GI	1	96	1.64	0.20
CI	1	96	0.61	0.44
Oxygen Experiment				
Dissolved oxygen	1	27	70.1	<0.001*
Shell length	1	27	0.11	0.74
GI	1	27	0.93	0.34
CI	1	27	1.77	0.20